INSTITUTO TECNOLÓGICO Y DE ESTUDIOS SUPERIORES DE MONTERREY

CAMPUS MONTERREY

PROGRAMA DE GRADUADOS EN MECATRÓNICA
Y TECNOLOGÍAS DE INFORMACIÓN

TECNOLÓGICO
DE MONTERREY®

Interference Estimation for Wireless Mesh Networks with IEEE 802.16 WiMAX

by

Rocio Elizalde Gómez

Thesis

Presented as a partial fulfillment of the requirements for the degree of

Master of Science in Electronic Engineering
Major in Telecommunications

Monterrey, N.L. May 2008

INSTITUTO TECNOLÓGICO Y DE ESTUDIOS SUPERIORES DE MONTERREY

CAMPUS MONTERREY

DIVISIÓN DE MECATRÓNICA Y TECNOLOGÍAS DE INFORMACIÓN

PROGRAMA DE GRADUADOS EN MECATRÓNICA Y TECNOLOGÍAS DE INFORMACIÓN

The members of the thesis committee hereby approve the thesis of Rocio Elizalde Gómez, B.S. as a partial fulfillment of the requirements for the degree of Master of Science in

Electronic Engineering

Major in Telecommunications

Thesis Committee:

David Muñoz Rodríguez, Ph.D.
Thesis Advisor

César Vargas Rosales, Ph.D.
Synodal

Oscar Rodríguez Morales, M.Sc.
Synodal

Joaquín Acevedo Mascarúa, Ph.D.
Director of the Graduate Program

May 2008

To my family,

Luz María Gómez Velarde, José Fernando Elizalde Romo,
Lucero Elizalde Gómez and Sebastián Reynoso Elizalde.

Acknowledgments

To my parents, Luz María and José Fernando, for their unconditional support in all my life. To my sister Lucero for support to me at any moment.

I am very grateful to my thesis advisor David Muñoz Rodríguez, Ph.D. for all this time in which we works together, for all his professional advice for the accomplishment of this work. Because, without his guidance this thesis would not have been possible. Also I want to thank to César Vargas Rosales, Ph.D. and Oscar Rodríguez Morales, M.Sc. for their valuable comments for the enhancement of this work.

To the ITESM and CONACYT for give me the opportunity of realize my graduate studies.

To my friends, for everything we went through during this wonderful time.

Rocio Elizalde Gómez

INSTITUTO TECNOLÓGICO Y DE ESTUDIOS SUPERIORES DE MONTERREY
May 2008

Interference Estimation for Wireless Mesh Networks with IEEE 802.16 WiMAX

Rocio Elizalde Gómez, M.Sc.
INSTITUTO TECNOLÓGICO Y DE ESTUDIOS SUPERIORES DE MONTERREY, 2008

Thesis advisor: David Muñoz Rodríguez, Ph.D.

IEEE 802.16 (WiMAX) is a wireless metropolitan area network standard with high transmission speed and great coverage. There are several ways of quantifying the performance of a broadband system. This work will address the interference analysis; an important issue of WiMAX system design. This thesis considers the factors affecting this performance measure for the two WiMAX transmission modes. Point-to-multipoint (PMP) is the traditional WiMAX transmission mode. Wireless mesh network (WMN) is an attractive and useful structure which is suggested to be adopted in WiMAX.

We study in this thesis the interference of the downlink and uplink of OFDMA-based IEEE802.16 WiMAX system. We focus in particular on the impact of Adaptive Modulation and Coding (AMC) as well as inter-cell interference resulting from different frequency reuse schemes.

We demonstrate that the mesh mode offers a significantly advantage over the traditional PMP mode. The mesh mode allow to offer best quality of service to more users using a higher rate modulation.

Contents

List of Figures

List of Tables

Chapter 1

Introduction

WiMAX (Worldwide Interoperability for Microwave Access) is based on the IEEE 802.16 standard for Metropolitan Area Networks (MAN). Its goal is to deliver wireless broadband access to customers using base stations with coverage distances in the order of miles. Originally, the standard considered only fixed and nomadic links (802.16-2004) that could be used for "last mile" connectivity providing an alternate to T1 and DSL wired lines or as a back-haul for cellular or Wi-Fi networks. In order to address mobile subscribers, WiMAX was expanded to include portable devices (802.16e) such as personal digital assistants (PDAs), laptops, or phones. Supporting mobility required including provisions for roaming and inter-cell handoff and incorporating more flexibility into the standard to sustain multiple users demanding various types of services. In mobile WiMAX, the system's resources are dynamically allocated to deliver high data rates seamlessly to terminals traveling at vehicular speeds.

The IEEE 802.16e specifications define three different PHY layers: single carrier transmission, Orthogonal Frequency-Division Multiplexing (OFDM), and OFD Multiple Access (OFDMA). The multiple access technique used in the first two of these PHY specifications is pure TDMA, while the third technique uses both the time and frequency dimensions for resource allocation. From these three PHY technologies, OFDMA has been selected by WiMAX Forum [5] as the basic technology for portable and mobile applications.

A WiMAX network consists of a Base Station (BS) and multiple Subscriber Stations (SS). A WiMAX network can operate under two modes. The first mode is the Point-to-Multipoint (PMP) mode. In PMP, all the SSs are directly connect to the BS through a single-hop wireless link, hence, data transmissions between two SSs are routed through the BS. The second mode is the mesh mode, in which a SS can com-

municate with either the BS or other SSs through multi-hop routes. A station in the wireless network, termed Mesh BS, acts like a BS in PMP mode and interfaces the network to the backhaul links. The mesh mode extends the coverage of the network and is able to support non-LOS transmission.

WiMAX uses a combination of adaptive modulation schemes and coding ranging from 1/2 rate QPSK to 3/4 rate 64QAM. The amount of error correction applied to each transmission is adjustable and can be changed depending on the required QoS and based on the reliability of the link between each user and the base station. Assigning modulations based on the link conditions increases the overall capacity of the system. In OFDMA, modulation and/or coding scheme can be chosen differently for each sub-carrier, and it can also change with time. It has been shown that systems using adaptive modulation perform better than systems whose modulation and coding are fixed.

1.1. Problem Description

To gain widespread success, broadband wireless systems must deliver multimegabit per second throughput to end users, with robust QoS to support a variety of services, such as voice, data, and multimedia. Given the remarkable success of the Internet and the large variety of emerging IP-based applications, it is critical that broadband wireless systems be built to support these IP-based applications and services efficiently.

IEEE 802.16 WiMAX is coming popular due to the promise of coverage distances in the order of miles and higher bitrates compared to other wireless technologies. However limitations in the amount of available spectrum dictate that users share the available bandwidth. This sharing can cause signals from different users to interfere with one another. In capacity-driven networks, interference typically poses a larger impairment than noise and hence needs to be addressed. Interference estimation is way of quantifying the performance of a broadband system and it is essential to the development of effective solutions for broadband wireless.

1.2. Objective

As a way of quantifying the performance of a WiMAX system, the purpose of this thesis is to estimate the interference in the two possible network topologies defined in the IEEE 802.16 standard: point-to-multipoint and mesh mode. We focus in particular on the impact of Adaptive Modulation and Coding (AMC) as well as inter-cell interference resulting from different frequency reuse schemes.

1.3. Justification

The goal of all communication systems is to provide service to the all users at any time, and this service needs to be fast, efficient and of good quality. But the achievement of these goals is more difficult to reach. This is due to the limited resources of the system, the subscriber's mobility, the geographical characteristics of the region, etc.

Due to the importance of the performance quantification, we can find several works that present some results in this matter. In [6] is discussed an analytical approach to dimension cellular multihop networks based on the WiMAX technology and a performance evaluation is presented in order to compare singlehop and multihop deployments in terms of capacity but AMC schemes were not considered.

Furthermore, in [7] a WiMAX structure with mesh is proposed, which supports direct data transmission between SSs (subscribe stations) with the control of the BS if possible. Simulation results are presented in this article to show the enhancement gain of the system performance by the smart model where AMC scheme is considered too. However, they considered just the intra-cell interference but actually the system model try to avoid this interference in order to improve the system performance.

1.4. Contribution

IEEE 802.16 (WiMAX) is a wireless metropolitan area network standard with high transmission speed and great coverage. It is important to quantify the performance of a broadband system. This work will focus in the interference analysis; an important issue of WiMAX system design. The analysis will be done in the two WiMAX transmission modes—Point-to-multipoint (PMP) mode and Mesh mode—in order to have

comparative results between them.

We study in this thesis the interference of the downlink and uplink of OFDMA-based IEEE802.16 WiMAX system. We focus in particular on the impact of Adaptive Modulation and Coding (AMC) as well as inter-cell interference resulting from different frequency reuse schemes.

1.5. Thesis Organization

This work is organized as follows, Chapter 2 presents the necessary Theoretical Background to understand the analysis performed in the research. Some of the concepts used throughout the thesis like co-channel interference and propagation models are explained here. Chapter 3 presents the considerations taken for the WiMAX deployments presented and analyzed. Comparisons of simulation results and analytical evaluations are presented in Chapter 4. Finally Chapter 5 presents the conclusions of this work and further research under the same line of study.

Chapter 2

Overview of WiMAX

After years of development and uncertainty, a standards-based interoperable solution is emerging for wireless broadband. A broad industry consortium, the Worldwide Interoperability for Microwave Access (WiMAX) Forum has begun certifying broadband wireless products for interoperability and compliance with a standard. WiMAX is based on wireless metropolitan area networking (WMAN) standards developed by the IEEE 802.16 group and adopted by both IEEE and the ETSI HIPERMAN group.

The IEEE 802.16 group was formed in 1998 to develop an air-interface standard for wireless broadband. The group's initial focus was the development of a LOS-based point-to-multipoint wireless broadband system for operation in the 10GHz-66GHz millimeter wave band. The resulting standard—the original 802.16 standard, completed in December 2001—was based on a single-carrier physical (PHY) layer with a burst time division multiplexed (TDM) MAC layer. Many of the concepts related to the MAC layer were adapted for wireless from the popular cable modem DOCSIS (data over cable service interface specification) standard [1].

The IEEE 802.16 group subsequently produced 802.16a, an amendment to the standard, to include non-line-of-sight (NLOS) applications in the 2GHz-11GHz band, using an *orthogonal frequency division multiplexing* (OFDM)-based physical layer. Additions to the MAC layer, such as support for *orthogonal frequency division multiple access* (OFDMA), were also included. Further revisions resulted in a new standard in 2004, called IEEE 802.16-2004, which replaced all prior versions and formed the basis for the first WiMAX solution. These early WiMAX solutions based on IEEE 802.16-2004 targeted fixed applications, and we will refer to these as fixed WiMAX (REF STD 2004). In December 2005, the IEEE group completed and approved IFEEE 802.16e-2005, an amendment to the IEEE 802.16-2004 standard that added mobility

support. The IEEE 802.16e-2005 forms the basis for the WiMAX solution for nomadic and mobile applications and is often referred to as mobile WiMAX [3].

The basic characteristics of the various IEEE 802.16 standards are summarized in Table 2.1. Note that these standards offer a variety of fundamentally different design options. For example, there are multiple physical-layer choices: a single-carrier-based physical layer called Wireless-MAN-SCa, an OFDM-based physical layer called WirelessMAN-OFDM, and an OFDMA based physical layer called Wireless-OFDMA. Similarly, there are multiple choices for MAC architecture, duplexing, frequency band of operation, etc. These standards were developed to suit a variety of applications and deployment scenarios, and hence offer a plethora of design choices for system developers. In fact, one could say that IEEE 802.16 is a collection of standards, not one single interoperable standard [1].

2.1. Salient Features of WiMAX [1]

WiMAX is a wireless broadband solution that offers a rich set of features with a lot of flexibility in terms of deployment options and potential service offerings. Some of the more salient features that deserve highlighting are as follows:

OFDM-based physical layer: The WiMAX physical layer (PHY) is based on orthogonal frequency division multiplexing, a scheme that offers good resistance to multipath, and allows WiMAX to operate in NLOS conditions. OFDM is now widely recognized as the method of choice for mitigating multipath for broadband wireless.

Very high peak data rates: WiMAX is capable of supporting very high peak data rates. In fact, the peak PHY data rate can be as high as 74Mbps when operating using a 20MHz[1] wide spectrum. More typically, using a 10MHz spectrum operating using TDD scheme with a 3:1 downlink-to-uplink ratio, the peak PHY data rate is about 25Mbps and 6.7Mbps for the downlink and the uplink, respectively. These peak PHY data rates are achieved when using 64 QAM modulation with rate 5/6 error-correction coding. Under very good signal conditions, even higher peak rates may be achieved using multiple antennas and spatial multiplexing.

[1]Initial WiMAX profiles do not include 20MHz support; 74Mbps is combined uplink/downlik PHY throughput

Table 2.1: Basic Data on IEEE 802.16 Standards

	IEEE 802.16	IEEE 802.16-2004	IEEE 802.16e-2005
Status	Completed December 2001	Completed June 2004	Completed December 2005
Frequency Band	10GHz-66GHz	2GHz-11GHz	2GHz-11GHz for fixed; 2GHz-6GHz for mobile applications
Application	Fixed LOS	Fixed NLOS	Fixed and mobile NLOS
MAC architecture	Point-to-multipoint, mesh	Point-to-multipoint, mesh	Point-to-multipoint, mesh
Transmission scheme	Single carrier only	Single carrier, 256 OFDM or 2048 OFDM	Single carrier, 256 OFDM or scalable OFDM with 128, 512, 1024 or 2048 subcarriers
Modulation	QPSK, 16 QAM, 64 QAM	QPSK, 16 QAM, 64 QAM	QPSK, 16 QAM, 64 QAM
Gross data rate	32Mbps-134.4Mbps	1Mbps-75Mbps	1Mbps-75Mbps
Multiplexing	Burst TDM/TDMA	Burst TDM/TDMA/OFDMA	Burst TDM/TDMA/OFDMA
Duplexing	TDD and FDD	TDD and FDD	TDD and FDD
Channel bandwidths	20MHz, 25MHz, 28MHz	1.75MHz, 3.5MHz, 7MHz, 14MHz, 1.25MHz, 5MHz, 10MHz, 15MHz, 8.75MHz	1.75MHz, 3.5MHz, 7MHz, 14MHz, 1.25MHz, 5MHz, 10MHz, 15MHz, 8.75MHz
Air-interface designation	WirelessMAN-SC	WirelessMAN-SCa, WirelessMAN-OFDM, WirelessMAN-OFDMA	WirelessMAN-SCa, WirelessMAN-OFDM, WirelessMAN-OFDMA
WiMAX implementation	None	256 - OFDM as Fixed WiMAX	Scalable OFDMA as Mobile WiMAX

Scalable bandwidth and data rate support: WiMAX has a scalable physical-layer architecture that allows for the data rate to scale easily with available channel bandwidth. This scalability is supported in the OFDMA mode, where the FFT (fast fourier transform) size may be scaled based on the available channel bandwidth. For example, a WiMAX system may use 128-, 512-, or $1,048$-bit FFTs based on whether the channel bandwidth is 1.25MHz, 5MHz, or 10MHz, respectively. This scaling may be done dynamically to support user roaming across different networks that may have different bandwidth allocations.

Adaptive modulation and coding (AMC): WiMAX supports a number of modulation and forward error correction (FEC) coding schemes and allows the scheme to be changed on a per user and per frame basis, based on channel conditions. AMC is an effective mechanism to maximize throughput in a time-varying channel. The adaptation algorithm typically calls for the use of the highest modulation and coding scheme that can be supported by the signal-to-noise and interference ratio at the receiver such that each user is provided with the highest possible data rate that can be supported in their respective links.

Link-layer retransmissions: For connections that require enhanced reliability, WiMAX supports automatic retransmission requests (ARQ) at the link layer. ARQ-enabled connections require each transmitted packet to be acknowledged by the receiver; unacknowledged packets are assumed to be lost and are retransmitted. WiMAX also optionally supports hybrid-ARQ, which is an effective hybrid between FEC and ARQ.

Support for TDD and FDD: IEEE 802.16-2004 and IEEE 802.16e-2005 supports both time division duplexing and frequency division duplexing, as well as a half-duplex FDD, which allows for a low-cost system implementation. TDD is favored by a majority of implementations because of its advantages: (1) flexibility in choosing uplink-to-downlink data rate ratios, (2) ability to exploit channel reciprocity, (3) ability to implement in nonpaired spectrum, and (4) less complex transceiver design. All the initial WiMAX profiles are based on TDD, except for two fixed WiMAX profiles in 3.5GHz.

Orthogonal frequency division multiple access (OFDMA): Mobile WiMAX uses OFDM as a multiple-access technique, whereby different users can be allocated different subsets of the OFDM tones. OFDMA facilitates the exploitation of frequency diversity and multiuser diversity to significantly improve the system capacity.

Flexible and dynamic per user resource allocation: Both uplink and downlink resource allocation are controlled by a scheduler in the base station. Capacity is shared among multiple users on a demand basis, using a burst TDM scheme. When using the OFDMA-PHY mode, multiplexing is additionally done in the frequency dimension, by allocating different subsets of OFDM subcarriers to different users. Resources may be allocated in the spatial domain as well when using the optional advanced antenna systems (AAS). The standard allows for bandwidth resources to be allocated in time, frequency, and space and has a flexible mechanism to convey the resource allocation information on a frame-by-frame basis.

Support for advanced antenna techniques: The WiMAX solution has a number of hooks built into the physical-layer design, which allows for the use of multiple-antenna techniques, such as beamforming, space-time coding, and spatial multiplexing. These schemes can be used to improve the overall system capacity and spectral efficiency by deploying multiple antennas at the transmitter and/or the receiver.

Quality-of-service support: The WiMAX MAC layer has a connection-oriented architecture that is designed to support a variety of applications, including voice and multimedia services. The system offers support for constant bit rate, variable bit rate, real-time, and non-real-time traffic flows, in addition to best-effort data traffic. WiMAX MAC is designed to support a large number of users, with multiple connections per terminal, each with its own QoS requirement.

Robust security: WiMAX supports strong encryption, using Advanced Encryption Standard (AES), and has a robust privacy and key-management protocol. The system also offers a very flexible authentication architecture based on Extensible Authentication Protocol (EAP), which allows for a variety of user credentials, including username/password, digital certificates, and smart cards.

Support for mobility: The mobile WiMAX variant of the system has mechanisms to support secure seamless handovers for delay-tolerant full-mobility applications, such as VoIP. The system also has built-in support for power-saving mechanisms that extend the battery life of handheld subscriber devices. Physical-layer enhancements, such as more frequent channel estimation, uplink subchannelization, and power control, are also specified in support of mobile applications.

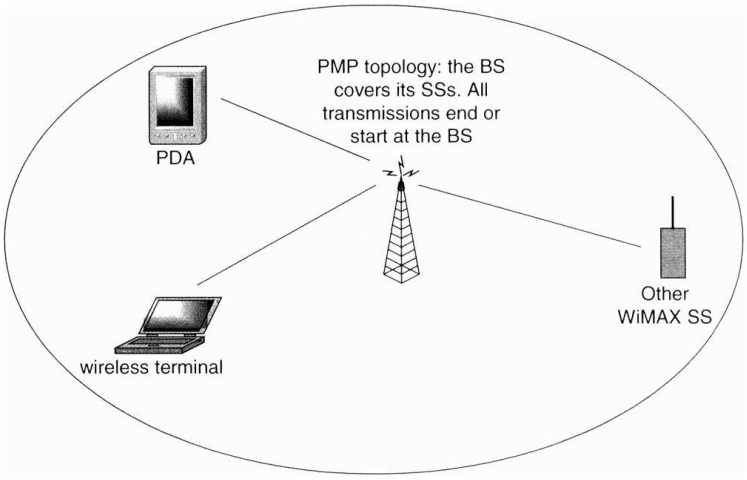

Figure 2.1: PMP topology

IP-based architecture: The WiMAX Forum has defined a reference network architecture that is based on an all-IP platform. All end-to-end services are delivered over an IP architecture relying on IP-based protocols for end-to-end transport, QoS, session management, security, and mobility. Reliance on IP allows WiMAX to ride the declining cost curves of IP processing, facilitate easy convergence with other networks, and exploit the rich ecosystem for application development that exists for IP.

2.1.1. WiMAX topologies

The IEEE 802.16 standard defines two possible network topologies:

- PMP (Point-to-Multipoint) topology (see Figure 2.1);
- Mesh topology or Mesh mode (see Figure 2.2).

The main difference between the two modes is the following: in the PMP mode, traffic may take place only between a BS and its SSs, while in the Mesh mode the traffic can be routed through other SSs until the BS and can even take place only between SSs. PMP is a centralized topology where the BS is the center of the system while in Mesh topology it is not. The elements of a Mesh network are called nodes, e.g. a Mesh SS is a node.

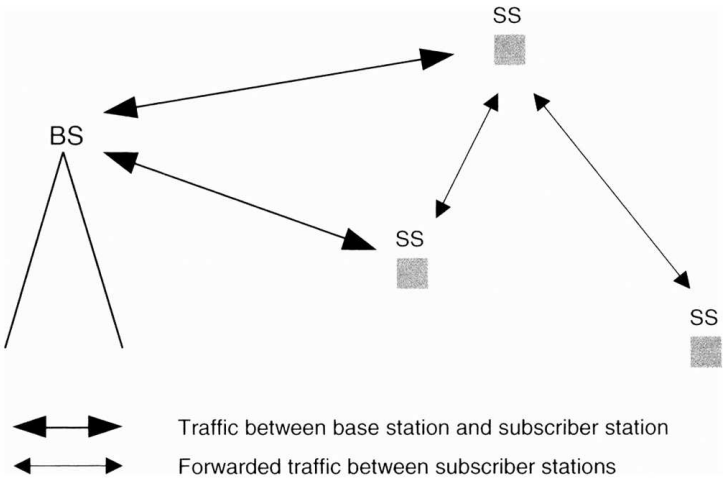

Figure 2.2: Mesh topology. The BS is no longer the center of the topology, as in the classical PMP mode

In Mesh topology, each station can create its own communication with any other station in the network and is then not restricted to communicate only with the BS. Thus, a major advantage of the Mesh mode is that the reach of a BS can be much greater, depending on the number of hops, until the most distant SS. On the other hand, using the Mesh mode brings up the now thoroughly studied research topic of ad hoc (no fixed infrastructure) networks routing.

When authorized to a Mesh network, a candidate SS node receives a 16-bit Node ID (IDentifier) upon a request to an SS identified as the Mesh BS. The Node ID is the basis of node identification. The Node ID is transferred in the Mesh subheader of a generic MAC frame in both unicast and broadcast messages [8].

2.1.2. Duplexing

In the majority of point-to-point wireless communication applications, full duplex operation is required, that is the flow of data needs to be bi-directional. Therefore, most radio technologies require a method to support the transfer of data in both directions.

The WiMAX/802.16 standard includes the two main duplexing techniques: Time Division Duplexing (TDD) and Frequency Division duplexing (FDD). The choice of

one duplexing technique or the other may affect certain PHY parameters as well as impact on the features that can be supported.

FDD mode

In an FDD system, the uplink and downlink channels are located on separate frequencies. A fixed duration frame is used for both uplink and downlink transmissions. This facilitates the use of different modulation types. It also allows simultaneous use of both full-duplex SSs, which can transmit and receive simultaneously and, optionally, half-duplex SSs which cannot. A full-duplex SS is capable of continuously listening to the downlink channel, while a half-duplex SS can listen to the downlink channel only when it is not transmitting on the uplink channel.

TDD mode

In the case of TDD, the uplink and downlink transmissions share the same frequency but they take place at different times. A TDD frame has a fixed duration and contains one downlink and one uplink subframe. The frame is divided into an integer number of Physical Slots (PSs), which help to partition the bandwidth easily. For OFDM and OFDMA PHYsical layers, a PS is defined as the duration of four modulation symbols. The frame is not necessarily divided into two equal parts. The TDD framing is adaptive in that the bandwidth allocated to the downlink versus the uplink can change. The split between the uplink and downlink is a system parameter and the 802.16 standard states that it is controlled at higher layers within the system [8].

Mesh topology supports only TDD duplexing.

Comparing the two modes, a fixed duration frame is used for both uplink and downlink transmissions in FDD while the TDD distribution is adaptive. Therefore TDD duplexing is more suitable when data rates are asymmetrical (between the uplink and downlink), e.g. for an Internet transmission.

After settling the question of duplexing, many users have to share the bandwidth resource in each kind of transmission.

2.2. The Cellular Concept

In this section, we briefly explore the key aspects of cellular systems and the closely related topics of sectoring and frequency reuse. Since WiMAX systems are expected to be deployed primarily in a cellular architecture, the concepts presented here are fundamental to understanding WiMAX system design and performance.

The cellular concept was a major breakthrough in solving the problem of spectral congestion and user capacity. It offered very high capacity in limited spectrum allocation without any major technological changes. The cellular concept is a system-level idea which calls for replacing a single, high power transmitter (large cell) with many low power transmitters (small cells), each providing coverage to only a small portion of the service area. Each base station is allocated a portion of the total number of channels available to the entire system, and nearby base stations are assigned different groups of channels so that all the available channels are assigned to a relatively small number of neighboring stations. Neighboring base stations are assigned different groups of channels so that the interference between base stations (and the mobile users under their control) is minimized. By systematically spacing base stations and their channel groups throughout a market, the available channels are distributed throughout the geographic region and may be reused as many times as necessary so long as the interference between co-channel stations is kept below acceptable levels.

2.2.1. Cluster Size Considerations: Frequency Reuse

Cellular radio systems rely on an intelligent allocation and reuse of channels throughout a coverage region [9]. Each cellular base station is allocated a group of radio channels to be used within a small geographic area called a *cell*. Base stations in adjacent cells are assigned channel groups which contain completely different channels than neighboring cells. The base station antennas are designed to achieve the desired coverage within the particular cell. By limiting the coverage area to within the boundaries of a cell, the same group of channels may be used to cover different cells that are separated from one another by distances large enough to keep interference levels within tolerable limits [10]. The design process of selecting and allocating channel groups for all of the cellular base stations within a system is called *frequency reuse* or *frequency planning*[11].

Figure 2.3 illustrates the concept of cellular frequency reuse, where cells labeled

with the same letter use the same group of channels. In this model, a cluster is outlined in boldface and consists of seven cells with different frequency channels. The hexagonal cell shape shown in Figure 2.3 is conceptual and is a simplistic model of the radio coverage for each base station, but it has been universally adopted since the hexagon permits easy and manageable analysis of a cellular system. The actual radio radio coverage of a cell is known as the *footprint* and is determined from field measurements or propagation prediction models [10]. Although the real footprint is amorphous in nature, a regular cell shape is needed for systematic system design and adaptation for future growth. While it might seem natural to choose a circle to represent the coverage area of a base station, adjacent circles cannot be overlaid upon a map without leaving gaps or creating overlapping regions. Thus, when considering geometric shapes which cover an entire region without overlap and with equal area, there are three sensible choices—a square, an equilateral triangle, and a hexagon (see Figure 2.4). A cell must be designed to serve the weakest mobiles within the footprint, and these are typically located at the edge of the cell. For a given distance between the center of a polygon and its farthest perimeter points, the hexagon has the largest of the three. Thus, by using the hexagon geometry, the fewest number of cells can cover a geographic region, and the hexagon closely approximates a circular radiation pattern which will occur for an omnidirectional base station antenna and free space propagation [10].

To understand the frequency reuse concept, consider a cellular system which has a total of S duplex channels available for use. If each cell is allocated a group of k channels ($k < S$), and if the S channels are divided among N cells into unique and disjoint channel groups which each have the same number of channel, the total number of available radio channels can be expressed as

$$S = kN \tag{2.1}$$

The N cells which collectively use the complete set of available frequencies is called a *cluster*. If a cluster is replicated M times within the system, the total number of duplex channels, C, can be used as a measure of capacity and is given by

$$C = MkN = MS \tag{2.2}$$

As seen from Equation 2.2, the capacity of a cellular system is directly proportional to the number of times a cluster is replicated in a fixed service area. The factor N is called the *cluster size* and for WiMAX systems is typically equal to 1 or 3 [8]. If the cluster size N is reduced while the cell size is kept constant, more cluster are re-

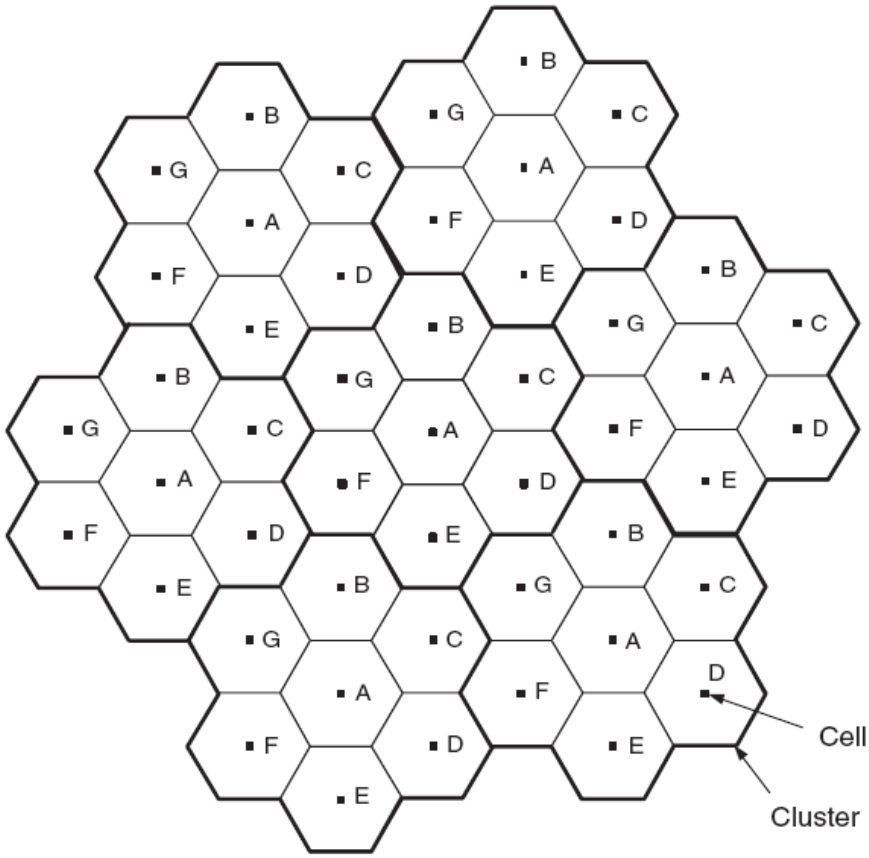

Figure 2.3: Standard figure of a hexagonal cellular system with $FRF = 1/7$

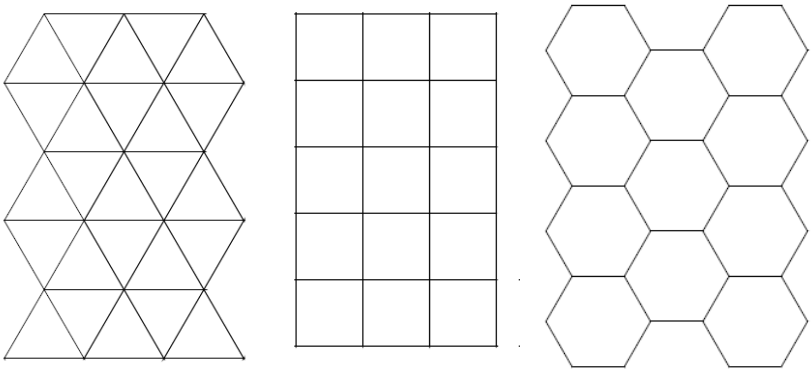

(a) Equilateral triangles (b) Squares (c) Regular hexagons

Figure 2.4: Regular polygons as cells

quired to cover a given area, and hence more capacity (a larger value of C) is achieved. A larger cluster size causes the ratio between the cell radius and the distance between co-channel cells to decrease, leading to weaker co-channel interference. Conversely, a small cluster size indicates that co-channel cells are located much closer together. The value for N is a function of how much interference a mobile or base station can tolerate while maintaining a sufficient quality of communications [10]. From a design viewpoint, the smallest possible value of N is desirable in order to maximize capacity over a given coverage area (i.e., to maximize C in Equation 2.2). The *frequency reuse factor* (FRF) of a cellular system is given by $1/N$, since each cell within a cluster is only assigned $1/N$ of the total available channels in the system.

Due to the fact that the hexagonal geometry of Figure 2.3 has exactly six equidistant neighbors and that the lines joining the centers of any cell and each of its neighbors are separated by multiples of 60 degrees, there are only certain cluster sizes and cell layouts which are possible [11]. In order to tessellate—to connect without gaps between adjacent cells—the geometry of hexagons is such that the number of cells per cluster, N, can only have values which satisfy Equation 2.3.

$$N = i^2 + ij + j^2 \tag{2.3}$$

where i and j are non-negative integers. To find the nearest co-channel neighbors of a particular cell, one must do the following: (1) move i cells along any chain of hexagons and then (2) turn 60 degrees counter-clockwise and move j cells. This is illustrated in Figure 2.5 for $i = 3$ and $j = 2$ (example, $N = 19$).

Refer to [11] for further information about fundamentals of hexagonal cellular geometry.

2.2.2. Interference and System Capacity

Interference is the major limiting factor in the performance of cellular radio systems. Sources of interference include another mobile in the same cell, a call in progress in a neighboring cell, other base stations operating in the same frequency band, or any noncellular system which inadvertently leaks energy into the cellular frequency band. Interference is more severe in urban areas, due to the greater RF noise floor and the large number of base stations and mobiles. The two major types of system-generated cellular interference are *co-channel interference* and *adjacent channel interference*.

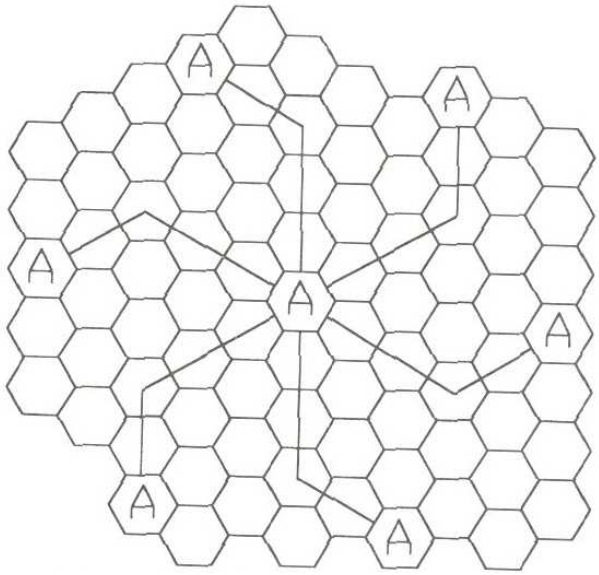

Figure 2.5: Method of locating co-channel cells in a cellular system. In this example, $N = 19$ (i.e., $i = 3$, $j = 2$)

Co-channel Interference

Frequency reuse implies that in a given coverage area there are several cells that use the same set of frequencies. These cells are called *co-channel cells*, and the interference between signals from these cells is called *co-channel interference*. Unlike thermal noise which can be overcome by increasing the signal-to-noise ratio (SNR), co-channel interference cannot be combated by simply increasing the carrier power of a transmitter. This is because an increase in carrier transmit power increases the interference to neighboring co-channel cells. To reduce co-channel interference, co-channel cells must be physically separated by a minimum distance to provide sufficient isolation due to propagation.

When the size of each cell is approximately the same and the base stations transmit the same power, the co-channel interference ratio is independent of the transmitted power and becomes a function of the radius of the cell(R) and the distance between centers of the nearest co-channel cells (D). By increasing the ratio D/R, the spatial separation between co-channel cells relative to the coverage distance of a cell is increased. Thus, interference is reduced from improved isolation of RF energy from the

co-channel cell [10]. The parameter Q, called the *co-channel reuse ratio*, is related to the cluster size (see Table 2.2 and Equation 2.3). For a hexagonal geometry

$$Q = \frac{D}{R} = \sqrt{3N} \tag{2.4}$$

A small value of Q provides larger capacity since the cluster size N is small, whereas a larger value of Q improves the transmission quality, due to a smaller level of co-channel interference. A trade-off must be made between these two objectives in actual cellular design.

Table 2.2: Co-channel Reuse Ratio for Some Values of N

	Cluster Size (N)	Co-channel Reuse Ratio (Q)
$i = 1$, $j = 1$	3	3
$i = 1$, $j = 2$	7	4.58
$i = 0$, $j = 3$	9	5.20
$i = 2$, $j = 2$	12	6

Since the background-noise power is negligible compared to the interference power in an interference-limited environment, the received SIR can be used instead of $SINR$. Let i_0 be the number of co-channel interfering cells. Then, the signal-to-interference ratio (S/I or SIR) for a mobile receiver which monitors a forward channel can be expressed as

$$\frac{S}{I} = \frac{S}{\sum_{i=1}^{i_0} I_i}, \tag{2.5}$$

where S is the desired signal power from the desired base station and I_i is the interference power caused by the ith interfering co-channel cell base station. If the signal levels of co-channel cells are known, then the S/I ratio for the forward link can be found using Equation 2.5.

Propagation measurements in a mobile radio channel show that the average received signal strength at any point decays as a power law of the distance of separation between a transmitter and receiver. The average received power P_r at a distance d from the transmitting antenna is approximated by

$$P_r = P_0(\frac{d}{d_0})^{-\gamma} \tag{2.6}$$

or

$$P_r(\text{dBm}) = P_0(\text{dBm}) - 10\gamma \log(\frac{d}{d_0}), \tag{2.7}$$

where P_0 is the power received at a close-in reference point in the far field region of the antenna at a small distance d_0 from the transmitting antenna and γ is the path loss exponent [10]. Now consider the forward link where the desired signal is the serving base station and where the interference is due to co-channel base stations. If D_i is the distance of the ith interferer from the mobile, the received power at a given mobile due to the ith interfering cell will be proportional to $(D_i)^{-\gamma}$. The path loss exponent typically ranges between two and four in urban cellular systems [10].

When the transmit power of each base station is equal and the path loss exponent is the same throughout the coverage area, S/I for a mobile can be approximated as

$$\frac{S}{I} = \frac{R^{-\gamma}}{\sum_{i=1}^{i_0}(D_i)^{-\gamma}}. \tag{2.8}$$

Considering only the first layer of interfering cells, if all the interfering base stations are equidistant from the desired base station and if this distance is equal to the distance D between cell centers, then Equation 2.8 simplifies to

$$\frac{S}{I} = \frac{(D/R)^{\gamma}}{i_0} = \frac{(\sqrt{3N})^{\gamma}}{i_0} \tag{2.9}$$

Equation 2.9 relates S/I to the cluster size N, which in turn determines the overall capacity of the system from Equation 2.2.

Figure 2.6 highlights the co-channel interference problem in a cellular system if universal frequency reuse is adopted. The figure shows the regions of a cell in various SIR bins of the systems with universal frequency reuse and $f = 1/3$ frequency reuse. The figure is based on a two-tier cellular structure and the free-space pathloss model given in Equation 2.10 with $\gamma = 3.5$. The SIR in most parts of the cell is very low if universal frequency reuse is adopted. The co-channel interference problem can be mitigated if higher frequency reuse is adopted, as shown in Figure 2.6(b). However, as previously emphasized, this improvement in the quality of communication is

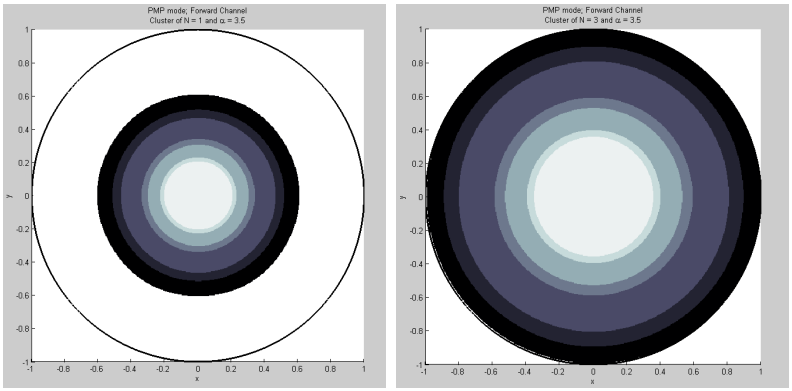

(a) Universal frequency reuse, $FRF = 1$ (b) Frequency reuse, $FRF = 1/3$

Figure 2.6: The received SIR in a cell using AMC with pathloss exponent $\gamma = 3.5$. Darker color indicates lower SIR

achieved at the sacrifice of spectral efficiency: In this case, the available bandwidth is cut by a factor of 3. Frequency planning is a delicate balancing act of using the highest reuse factor possible while still having most of the cell have at least some minimum SIR.

Adjacent Channel Interference

Interference resulting from signals which are adjacent in frequency to the desired signal is called *adjacent channel interference*. Adjacent channel interference results from imperfect receiver filters which allow nearby frequencies to leak into the passband [10]. The problem can be particularly serious if an adjacent channel user is transmitting in very close range to a subscriber's receiver, the *near-far* effect, where a nearby transmitter (which may or may not be of the same type as that used by the cellular system) captures the receiver of the subscriber. Alternatively, the near-far effect occurs when a mobile close to a base station transmits on a channel close to one being used by a weak mobile. The base station may have difficulty in discriminating the desired mobile user form the "bleedover" caused by the close adjacent channel mobile.

Adjacent channel interference can be minimized through careful filtering and channel assignments. Since each cell is given only a fraction of the available channels, a cell need not be assigned channels which are all adjacent in frequency. By keeping the frequency separation between each channel in a given cell as large as possible, the adjacent channel interference may be reduced considerably [10].

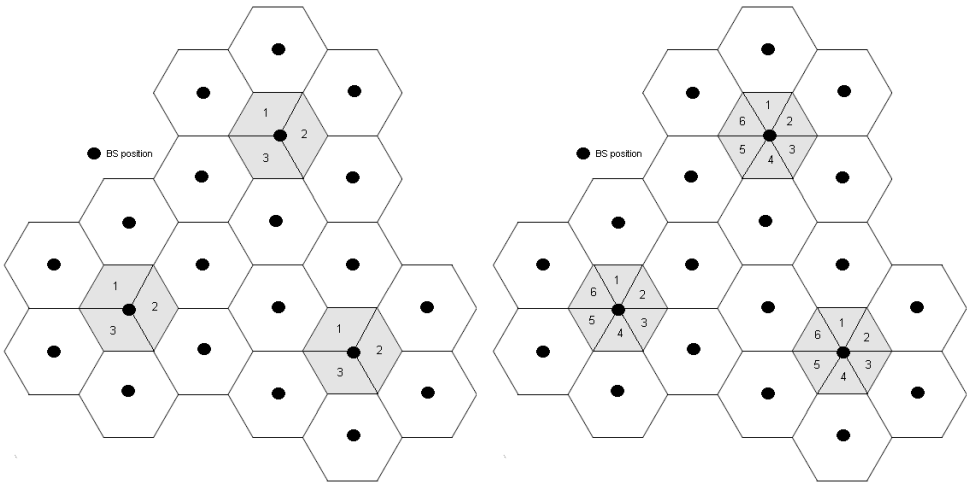

(a) Three-sector (120°) cells (b) Six-sector (60°) cells

Figure 2.7: Illustration of sectoring

2.2.3. Sectoring

Since the SIR is so low in most of the cell, it is desirable to find techniques to improve it without sacrificing so much bandwidth, as frequency reuse does. A popular technique is to sectorize the cells, which is effective if frequencies are reused in each cell. Using directional antennas instead of an omnidirectional antenna at the base station can significantly reduced the co-channel interference. An illustration of sectoring is shown in Figure 2.7. Although the absolute amount of bandwidth used is three times before (assuming three sector cells), the capacity increase is in fact more than three times. No capacity is lost from sectoring, because each sector can reuse time and code slots, so each sector has the same nominal capacity as an entire cell. Furthermore, the capacity in each sector is higher than that in a nonsectored cellular system, because the interference is reduced by sectoring, since users experience only interference from the sectors at their frequency. In Figure 2.7(a), if each sector 1 points in the same direction in each cell, the interference caused by neighboring cells will be dramatically reduced. An alternative way to use sectors, not shown in Figure 2.7, is to reuse frequencies in each sector. In this case, all the time/code/frequency slots can be reused in each sector, but there is no reduction in the experienced interference.

Figure 2.8 shows the regions of a three-sector cell in various SIR bins of the sys-

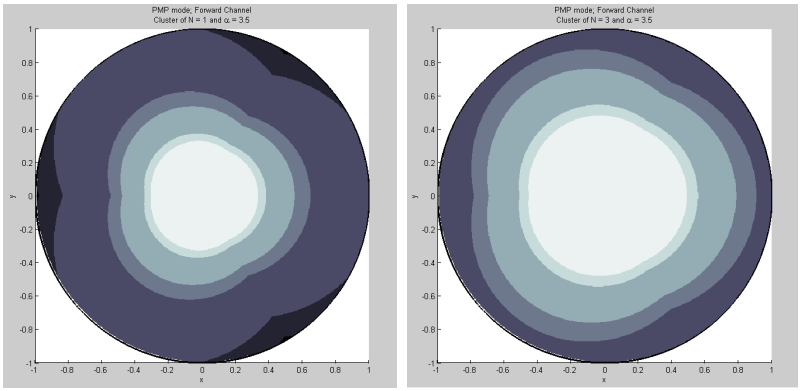

(a) Universal frequency reuse, $FRF = 1$ (b) Frequency reuse, $FRF = 1/3$

Figure 2.8: The received SIR in a sectorized cell (three sectors) using AMC with pathloss exponent $\gamma = 3.5$. Darker color indicates lower SIR

tems with universal frequency reuse and 1/3 frequency reuse. All the configurations are the same as those of Figure 2.6 except that sectoring is added. Compared to Figure 2.6, sectoring improves SIR, especially at the cell boundaries, even when universal frequency reuse is adopted. If sectoring is adopted with frequency reuse, the received SIR can be significantly improved, as shown in Figure 2.8(b), where both $f = 1/3$ frequency reuse and 120° sectoring are used.

Although sectoring is an effective and practical approach to the OCI problem, it is not without cost. Sectoring increases the number of antennas at each base station and reduces trunking efficiency, owing to channel sectoring at the base station. Even though intersector handoff is simpler than intercell handoff, sectoring also increases the overhead, owing to the increased number of intersector handoffs. Finally, in channels with heavy scattering, desired power can be lost into other sectors, which can cause inter-sector interference as well as power loss.

2.3. Propagation model

The mechanism behind electromagnetic wave propagation are diverse, but can generally be attributed to reflection, diffraction, and scattering. Most cellular radio systems operate in urban areas where there is no direct line-of-sight path between the transmitter and the receiver, and where the presence of high-rise buildings causes severe

diffraction loss.

Propagation models have traditionally focused on predicting the average received signal strength at a given distance from the transmitter, as well as the variability of the signal strength in close spatial proximity to a particular location. Propagation models that predict the mean signal strength for an arbitrary transmitter-receiver (T-R) separation distance are useful in estimating radio coverage area of a transmitter and are called *large-scale* propagation models, since they characterize signal strength over large T-R separation distances (several hundreds or thousands of meters). On the other hand, propagation models that characterize the rapid fluctuations of the received signal strength over very short travel distances (a few wavelengths) or short time durations (on the order of seconds) are called *small-scaled* or *fading* models.

2.3.1. Free Space Propagation Model

The free space propagation model is used to predict received signal strength when the transmitted and receiver have a clear, unobstructed line-of-sight path between them. Satellite communication systems and microwave line-of-sight radio links typically undergo free space propagation. As with most large-scale radio wave propagation models, the free space model predicts that received power decays as a function of the T-R separation distance raised to some power (i.e. a power law function). The free space power received by a receiver antenna which is separated from a radiating transmitter antenna by a distance d, is given by the *free-space pathloss formula*,or Friis equation,

$$P_r(d) = \frac{P_t G_t G_r \lambda^2}{(4\pi)^2 d^2 L} \tag{2.10}$$

where P_t is the transmitted power, $P_r(d)$ is the received power which is a function of the T-R separation, G_t is the transmitter antenna gain, G_r is the receiver antenna gain, d is the T-R separation distance in meters, L is the system loss factor not related to propagation ($L \geq 1$), and λ is the wavelength in meters [10]. The gain of an antenna is related to its effective aperture, A_e, by

$$G = \frac{4\pi A_e}{\lambda^2} \tag{2.11}$$

The effective aperture A_e is related to the physical size of the antenna, and λ is related to the carrier frequency by

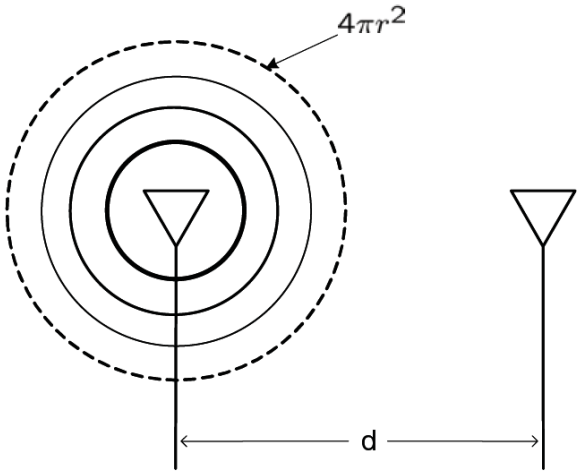

Figure 2.9: Free-space propagation

$$\lambda = \frac{c}{f} = \frac{2\pi c}{\omega_c} \tag{2.12}$$

where f is the carrier frequency in Hertz, ω_c is the carrier frequency in radians per second, and c is the speed of light given in meters/s. The values for P_t and P_r must be expressed in the same units, and G_t and G_r are dimensionless quantities. The miscellaneous losses L ($L \geq 1$) are usually due to transmission line attenuation, filter losses, and antenna losses in the communication system. A value of $L = 1$ indicates no loss in the system hardware [10].

The Friis free space equation of 2.10 shows that the received power falls off as the square of the T-R separation distance. This implies that the received power decays with distance at a rate of 20 dB/decade [10].

An isotropic radiator is an ideal antenna which radiates power with unit gain uniformly in all direction, and is often used to reference antenna gains in wireless systems. The effective isotropic radiated power ($EIRP$) is defined as

$$EIRP = P_t G_t \tag{2.13}$$

and represents the maximum radiated power available from a transmitter in the direction of maximum antenna gain, as compared to an isotropic radiator [10].

In practice, effective radiated power (ERP) is used instead of $EIRP$ to denote

the maximum radiated power as compared to a half-wave dipole antenna (instead of an isotropic antenna). Since a dipole antenna has a gain of 1.64 (2.15 dB above an isotrope), the *ERP* will be 2.15 dB smaller than the *EIRP* for the same transmission system. In practice, antenna gains are given in units of dBi (dB gain with respect to an isotropic antenna) or dBd (dB gain with respect to a half-wave dipole [12].

[10] The path loss, which represents signal attenuation as a positive quantity measured in dB, is defined as the difference (in dB) between the effective transmitted power and the received power, and may or may not include the effect of the antenna gains. The path loss for the free space model when antenna gains are included is given by

$$PL(dB) = 10\log_{10}\frac{P_t}{P_r} = -10\log_{10}\frac{G_t G_r \lambda^2}{(4\pi)^2 d^2} \tag{2.14}$$

when antenna gains are excluded, the antennas are assumed to have unity gain, and path loss is given by

$$PL(dB) = 10\log_{10}\frac{P_t}{P_r} = -10\log_{10}\frac{\lambda^2}{(4\pi)^2 d^2} \tag{2.15}$$

The Friis free space model is only a valid predictor for P_r for values of d which are in the far-field of the transmitting antenna. The far-field, of Fraunhofer region, of a transmitting antenna is defined as the region beyond the far-field distance d_f, which is related to the largest linear dimension of the transmitter antenna aperture and the carrier wavelength [10]. The Fraunhofer distance is given by

$$d_f = \frac{2D^2}{\lambda} \tag{2.16}$$

where D is the largest physical dimension of the antenna. Additionally, to be in the far-field region, d_f must satisfy

$$d_f \gg D \tag{2.17}$$

and

$$d_f \gg \lambda \tag{2.18}$$

Furthermore, it is clear that Equation 2.10 does not hold for $d = 0$. For this reason, large-scale propagation models use a close-in distance, d_0, as a known received power reference point. The received power, $P_r(d)$, at any distance $d > d_0$, may be related to

P_r at d_0. The value $P_r(d_0)$ may be predicted from Equation 2.10, or may be measured in the radio environment by taking the average received power at many points located at a close-in radial distance d_0 from the transmitter. The reference distance must be chosen such that it lies in the far-field region, that is, $d_0 \geq d_f$, and d_0 is chosen to be smaller than any practical distance used in the mobile communication system [10]. Thus, using Equation 2.10, the received power in free space at a distance greater than d_0 is given by

$$P_r(d) = P_r(d_0)\left(\frac{d_0}{d}\right)^2 \quad d \geq d_0 \geq d_f \tag{2.19}$$

Where $P_r(d_0)$ is in units of watts [10].

In mobile radio systems, it is not uncommon to find that P_r may change by many orders of magnitude over a typical coverage area of several kilometers. Because of the large dynamic range of received power levels, often dBm or dBW units are used to express received power levels [10]. Equation 2.19 may be expressed in units of dBm or dBW by simply taking the logarithm of both sides and multiplying by 10.

$$P_r(d)dBm = 10\log_{10}\frac{P_r(d_0)}{0.001W} + 20\log_{10}\frac{d_0}{d} \quad d \geq d_0 \geq d_f \tag{2.20}$$

or

$$P_r(d)dBW = 10\log_{10}P_r(d_0) + 20\log_{10}\frac{d_0}{d} \quad d \geq d_0 \geq d_f \tag{2.21}$$

2.3.2. Suburban Path Loss Model (Erceg Model)

The most widely used path loss model for signal strength prediction and simulation in macrocellular environments is the Hata-Okumura model [13, 14]. This model is valid for the 500–1500 MHz frequency range, receiver distances greater than 1 km from the base station, and base station antenna heights greater than 30 m. It was found that these models are not suitable for lower base station antenna heights, and hilly or moderate-to-heavy wooded terrain. To correct for these limitations, it was proposed the model presented in [2]. The model covers three most common terrain categories found across the United States. However, other sub-categories and different terrain types can be found around the world.

The maximum path loss category is hilly terrain with moderate-to-heavy tree densities (Category A). The minimum path loss category is mostly flat terrain with light

tree densities (Category C). Intermediate path loss condition is captured in Category B. The middle category can be characterized as either mostly flat terrain with moderate-to-heavy tree densities, or hilly terrain with light tree densities. This intermediate condition is captured in Category B. The extensive experimental data was collected by AT&T Wireless Services across the United States in 95 existing macrocells at 1.9 GHz. For a given close-in reference distance d_0, the median path loss (PL in dB) is given by

$$PL = A + 10\gamma \log(d/d_0) + s \quad \text{for } d > d_0 \tag{2.22}$$

where $A = 20\log(4\pi d_0/\lambda)$ (λ being the wavelength in m), γ is the path-loss exponent, $d_0 = 100$m.

The path loss exponent γ depends on propagation environment, e.g. free space path loss exponent is $\gamma = 2$. The path loss exponent γ is a Gaussian random variable over the population of macrocells within each terrain category [2]. It can be written as

$$\gamma = (a - bh_b + c/h_b) \quad \text{for } 10 \text{ m} \leq h_b \leq 80 \text{ m} \tag{2.23}$$

where h_b is the height of the base station in meters, and a, b and c are constants dependent on the terrain category given in Table 2.3. If the base station antenna heights increased, path loss exponent decreased (see Figure 2.10).

Table 2.3: Numerical Values of Model Parameters [2]

	Terrain type A	Terrain type B	Terrain type C
a	4.6	4	3.6
b	0.0075	0.0065	0.005
c	12.6	17.1	20

The shadowing effect is represented by s, which follows the lognormal distribution. The typical value of the standard deviation for s is between 8.2 and 10.6 dB depending on the terrain/tree density type [2].

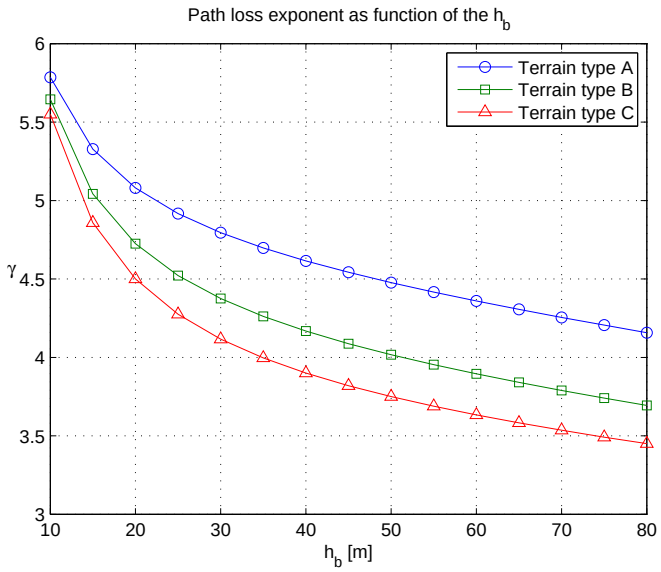

Figure 2.10: Path loss exponent as function of the h_b

Receive Antenna Height and Frequency Correction Terms

The above path loss model is based on published literature for frequencies close to 2 GHz and for receive antenna heights close to 2 m. In order to use the model for other frequencies and for receive antenna heights between 2 m and 10 m, correction terms have to be included. The path loss model (in dB) with the correction terms would be

$$PL_{\text{modified}} = PL + \Delta PL_f + \Delta PL_h \tag{2.24}$$

where PL is the path loss given in Eq. 2.22, ΔPL_f (in dB) is the frequency correction term given by

$$\Delta PL_f = 6\log(f/2000) \tag{2.25}$$

where f is the frequency in MHz, and ΔPL_h (in dB) is the receive antenna height correction term given by

$$\begin{aligned} \Delta PL_h &= -10.8\log(h/2) \quad \text{for Categories A and B} \\ \Delta PL_h &= -20\log(h/2) \quad \text{for Category C} \end{aligned} \tag{2.26}$$

where h is the receive antenna height between 2 m and 10 m.

2.4. Digital Modulation, OFDM and OFDMA

2.4.1. Digital Modulations

Digital modulation involves choosing a particular signal waveform $s_i(t)$, from a finite set of possible signal waveforms (or symbols) based on the information bits applied to the modulator. If there are a total of M possible signals, the modulation signal set S can be represented as

$$S = s_1(t), s_2(t), \ldots, s_M(t) \tag{2.27}$$

For binary modulation schemes, a binary information bit is mapped directly to a signal and S will contain only two signals. For higher modulation schemes (M-ary keying) the signal set will contain more than two signals, and each signal (or symbol) will represent more than a single bit of information. With a signal set of size M, it is possible to transmit a maximum of $\log_2 M$ bits of information per symbol [10].

The constellation diagram is geometrically representation of the signal set which provides a graphical representation of the complex envelope of each possible symbol state. The x-axis of a constellation diagram represents the in-phase component of the complex envelope, and the y-axis represents the quadrature component of the complex envelope. The distance between signals on the constellation diagram relates to how different the modulation waveforms are, and how well a receiver can differentiate between all possible symbols when random noise is present [10].

Some of the properties of a modulation scheme can be inferred from its constellation diagram. For example, the bandwidth occupied by the modulation signals decreases as the number of signal points increases. Therefore, if a modulation scheme has a constellation that is densely packed, it is more bandwidth efficient than a modulation scheme with a sparsely packed constellation.

The probability of bit error is proportional to the distance between the closest points in the constellation. This implies that a modulation scheme with a constellation that is densely packed is less energy efficient than a modulation scheme that has a sparse constellation.

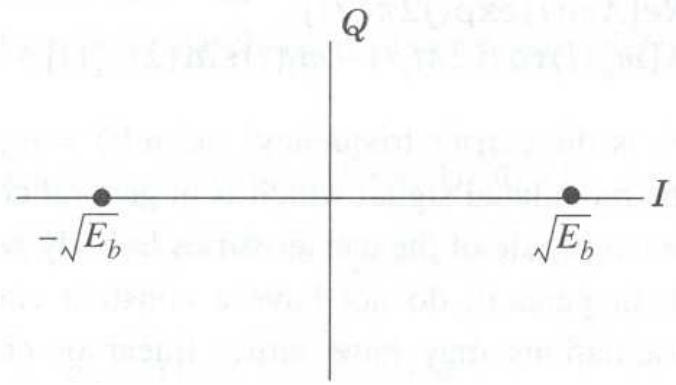

Figure 2.11: The BPSK constellation

Binary Phase Shift Keying (BPSK)

The BPSK is a binary digital modulation; i.e. one modulation symbol is one bit. This gives high immunity against noise and interference an a very robust modulation. A digital phase modulation, which is the case for BPSK modulation, uses phase variation to encode bits: each modulation symbol is equivalent to one phase. The phase of the BPSK modulated signal is π or $-\pi$ according to the value of the data bit. An often used illustration for digital modulation is the constellation. Figure 2.11 shows the BPSK constellation; the values that the signal phase can take are 0 to π.

Quadrature Phase Shift Keying (QPSK)

When a higher spectral efficiency modulation is needed, i.e. more b/s/Hz, greater modulation symbols can be used. For example, QPSK considers two-bit modulation symbols. Table 2.4 shows the possible phase values as function of the modulation symbol. Many variants of QPSK can be used but QPSK always has four-point constellation (see Figure 2.12). The decision at the receiver, e.g. between symbol '00' and symbol '01', is less easy than decision between '0' and '1'. The QPSK modulation is therefore less nose-resistant than BPSK as it has a smaller immunity against interference. A well-known digital communication principle must be kept in mind: 'A greater data symbol modulation is more spectrum efficient but also less robust.'

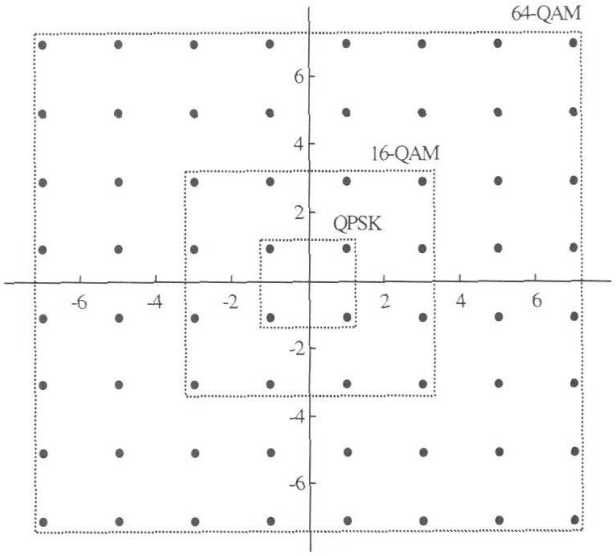

Figure 2.12: Constellation diagram for QPSK, 16QAM and 64QAM modulation

Table 2.4: Possible phase values for QPSK modulation

Even Bits	Odd bits	Modulation symbol	φ_k
0	0	00	$\pi/4$
1	0	01	$3\pi/4$
1	1	11	$5\pi/4$
0	1	10	$7\pi/4$

Quadrature Amplitude Modulation (QAM): 16-QAM and 64-QAM

The QAM changes the amplitude of two sinusoidal carriers depending on the digital sequence that must be transmitted; the two carriers being out of phase of $+\pi/2$, this amplitude modulation is called quadrature. It should be mentioned that according to digital communication theory, QAM-4 and QPSK are the same modulation (considering complex data symbols). Both 16-QAM (4 bits/modulation symbol) and 64-QAM (6 bits/modulation symbol) modulations are included in the IEEE 802.16 standard. The 64-QAM is the most efficient modulation of 802.16 (see Figure 2.12). Indeed, 6 bits are transmitted with each modulation symbol.

The 64-QAM modulation is optional in some cases:

- license-exempt bands, when the OFDM PHYsical Layer is used
- for OFDMA PHY, yet the Mobile WiMAX profiles indicates that 64-QAM is mandatory in the downlink

Adaptive Modulation and Coding in WiMAX

WiMAX supports a variety of modulation and coding schemes and allows for the scheme to change on a burst-by-burst basis per link, depending on channel conditions. Using the channel-quality feedback indicator, the mobile can provide the base station with feedback on the downlink channel quality. For the uplink, the base station can estimate the channel quality, based on the received signal quality. The base station scheduler can take into account the channel quality of each user's uplink and downlink and assign a modulation and coding scheme that maximizes the throughput for the available signal-to-noise ratio. Adaptive modulation and coding significantly increases the overall system capacity, as it allows real-time trade-off between throughput and robustness on each link.

The principle of link adaptation is rather simple: when the radio link is good, use a high-level modulation; when the radio link is bad, use a low-level, but also robust, modulation. Figure 2.13 shows this principle, illustrating the fact that the radio channel is better when an SS is close to the BS. Another dimension is added to this figure when the coding rate is also changed.

Table 2.5 lists the various modulation and coding schemes supported by WiMAX. In the downlink, QPSK, 16 QAM, and 64 QAM are mandatory for both fixed and mobile WiMAX; 64 QAM is optional in the uplink. FEC coding using convolutional codes is mandatory. Convolutional codes are combined with an outer Reed-Solomon code in the downlink for OFDM-PHY. The standard optionally supports turbo codes and low-density parity check (LDPC) codes at a variety of code rates as well. A total of 52 combinations of modulation and coding schemes are defined in WiMAX as burst profiles.

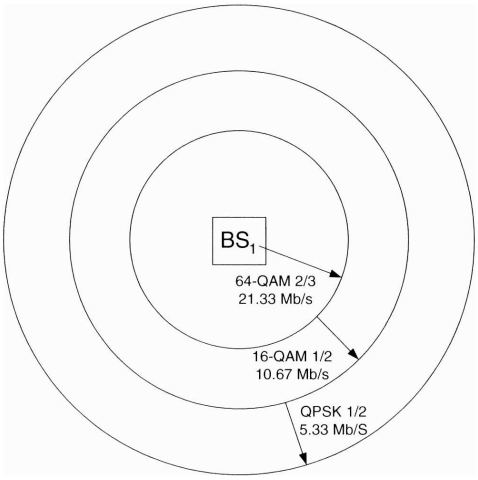

Figure 2.13: Illustration of link adaptation. A good radio channel corresponds to a high-efficiency Modulation and Coding Scheme (MCS)

Table 2.5: Modulation and Coding Supported in WiMAX

	Downlink	Uplink
Modulation	BPSK, QPSK, 16 QAM, 64 QAM; BPSK optional for OFDMA-PHY	BPSK, QPSK, 16 QAM; 64 QAM optional
Coding	Mandatory: convolutional codes at rate 1/2, 2/3, 3/4, 5/6 Optional: convolutional turbo codes at rate 1/2, 2/3, 3/4, 5/6; repetition codes at rate 1/2, 1/3, 1/6, LDPC, RS-Codes for OFDM-PHY	Mandatory: convolutional codes at rate 1/2, 2/3, 3/4, 5/6 Optional: convolutional turbo codes at rate 1/2, 2/3, 3/4, 5/6; repetition codes at rate 1/2, 1/3, 1/6, LDPC

The choice between different burst profiles or, equivalently, between different MCSs is a powerful tool. Specifically, choosing the MCS most suitable for the state of the radio channel, at each instant, leads to an optimal (highest) average data rate. The link adaptation algorithm itself is not indicated in the 802.16 standard. It is left to the vendor or operator.

Table 2.6: Received SNR threshold assumptions. (Table 266 from [3])

Modulation	Coding Rate	Receiver SNR (dB)
BPSK	1/2	3.0
QPSK	1/2	6.0
QPSK	3/4	8.5
16-QAM	1/2	11.5
16-QAM	3/4	15.0
64-QAM	2/3	19.0
64-QAM	3/4	21.0

The order of magnitudes of SNR thresholds can be obtained from Table 2.6, proposed in the standard for some test conditions. These SNR thresholds are for a BER, Bit-Error Rate, measured after the FEC, that is smaller than 10^{-6}.

2.4.2. OFDM Transmission

OFDM is a very powerful transmission technique. It is based on the principle of transmitting simultaneously many narrow-band orthogonal frequencies, often also called OFDM subcarriers or subcarriers. The number of subcarriers is often noted N. These frequencies are orthogonal to each other which (in theory) eliminates the interference between channels. Each frequency channel is modulated with a possibly different digital modulation. The frequency bandwidth associated with each of these channels is then much smaller than if the total bandwidth was occupied by a single modulation (Single Carrier) [8].

Basic Principle

The basic principle of OFDM is to split a high-rate datastream into a number of lower rate streams that are transmitted simultaneously over a number of subcarriers. Because the symbol duration increases for the lower rate parallel subcarriers, the relative amount of dispersion in time caused by multipath delay spread is decreased. Intersymbol interference (ISI) is eliminated almost completely by introducing a guard time in every OFDM symbol. In the guard time, the OFDM symbol is cyclically ex-

tended to avoid intercarrier interference [15].

The FFT is the Fast Fourier Transform operator. This is a matrix computation that allows the discrete Fourier transform to be computed (while respecting certain conditions). The FFT works for any number of points but the operation is simpler when applied for a number N which is a power of 2 (e.g. $N = 256$). The IFFT is the Inverse Fast Fourier Transform operator and realizes the reverse operation. OFDM theory (see, for example, Reference [15]) shows that the IFFT of magnitude N, applied on N symbols, realizes an OFDM signal, where each symbol is transmitted on one of the N orthogonal frequencies. The symbols are the data symbols of the type BPSK, QPSK, QAM-16 and QAM-64 introduced in the previous section.

OFDM Pros and Cons

OFDM enjoys several advantages over other solutions for high-speed transmission.

- **Reduced computational complexity:** OFDM can be easily implemented using FFT/IFFT, and the processing requirements grow only slightly faster than linearly with data rate or bandwidth. The computational complexity of OFDM can be shown to be $O(B \log BT_m)$, where B is the bandwidth and T_m is the delay spread. This complexity is much lower than that of a standard equalizer-based system, which has a complexity $O(B^2T_m)$.
- **Graceful degradation of performance under excess delay:** The performance of an OFDM system degrades gracefully as the delay spread exceeds the value designed for. Greater coding and low constellation sizes can be used to provide fallback rates that are significantly more robust against delay spread. In other words, OFDM is well suited for adaptive modulation and coding, which allows the system to make the best of the available channel conditions. This contrasts with the abrupt degradation owing to error propagation that single-carrier systems experience as the delay spread exceeds the value for which the equalizer is designed.
- **Exploitation of frequency diversity:** OFDM facilitates coding and interleaving across subcarriers in the frequency domain, which can provide robustness against burst errors caused by portions of the transmitted spectrum undergoing deep fades. In fact, WiMAX defines subcarrier permutations that allow systems to exploit this.

- **Use as a multiaccess scheme**: OFDM can be used as a multiaccess scheme, where different tones are partitioned among multiple users. This scheme is referred to as OFDMA and is exploited in mobile WiMAX. This scheme also offers the ability to provide fine granularity in channel allocation. In relatively slow time-varying channels, it is possible to significantly enhance the capacity by adapting the data rate per subscriber according to the signal-to-noise ratio of that particular subcarrier.
- **Robust against narrowband interference:** OFDM is relatively robust against narrowband interference, since such interference affects only a fraction of the subcarriers.
- **Suitable for coherent demodulation:** It is relatively easy to do pilot-based channel estimation in OFDM systems, which renders them suitable for coherent demodulation schemes that are more power efficient.

Despite these advantages, OFDM techniques also face several challenges. First, there is the problem associated with OFDM signals having a high peak-to-average ratio that causes nonlinearities and clipping distortion. This can lead to power inefficiencies that need to be countered. Second, OFDM signals are very susceptible to phase noise and frequency dispersion, and the design must mitigate these imperfections. This also makes it critical to have accurate frequency synchronization.

OFDM symbol parameters and some simple computations

The choice of various OFDM parameters is a tradeoff between various, often conflicting requirements. Usually, there are three main requirements to start with: bandwidth, bit rate, and delay spread. The delay spread directly dictates the guard time. As a rule, the guard time should be about two or four times the root-mean-squared delay spread [15]. This value depends on the type of coding and QAM modulation. Higher order QAM (like 64-QAM) is more sensitive to ICI and ISI than QPSK; while heavier coding obviously reduces the sensitivity to such interference.

Now that the guard time has been set, the symbol duration can be fixed. To minimize the signal-to-noise ratio (SNR) loss caused by the guard time, it is desirable to have the symbol duration much larger than the guard time. It cannot be arbitrarily large, however, because a larger symbol duration means more subcarriers with a smaller subcarrier spacing, a larger implementation complexity, and more sensitivity to phase

noise and frequency offset, as well as an increased peak-to-average power ratio. Hence, a practical design choice is to make the symbol duration at least five times the guard time, which implies a 1-dB SNR loss because of the guard time [15].

After the symbol duration and guard time are fixed, the number of subcarriers follows directly as the required -3dB bandwidth divided by the subcarrier spacing, which is the inverse of the symbol duration less the guard time. Alternatively, the number of subcarriers may be determined by the required bit rate divided by the bit rate per subcarrier. The bit rate per subcarrier is defined by the modulation type (e.g., 16-QAM), coding rate, and symbol rate.

For WiMAX OFDM, the symbol parameters are the following:

- The total number of subcarriers or, equivalently, the IFFT magnitude. For OFDM PHY, $N_{FFT} = 256$, the number of lower-frequency guard subcarriers is 28 and the number of higher-frequency guard subcarriers is 27. Considering also the DC subcarrier, there remains N_{used}, the number of used subcarriers, excluding the null subcarriers. Hence $N_{used} = 200$ for OFDM PHY, of which 192 are used for useful data transmission, after deducing the pilot subcarriers.
- BW, the nominal channel bandwidth
- n, the sampling factor.

The sampling frequency, denoted f_s, is related to the occupied channel bandwidth by the following (simplified) formula:

$$f_s = n\text{BW} \tag{2.28}$$

This is a simplified formula because, according to the standard, f_s is truncated to an 8kHz multiple. According to the 802.16 standard, the numerical value of n depends of the channel bandwidths. Possible values are 8/7, 86/75, 144/125, 316/275 and 57/50 for OFDM PHY and 8/7 and 28/25 for OFDMA PHY.

Based on the above-defined parameters, the time duration of an OFDM symbol can be computed:

$$\text{OFDM symbol duration} = \text{useful symbol time} + \text{guard time (CP time)}$$

$$\begin{aligned} &= 1/(\text{one subcarrier spacing}) + \text{G} \times \text{useful symbol time} \\ &= (1/\Delta f)(1+\text{G}) \\ &= [1/(f_s/N_{FFT})](1+\text{G}) \\ &= [1/(n\text{BW}/N_{FFT})](1+\text{G}) \end{aligned} \tag{2.29}$$

The OFDM symbol duration is a basic parameter for data rate computations. In OFDM PHY, one OFDM symbol represents 192 subcarriers, each transmitting a modulation data symbol. One can then compute the number of data transmitted for the duration of an OFDM symbol (which value is already know). Knowing the coding rate, the number of uncoded bits can be computed. Table 2.7 shows the data rates for different Modulation and Coding Schemes (MCSs) and G values. The occupied bandwidth considered is 7 MHz and the sampling factor is 8/7 (the value corresponding to 7 MHz according to the standard).

Consider the following case in Table 2.7: 16-QAM, coding rate = 3/4 and G = 1/16. It can be verified that the data rate is equal to:

$$\begin{aligned} \text{Data rate} &= \text{number of uncoded bits per OFDM symbol/OFDM symbol duration} \\ &= 192 \times 4 \times (3/4)/[256/(7\text{MHz} \times 8/7)](1+1/16) \\ &= 16.94 \text{ Mb/s} \end{aligned} \tag{2.30}$$

Table 2.7: OFDM PHY data rates in Mb/s. [4]

G ratio	BPSK 1/2	QPSK 1/2	QPSK 3/4	16-QAM 1/2	16-QAM 3/4	64-QAM 2/3	64-QAM 3/4
1/32	2.92	5.82	8.73	11.64	17.45	23.27	26.18
1/16	2.82	5.65	8.47	11.29	16.94	22.59	25.41
1/8	2.67	5.33	8.00	10.67	16.00	21.33	24.00
1/4	2.40	4.80	7.20	9.60	14.40	19.20	21.60

It should be noted here that these data rate values do not take into account some overheads such as preambles (of the order of one or two OFDM symbols per frame) and signaling messages present in every frame. Hence these data rates, known as raw

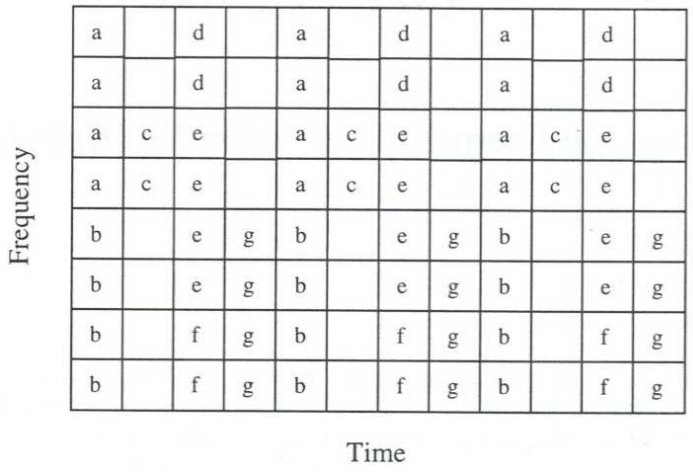

Figure 2.14: Example of the time-frequency grid with seven OFDMA users, a to g, which all have a fixed set of subcarriers every four timeslots

data rates, are optimistic values.

2.4.3. OFDMA

The OFDM transmission mode was originally designed for a single signal transmission. Thus, in order to have multiple user transmissions, a multiple access scheme such as TDMA or FDMA has to be associated with OFDM. In fact, an OFDM signal can be made from many user signals, giving the OFDMA (Orthogonal Frequency Division Multiple Access) multiple access.

An example of an OFDMA time-frequency grid is shown in Figure 2.14, where seven users a to g each use a certain fraction—which may be different for each user—of the available subcarriers. This particular example in fact is a mixture of OFDMA and Time Division Multiple Access (TDMA), because each user only transmits in one out of every four timeslots, which may contain one or several OFDM symbols [15].

In OFDMA, the OFDMA subcarriers are divided into subsets of subcarriers, each subset representing a subchannel (see Figure 2.15). In the downlink, a subchannel may be intended for different receivers or groups of receivers; in the uplink, a transmitter may be assigned one or more subchannels. The subcarriers forming one subchannel may be adjacent or not. The standard indicates that the OFDM symbol is divided

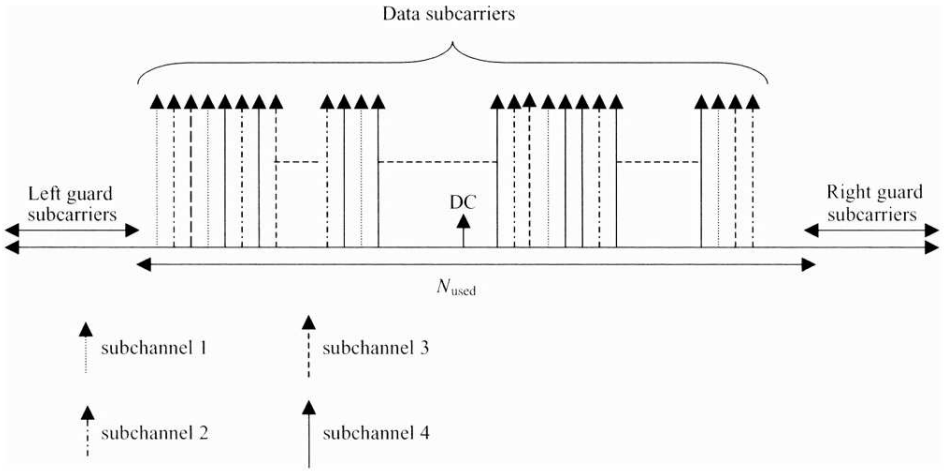

Figure 2.15: Illustration of the OFDMA principle

into logical subchannels to support scalability, multiple access and advance antenna array processing capabilities. The multiple access has a new dimension with OFDMA. A downlink or an uplink user will have a time and a subchannel allocation for each of its communications. Different subchannel distributions and logical renumberings are defined in the 802.16 standard [8].

Subchannelization: OFDMA

The available subcarriers may be divided into several groups of subcarriers called subchannels. Fixed WiMAX based on OFDM-PHY allows a limited form of subchannelization in the uplink only. The standard defines 16 subchannels, where 1, 2, 4, 8, or all sets can be assigned to a subscriber station (SS) in the uplink. Uplink subchannelization in fixed WiMAX allows subscriber stations to transmit using only a fraction (as low as 1/16) of the bandwidth allocated to it by the base station, which provides link budget improvements that can be used to enhance range performance and/or improve battery life of subscriber stations. A 1/16 subchannelization factor provides a 12 dB link budget enhancement.

Mobile WiMAX based on OFDMA-PHY, however, allows subchannelization in both the uplink and the downlink, and here, subchannels form the minimum frequency resource-unit allocated by the base station. Therefore, different subchannels may be allocated to different users as a multiple-access mechanism. This type of multiaccess

scheme is called orthogonal frequency division multiple access (OFDMA), which gives the mobile WiMAX PHY its name.

Subchannels may be constituted using either contiguous subcarriers or subcarriers pseudorandomly distributed across the frequency spectrum. Subchannels formed using distributed subcarriers provide more frequency diversity, which is particularly useful for mobile applications. WiMAX defines several subchannelization schemes based on distributed carriers for both the uplink and the downlink. One, called partial usage of subcarriers (PUSC), is mandatory for all mobile WiMAX implementations. The initial WiMAX profiles define 15 and 17 subchannels for the downlink and the uplink, respectively, for PUSC operation in 5MHz bandwidth. For 10MHz operation, it is 30 and 35 channels, respectively.

The subchannelization scheme based on contiguous subcarriers in WiMAX is called band adaptive modulation and coding (AMC). Although frequency diversity is lost, band AMC allows system designers to exploit multiuser diversity, allocating subchannels to users based on their frequency response. Multiuser diversity can provide significant gains in overall system capacity, if the system strives to provide each user with a subchannel that maximizes its received SINR. In general, contiguous subchannels are more suited for fixed and low-mobility applications.

Chapter 3

WiMAX Deployment Considerations

3.1. Licensed Spectrum for Wireless MANs

This work will focus on deployments using licensed spectrum in the 2.5 GHz and 3.5 GHz frequency bands. Although both the 3.5 GHz Band and the 2.5 GHz Band are not universally available worldwide for fixed wireless access, at least one the two bands is available in most every major country.

3.1.1. 3.5 GHz Band

The "3.5 GHz" band is available as a licensed band in many countries outside the United States for fixed broadband wireless access. Although the regulations for deployment and specific allocations vary considerably country by country, this band is undoubtedly the most used spectrum for wireless metropolitan area networks (MANs) today.

Typical characteristics for the 3.5 GHz band based on a limited country by country survey are:

Total available spectrum: Varies country by country but generally about 200 MHz between 3.4 GHz and 3.8 GHz

Services allowed: Fixed access is usually specified

FDD or TDD: This is mixed, some countries specify FDD only while other allow either FDD or TDD

Spectrum per license: Varies from 2×5 MHz to 2×56 MHz

License aggregation: Some countries allow license aggregation operators to gain access to more spectrum, others do not allow aggregation

3.1.2. 2.5 GHz Band

This band is allocated for fixed microwave services in many countries including the United States. Although many of these countries have rules which do not support two-way services it is expected that this will change as WiMAX equipment becomes more readily available worldwide and operators lobby for more licensed spectrum for both fixed and mobile broadband services. In the United States the FCC modified the rules for this band in 1998 to allow two-way services and in mid-2004, announced a realignment of the channel plan. With these rule modifications, this band is now well suited to a WiMAX-based deployment and makes up for the fact that the 3.5 GHz band is not available for wireless access in the United States. The following details for the 2.5 GHz band is based on the most recent FCC rules.

Total available spectrum: Total of 195 MHz, including guard-bands and MDS channels, between 2.495 GHz and 2.690 GHz

Services allowed: Fixed two-way or broadcast

FDD or TDD: Both TDD and FDD are allowed

Spectrum per license: 22.5 MHz per license, a 16.5 MHz block paired with a 6 MHz block, a total of 8 licenses

License aggregation: Operators can acquire multiple licenses in one geographical area to increase spectrum holdings

3.2. PMP Deployment Scenarios

The analysis will focus on deployments using licensed spectrum in the 2.5 GHz and 3.5 GHz frequency bands. In the 2.5 GHz band, a time division duplex (TDD) solution with a 5 MHz channel bandwidth will be used and in the 3.5 GHz band a frequency

Table 3.1: Relevant Radio Parameters

Attribute	2.5 GHz Band	3.5 GHz Band
Duplexing	TDD	FDD
Channel Bandwidth	5 MHz	2×3.5 MHz
Adaptive Modulation	BPSK, QPSK, 16QAM, 64QAM	
TDD DL/UL Traffic Split	60/40	n/a

division duplex (FDD) solution with dual 3.5 MHz bandwidth channels will be used. These are not the only WiMAX equipment solutions that are expected to be available in these two bands but they are representative and serve the purposes intended for this work. Other expected solutions include a TDD solution for the 3.5 GHZ band with a 7 MHz channel bandwidth and over a period of time, different channel bandwidths will be made available in both bands to provide operators with more deployment options. WiMAX-compliant equipment will also be available in other frequency bands. 5.8 GHz products for example, are anticipated at about the same time as 3.5 GHz and 2.5 GHz products.

For the 2.5 GHz TDD solution, a downlink/uplink traffic split of 60/40 is assumed to reflect what is expected to be a typical traffic pattern for data-centric services. This makes the effective downlink (DL) channel bandwidth 3 MHz and the effective uplink (UL) channel bandwidth 2 MHz. With the same asymmetric traffic split in the FDD case, the 3.5 MHz uplink channel would not be fully utilized. Table 3.1 provides a summary of the key downlink radio characteristics that are used for the interference and capacity estimates that follow in later sections of this thesis.

The propagation model that is used to predict the range is based on contributions to the IEEE 802.16 Broadband Wireless Access Working Group by Erceg, et al [2]. As we said in Chapter 2 this propagation model cover three terrain categories; A, B, and C.

In PMP mode, connections are established among the BS and SS, hence, data transmission between two SSs are routed through the BS. As we said on Chapter 2, PMP is a centralized topology where the BS is the center of the system while in Mesh topology it is not. Figure 3.1 shows the PMP topology that will be analyzed in next chapter.

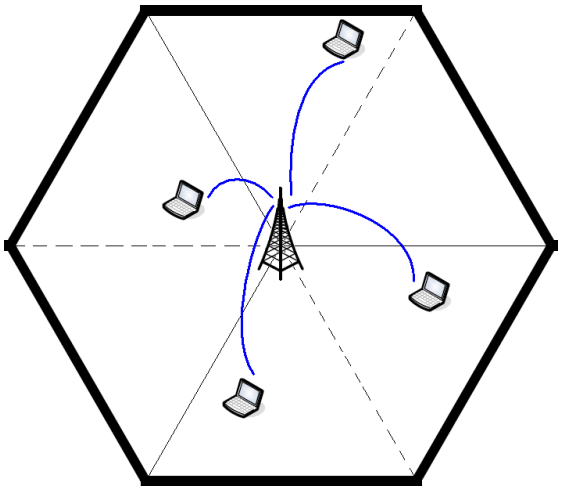

Figure 3.1: Point-to-Multipoint Scenario

3.3. Wireless Mesh Networks

Wireless Mesh Network (WMN) is a self-organizing multihop system formed by user nodes, it can connect and communicate with other user nodes directly without pre-existing infrastructure. WMN provides a reliable and flexible system that can quick-and-easy extended to thousands of devices. The signature of WMN is that each node acts as a relayed point for other nodes instead of being organized by a centralized control device.

For Mesh mode, we are going to use the same radio characteristics of the PMP mode for each hop. A station in the wireless network terms Mesh BS, acts like a BS in PMP mode and interfaces the network to the backhaul links. The MAC protocol for the Mesh mode has been designed to support both centralized (Mesh CS) and distributed (Mesh DS) scheduling.

The positioning of relay stations may vary according to the intended benefit. Two different scenarios are distinguished in the following.

- *Coverage scenario*
  In order to extend the coverage area of the cell, relays may be placed at the border of the BSs transmission range. The distance between the BS and the relay equals the original BS cell radius R. Figure 3.2(a) illustrates such scenario. It plots

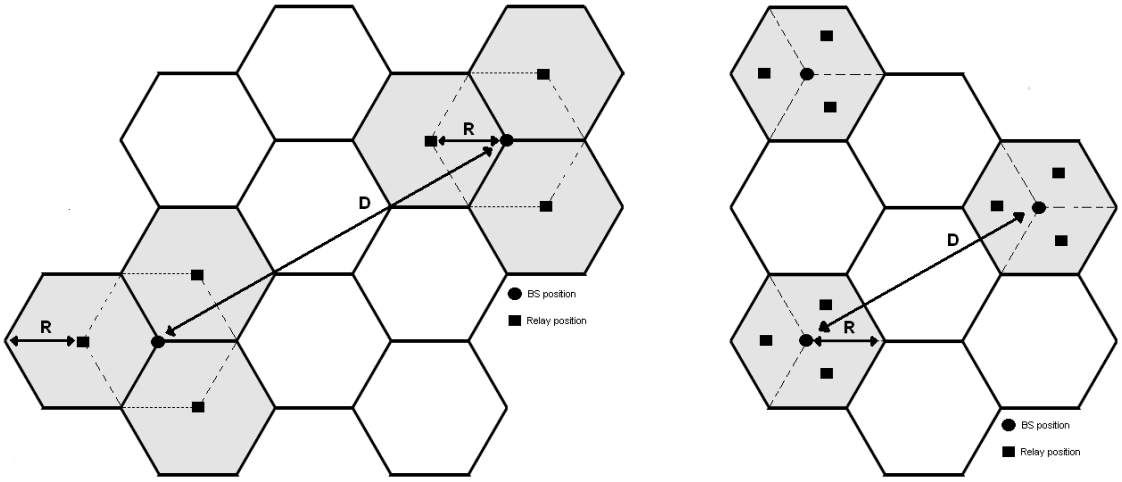

(a) Coverage Scenario (b) Throughput Scenario

Figure 3.2: Two different scenarios for relay positioning

the BSs coverage are with dashed lines. Three relays at the corners extend the coverage area of a singlehop deployment $A_{singlehop}$ by a factor of three.

$$A_{multihop} = 3\frac{3}{2}\sqrt{3}R^2 = 3 * A_{singlehop} \tag{3.1}$$

Due to the extended coverage of a relay enchanced cell, the co-channel distance is enlarged by a factor of $\sqrt{3}$ in these scenarios. Assuming a cluster order of k, the co-channel distance of the coverage scenarios can be calculated to $D = 3R\sqrt{k}$.

- *Throughput scenario*
  Placing relays within the BS's coverage, the CINR and therewith the link capacity is increased. The distance between the BS and the relay is half of the cell radius. The co-channel distance can be calculated to $D = R\sqrt{3k}$. From a dimensioning perspective, this scenario equals a singlehop case, since the entire cell area shall be covered by the BS.

Our main purpose is to estimate the interference in a WiMAX system, we model the Mesh mode as a multihop problem where relays foreseen to extend the range of the BS and to increase the cell capacity. We are trying to improve the throughput of the system in order to serve a more users with higher quality of service. For this reason

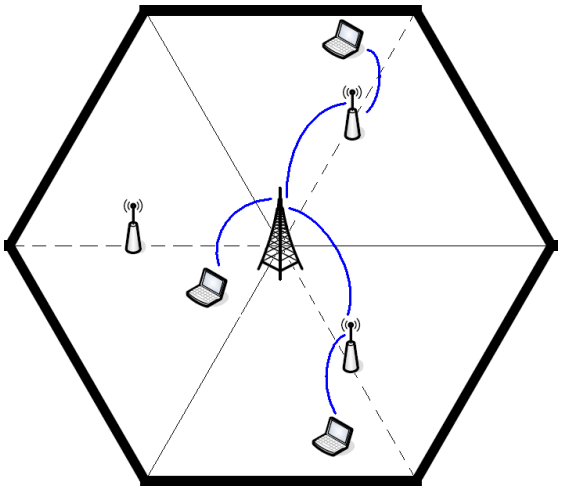

Figure 3.3: Multihop Scenario

the scenario that will analyze is shown in Figure 3.3.

3.4. Deployment Scenarios Based on the U.S. 700 MHz Band

The Mobile WiMAX Release 1.0 Profiles currently cover several frequency bands ranging from 2300 MHz to 3800 MHz. For comparison purposes these bands can be grouped into two categories, 2500 MHz and 3500 MHz. To accommodate the anticipated growth in mobile services and new broadband applications, there is ongoing pressure on regulators to make additional spectrum available for mobile applications. Bands below 1000 MHz are specially interesting due to the improved propagation conditions as compared to 2500 and 3500 MHz.

The frequency band between 470 MHz and 862 MHz has traditionally been allocated worldwide for radio and TV broadcasting and encompasses the UHF TV channels. With the planned transition to digital radio and TV formats, portions of this band will become available for other services and applications. The specifics and timing for revised allocations in this band will vary country by country but it is safe to conclude that regulators will give serious consideration to providing additional spectrum for fixed and mobile broadband services.

3.4.1. The "700 MHz Band" in the United States

Although locations will vary in detail from country to country, a characteristic that generally prevails is: there is less available spectrum for assignment to any single operator in the lower frequency bands than there is in higher bands. The 700 MHz allocation in the United States represents a good example for analysis sin it provides for several licenses ranging from 2 MHz of spectrum to 22 MHz of spectrum per license [16]. The US 700 MHz band allocation is shown in Figures 3.4 and 3.5. The spectrum designated as the "Lower 700 MHz Band", shown in Figure 3.4, supports five licenses. Three of the licenses have paired 6 MHz channels for a total of 12 MHz per license and two licenses consist of a single 6 MHz channel. Many of the lower band licenses were auctioned by the FCC in the year 2003.

The FCC plan for the "Upper 700 MHz Band", shown in Figure 3.5, provides for four additional licenses, one with paired 11 MHz channels for 22 MHz total, one with paired 5 MHz channels for a total of 10 MHz, and two licenses with paired 1 MHz channels. The latter two licenses comprising only 2 MHz of spectrum will not be considered further in this work since the spectrum is considered to be insufficient for a WiMAX deployment offering broadband services. The auctions for the "Upper 700 MHz Band" licenses were auctioned in the first quarter of 2008[1].

Assuming 700 MHz WiMAX equipment is available with either 5 or 10 MHz channel bandwidths, the US licenses in the 700 MHz band will support base station configurations as shown in Table 3.2 for TDD operation [17].

3.4.2. Path Loss Comparison

A number of channel models can be considered for 700 MHz and higher bands that include provision for mobile communication. For 700 MHz applications we based our path loss simulations on the Hata model [14] which is an analytical formulation based on the pathloss measurement data collected by Okumura in 1968 in Japan. The Hata model is one of the most widely used models for estimating median pathloss in macrocellular systems. The model provides an expression for median pathloss as a function of carrier frequency, BS and mobile station antenna heights, and the distance between the BS and the MS. The Hata model is valid only for the following range of

[1]700 MHz auction details can be found on the FCC website [16], Auction 73: 700 MHz Band

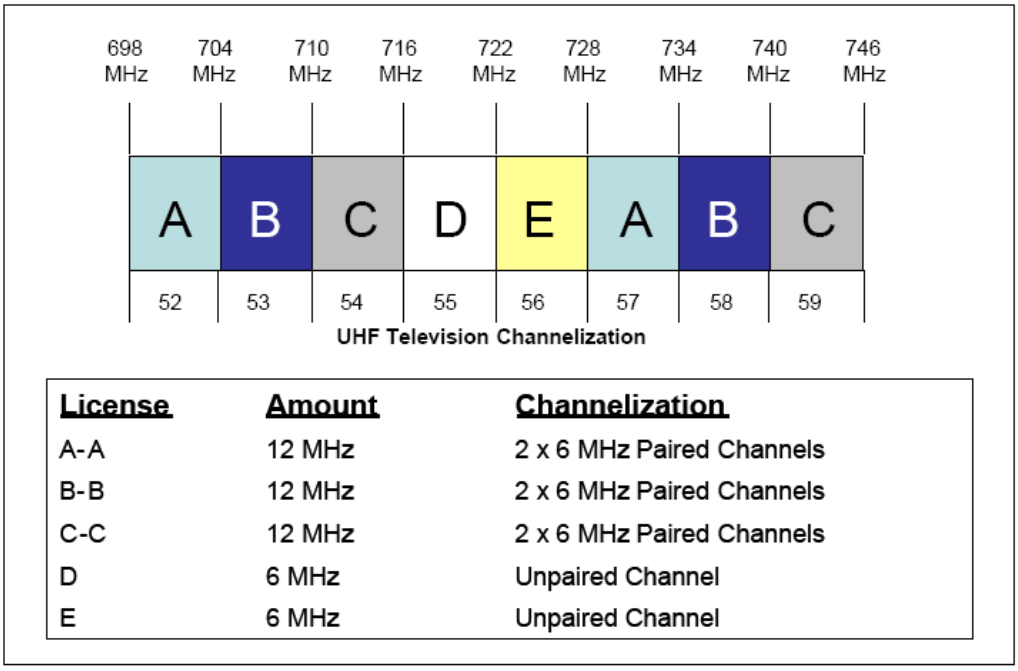

License	Amount	Channelization
A-A	12 MHz	2 x 6 MHz Paired Channels
B-B	12 MHz	2 x 6 MHz Paired Channels
C-C	12 MHz	2 x 6 MHz Paired Channels
D	6 MHz	Unpaired Channel
E	6 MHz	Unpaired Channel

Figure 3.4: "Lower" 700 MHz Band in the US

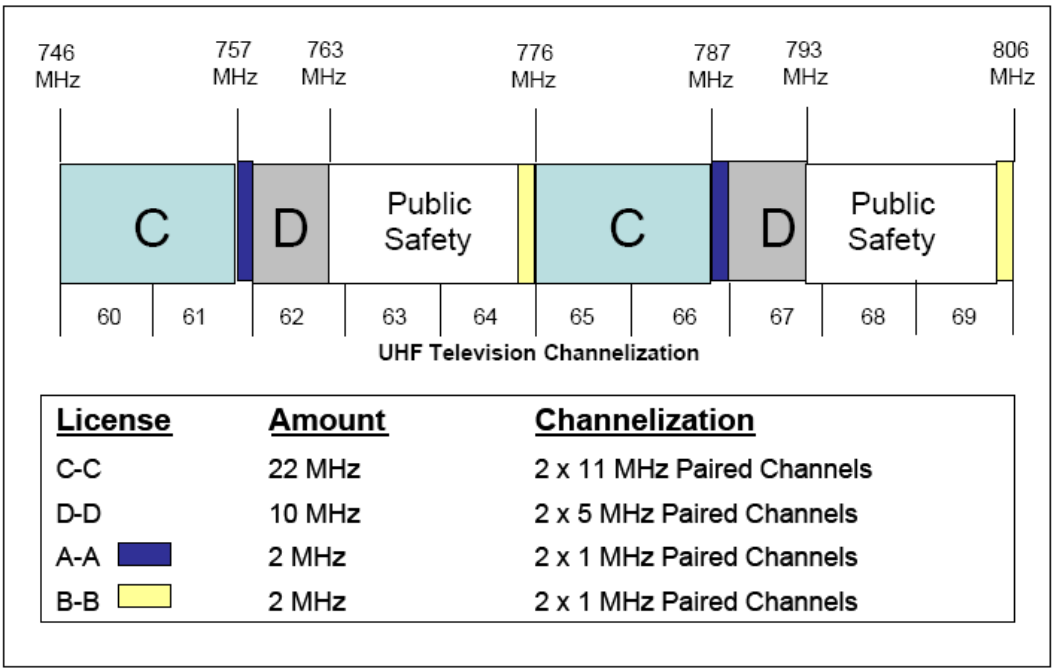

License	Amount	Channelization
C-C	22 MHz	2 x 11 MHz Paired Channels
D-D	10 MHz	2 x 5 MHz Paired Channels
A-A	2 MHz	2 x 1 MHz Paired Channels
B-B	2 MHz	2 x 1 MHz Paired Channels

Figure 3.5: "Upper" 700 MHz Band in the US

Table 3.2: Possible BS Configurations for US 700 MHz Band Plan

License	Channel BW	Maximum Channels per Sector	Average DL Sector Capacity
"Lower 700 MHz Band" D or E	5 MHz	1	4.6 Mbps
"Lower 700 MHz Band" A-A, B-B, or C-C	5 MHz	2	9.1 Mbps
"Upper 700 MHz Band" C-C	10 MHz	2	18.2 Mbps
"Upper 700 MHz Band" D-D	5 MHz	2	9.1 Mbps
"Upper 700 MHz Band" A-A, B-B	Not Applicable for WiMAX Deployment		

parameters:

- $150\text{MHz} \leq f \leq 1500\text{MHz}$
- $30\text{m} \leq h_b \leq 200\text{m}$
- $1\text{m} \leq h_m \leq 10\text{m}$
- $1\text{km} \leq d \leq 20\text{km}$

In these parameters, f is the carrier frequency in MHz, h_b is the BS antenna height in meters, h_m is the MS antenna height in meters, and d is the distance between the BS and the MS in km. According to the Hata model, the median pathloss in an urban environment is given by

$$\overline{PL}_{urban} = 69.55 + 26.16 \log f - 13.82 \log h_b + (44.9 - 6.55 \log(h_b)) \log d - a(h_m), \quad (3.2)$$

where $\overline{PL}_{urban}$ is expressed in the dB scale, and $a(h_m)$ is the MS antenna-correction factor. For a large city with dense building clutter and narrow streets, the MS antenna-correction factor is given by

$$a(h_m) = 8.29[\log[1.54 \cdot h_m]]^2 - 0.8 \quad f \leq 200\text{MHz}$$

$$a(h_m) = 3.20[\log[11.75 \cdot h_m]]^2 - 4.97 \quad f \geq 400\text{MHz} \quad (3.3)$$

For a small- or medium-size city, where the building-clutter density is smaller, the MS antenna-correction factor is given by

$$a(h_m) = (1.11 \log f - 0.7)h_m - (1.56 \log f - 0.8). \tag{3.4}$$

For a suburban area, the same MS antenna-correction factor as used for small cities is applicable, but the median pathloss is modified to be

$$\overline{PL}_{suburban} = \overline{PL}_{urban} - 2\left[\log\left(\frac{f}{28}\right)\right]^2 - 5.4. \tag{3.5}$$

For a rural area, the same MS antenna-correction factor as used for small cities is applicable, but the median pathloss is modified to be

$$\overline{PL}_{rural} = \overline{PL}_{urban} - 4.78[\log f]^2 - 18.33 \log f - 40.98. \tag{3.6}$$

The model may be also be generalized to any clutter environment, such that the median pathloss is modified from that of a small urban city as

$$\overline{PL} = \overline{PL}_{urban} + \text{Clutter Offset}. \tag{3.7}$$

In next chapter we are going to present some results about the path loss comparison between 700 MHz band and the 2.4 GHz band.

Chapter 4

Interference in WiMAX systems

Before addressing the interference of a deployed WiMAX system it is best to review how the sub-channels are divided among users in the uplink (UL) and downlink (DL). We are taking the 2.5 GHz scenario for this example. As we said before, for this case the Time Division Duplex (TDD) transmission scheme of the 802.16e standard was considered and 5 MHz bandwidth allocations was established. The available channel bandwidth is made up of sub-carriers each of which can be modulated individually with information. WiMAX uses Orthogonal Frequency Division Multiple Access (OFDMA) to assign sub-carriers to different users. The number of sub-carriers available for assignment in the UL and DL are a function of the channel bandwidth, the frame size, and the UL/DL transmit ratio. In mobile WiMAX, the smallest unit of frequency-time allocation available is a slot which contains 48 data sub-carriers. The sub-carriers comprising a slot can be made up of adjacent sub-carriers or can be allocated in a distributed fashion throughout the available carrier space. In general, distributed carrier allocations perform better in mobile environments, while adjacent sub-carriers are better suited for fixed links. The number of slots assigned to a particular user per frame is a function of their data needs.

Channel planning in WiMAX systems can be performed in several ways. Channel allocation is left up to the service providers and is based upon the amount of available spectrum and the density of the users requiring service. When enough bandwidth is at hand, the channels (for this case, 5 MHz portions of spectrum) can be allocated and reassigned among the available sectors in such a way as to minimize the co-channel interference at neighboring sites. This procedure corresponds to the traditional form of channel planning where a channel frequency re-use factor (FRF) can be picked to appropriately balance the trade off between spectral efficiency and interference. The interference between sectors operating on the same frequency is typically minimized

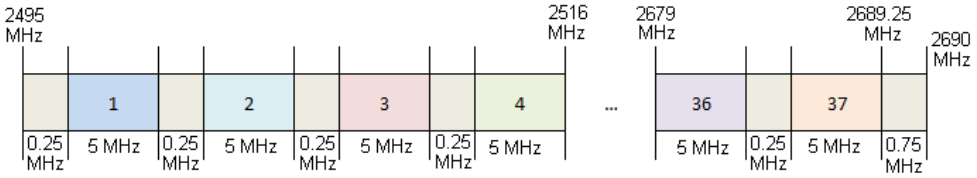

Figure 4.1: 2.5 GHz Band Channelization

through the use of directional antennas, sector spacing, and transmit power control in order to reduce the co-channel interference levels experienced by the users in the service area. Lower interference levels result in higher reliabilities and prevent the system from becoming unduly interference limited.

Actually the 2.5 GHz frequency band goes from 2.495 GHz to 2.690 GHz (see Figure 4.1); if all the 195 MHz of the spectrum is available we could have 37 channels of 5 MHz badwidth with a channel frequency step of 250 kHz to use in the cells depending on the FRF selected. For a $FRF = 1/3$, we could have 12 channels per cell and they could be assigned as in the Table 4.1 in order to minimize the adjacent channel interference.

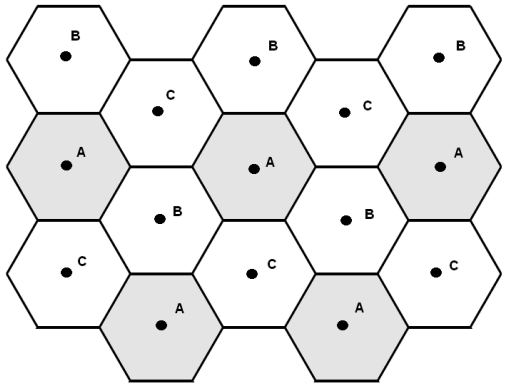

Figure 4.2: Hexagonal cellular system with $FRF = 1/3$

Table 4.1: Frequency allocation for $N = 3$

Cell	Channels assigned
Cell A	1, 4, 7, 10, 13, ..., 34, 37
Cell B	2, 5, 8, 11, 14, ..., 35
Cell C	3, 6, 9, 12, 15, ..., 36

However, it is typical that operators do not receive more than 25 MHz of the spectrum making not possible to use a cluster size bigger than 3 with a 5 MHz channel bandwidth.

Then each of the channels is made up of sub-carriers due to the OFDMA specifications. In [18] we can find the number of OFDM symbols per slot depending on the channel bandwidth and the DL/UL rate. In our example, we define a DL/UL of 60/40; this could be seen as 29/19 OFDM symbols per slot. Then the interference that BSs and SSs will experience come from neighboring sectors that use the same sub-carriers.

When analyzing the performance of a system using any level of FRF or sub-channelization the DL-only and UL-only interference cases are of the most significant concern. In the following sections we are going to calculate these interferences for both topologies (PMP and MSH). In Section 4.3 we present some estimations of the interference in DL/UL and UL/DL situations.

The interference estimation was made for the three terrain categories defined in [2]. The path loss exponent was calculate with Equation 2.23 for base station heights of 30, 40 and 50 meters. The Table 4.2 presents the results of this calculation.

For all interference calculations, it is assumed that the inter-cell interference is generated by the six co-channel cells of the first tier as in Figure 4.3. The interference caused from the second tier and beyond is insignificant compare to the one from the first tier.

Table 4.2: Path loss exponent for different terrain categories and base station heights

h_b	Terrain Category	PL exponent
30 m	A	4.795
	B	4.375
	C	4.1167
40 m	A	4.615
	B	4.1675
	C	3.9
50 m	A	4.477
	B	4.017
	C	3.75

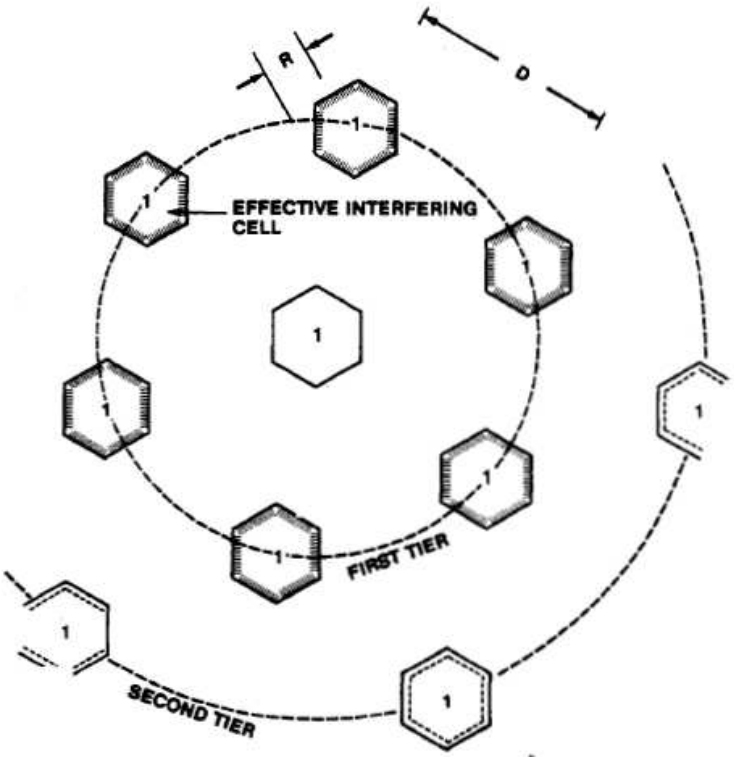

Figure 4.3: Six effective interfering cells of cell 1

4.0.3. About simulations

All simulations were made in MATLAB platform. In order to obtain the colored graphics, all interference equations were applied to each point of a grid drawn over the cell. Then each element of the SIR matrix obtained was compared to the thresholds defined in Table 2.6 in order to get the corresponding modulation scheme and the color assigned it.

Then the percentage corresponding to each modulation scheme was quantified. This process was repeated for each terrain category, base station antenna height and cluster size defined in this chapter resulting in several arrays. Finally, these arrays were plot in several comparative graphics in linear and bar styles.

4.1. Downlink Channel Interference Calculation

During the DL, a mobile experiences interference from neighboring sectors that use the same sub-carriers (see Figure 4.4). This type of analysis requires information on the channel and slot allocations at each sector and, if used, their frame frequency re-use factor zones. Since the cells and sectors are fixed in location and given a set of allotted time-frequency resources, a Signal-to-Interference (S/I) ratio could be estimated or measured for each point in space the system is deployed. In some cases there will be regions where the received S/I is not sufficient for reliable service. These areas could be identified and, if necessary, additional base stations erected to cover the affected areas. Note that this type of analysis is nonstochastic in nature once the resources are allocated to the different sectors and the locations of the sectors are fixed.

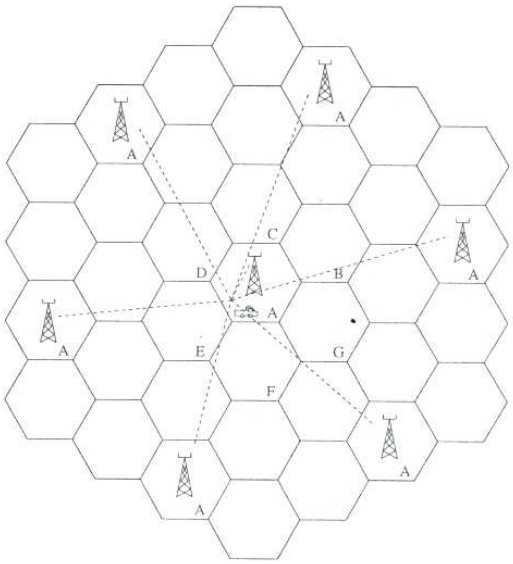

Figure 4.4: Downlink Co-Channel Interference

As we said before the propagation model that we are going to use is the Erceg model [2]. Considering the pathloss equation 2.24 we can obtain the received power as

$$P_r(d) = \left(\frac{P_t G_t G_r}{L_t L_r}\right)\left(\frac{\lambda^2}{(4\pi)^2 d_0^2}\right)\left(\frac{d}{d_0}\right)^{-\gamma}\left(\frac{1}{PL_f PL_h s}\right) \tag{4.1}$$

where P_t is the transmitted power, $P_r(d)$ is the received power which is a function of the T-R separation, G_t is the transmitter antenna gain, G_r is the receiver antenna gain, d is the T-R separation distance in meters, γ is the pathloss exponent factor, L is the system loss factor not related to propagation ($L \geq 1$), and λ is the wavelength in meters. PL_f and PL_h are the correction factor due to the frequency and receive antenna height respectively, while s represent the shadowing effect.

4.1.1. PMP scenario

The two PMP scenarios presented in Chapter 3 have the characteristic that their downlink (DL) and uplink (UL) channels are separated either by Time Division Duplex (TDD) or by Frequency Division Duplex (FDD). If it is assumed that these transmission channels are perfectly separated, the selected duplexing mode and the channel bandwidth are transparent for the interference calculation.

With Figure 4.4, Equation 2.5 and Equation 4.1 in mind, we can find the Downlink Co-Channel Interference for the PMP scenarios as follows:

$$\begin{aligned}
\frac{S}{I}_{DL} &= \frac{S}{\sum_{i=1}^{i_0} I_i} \\
\frac{S}{I}_{DL} &= \frac{P_r(R)}{\sum_{i=1}^{i_0} P_r(D_i)} \\
\frac{S}{I}_{DL} &= \frac{\left(\frac{P_{t_{BS}} G_{t_{BS}} G_{r_{MS}}}{L_{t_{BS}} L_{r_{MS}}}\right)\left(\frac{\lambda^2}{(4\pi)^2 d_0^2}\right)\left(\frac{R}{d_0}\right)^{-\gamma}\left(\frac{1}{PL_f PL_h s}\right)}{\sum_{i=1}^{i_0}\left(\frac{P_{t_{BS}} G_{t_{BS}} G_{r_{MS}}}{L_{t_{BS}} L_{r_{MS}}}\right)\left(\frac{\lambda^2}{(4\pi)^2 d_0^2}\right)\left(\frac{D_i}{d_0}\right)^{-\gamma}\left(\frac{1}{PL_f PL_h s}\right)}
\end{aligned} \tag{4.2}$$

where $P_{t_{BS}}$ is the BS transmitted power, $G_{t_{BS}}$ is the BS transmitter antenna gain, $G_{r_{MS}}$ is the MS receiver antenna gain, γ is the pathloss exponent factor, L is the system loss factor not related to propagation, and λ is the wavelength in meters. PL_f and PL_h are the correction factor due to the frequency and receive antenna height respectively, while s represent the shadowing effect. It was assumed that all BS have the same height, P_t and antennas characteristics; the same is assumed for all MS. Considering these, Equation 4.2 can be simplified as

$$\frac{S}{I}_{DL} = \frac{(R)^{-\gamma}}{\sum_{i=1}^{i_0}(D_i)^{-\gamma}} \tag{4.3}$$

where R is the distance between the BS and the MS in the cell of interest and D_i is the distance from the MS to the ith interfering co-channel cell base station. For a worst case scenario R is equal to the cell radio.

In order to obtain the interference throughout the cell, we applied Equation 4.3 to each point of a grid drawn over the cell. In order to use link adaptation, the thresholds defined in Table 2.6 are applied to the values obtained at each point. Then the area covered by each modulation scheme is quantified. This process was repeated several times changing the terrain type and the cluster size. For the cluster size we use the typical values of a WiMAX system (1 and 3) and a value of 7 for an illustrative case.

From Figure 4.5 to 4.7 we present the results obtained for the interference in PMP scenarios in the DL channel.

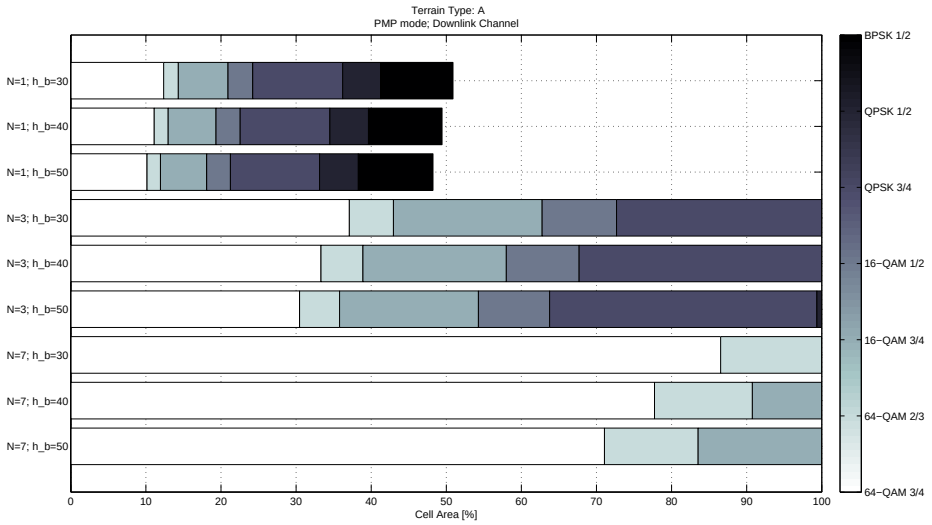

Figure 4.5: Terrain Type: A; PMP mode; Downlink Channel

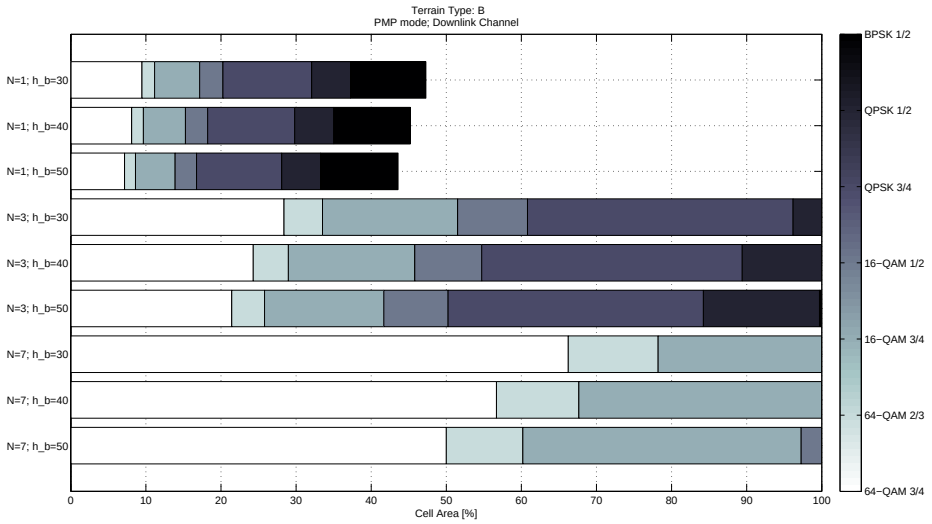

Figure 4.6: Terrain Type: B; PMP mode; Downlink Channel

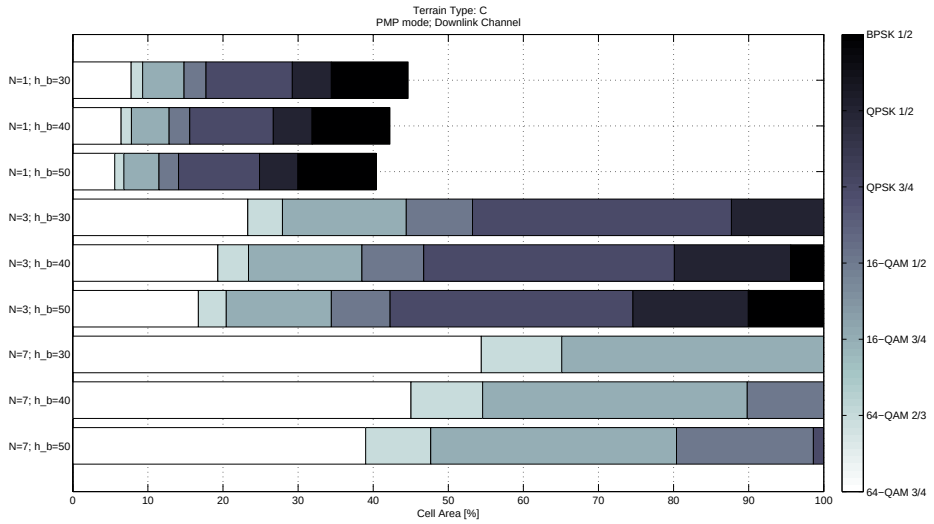

Figure 4.7: Terrain Type: C; PMP mode; Downlink Channel

We can observe from the previous figures that in all cases when the BS antenna height is bigger the co-channel interference increase and more robust modulation schemes are needed throughput the cell. With a bigger antenna it is assure a line-of sight transmission; this means that the transmission result more direct and affects more other cells.

In the same way, smaller cluster size results in a interference increasing due to the signals are more closer and, as a result, the transmitted power is attenuated less.

Also there are differences between the terrain types; these differences are due to the inherent characteristics of the terrains described before in chapter 2.

4.1.2. Mesh scenario

As it was stated before, for Mesh mode, we are going to use the same radio characteristics of the PMP mode. In the same way, for both interference calculations, it is assumed that the inter-cell interference is generated by the six co-channel cells of the first tier.

In downlink channel, BSs are interfered by co-channel BSs, which are centrally lo-

cated. Relays are interfered by co-channel relays, whose positions are also well known (see Figure 4.8). In uplink channel, co-channel SSs generate interference (see Figure 4.22). Their position is unknown and may vary within the cells coverage area; but as we said before we are going to take the mean value of the SS position.

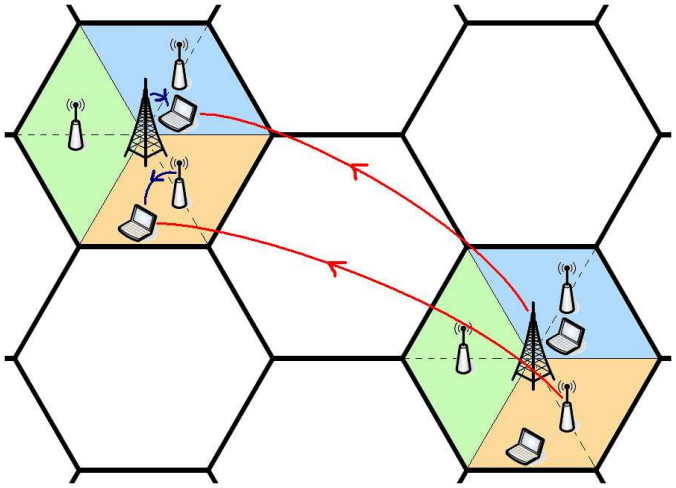

Figure 4.8: Diagram of the interference signals in Downlink Channel for Mesh mode

For the analysis of the downlink channel we can see it as two separate parts. In the first part the mobile station is located between the BS and the circle formed with the relays; the transmission is made in one hop directly to the BS. The SIR is calculated as follows,

$$\frac{S}{I}_{DL} = \frac{\left(\frac{P_{t_{BS}} G_{t_{BS}} G_{r_{MS}}}{L_{t_{BS}} L_{r_{MS}}}\right)\left(\frac{\lambda^2}{(4\pi)^2 d_0^2}\right)\left(\frac{d^{MS}}{d_0}\right)^{-\gamma}\left(\frac{1}{PL_f PL_h s}\right)}{\sum_{i=1}^{i_0}\left(\frac{P_{t_{BS}} G_{t_{BS}} G_{r_{MS}}}{L_{t_{BS}} L_{r_{MS}}}\right)\left(\frac{\lambda^2}{(4\pi)^2 d_0^2}\right)\left(\frac{D_i^{BS}}{d_0}\right)^{-\gamma}\left(\frac{1}{PL_f PL_h s}\right)}$$

$$\frac{S}{I}_{DL} = \frac{(d^{MS})^{-\gamma}}{\sum_{i=1}^{i_0}(D_i^{BS})^{-\gamma}} \quad \text{for } r \leq \frac{R}{2} \tag{4.4}$$

where $P_{t_{BS}}$ is the BS transmitted power, $G_{t_{BS}}$ is the BS transmitter antenna gain, $G_{r_{MS}}$ is the MS receiver antenna gain, γ is the pathloss exponent factor, L is the system loss factor not related to propagation, and λ is the wavelength in meters. PL_f and PL_h are the correction factor due to the frequency and receive antenna height respectively, while s represent the shadowing effect. d^{MS} is the distance between the BS and the

MS in the cell of interest and D_i^{BS} is the distance from the MS to the ith interfering co-channel cell base station.

In the second part the mobile station is located beyond the circle formed with the relays; the transmission is made in two hops: the first one to the relay, and the second to the BS. The SIR is defined as,

$$\frac{S}{I}_{DL} = \frac{\left(\frac{P_{t_{RS}} G_{t_{RS}} G_{r_{MS}}}{L_{t_{RS}} L_{r_{MS}}}\right)\left(\frac{\lambda^2}{(4\pi)^2 d_0^2}\right)\left(\frac{d^{MS}}{d_0}\right)^{-\gamma}\left(\frac{1}{PL_f PL_h s}\right)}{\sum_{i=1}^{i_0}\left(\frac{P_{t_{RS}} G_{t_{RS}} G_{r_{MS}}}{L_{t_{RS}} L_{r_{MS}}}\right)\left(\frac{\lambda^2}{(4\pi)^2 d_0^2}\right)\left(\frac{D_i^{RS}}{d_0}\right)^{-\gamma}\left(\frac{1}{PL_f PL_h s}\right)}$$

$$\frac{S}{I}_{DL} = \frac{(d^{MS})^{-\gamma}}{\sum_{i=1}^{i_0}(D_i^{RS})^{-\gamma}} \quad \text{for } r \geq \frac{R}{2} \tag{4.5}$$

where $P_{t_{RS}}$ is the RS transmitted power, $G_{t_{RS}}$ is the RS transmitter antenna gain, d^{MS} is the distance between the RS and the MS in the cell of interest and D_i^{RS} is the distance from the MS to the ith interfering co-channel cell relay station.

We follow the same process used in the PMP scenario in order to obtain the interference throughout the cell. Now, we applied Equations 4.4 and 4.5 to each point of a grid drawn over the cell. Then the thresholds defined in Table 2.6 are applied to the values obtained at each point, and as a result, the area covered by each modulation scheme is quantified. Again, the process was repeated several times changing the terrain type (A, B and C) and the cluster size (1, 3 and 7).

From Figure 4.9 to 4.25 we present the results obtained for the interference in MSH scenarios in the DL channel.

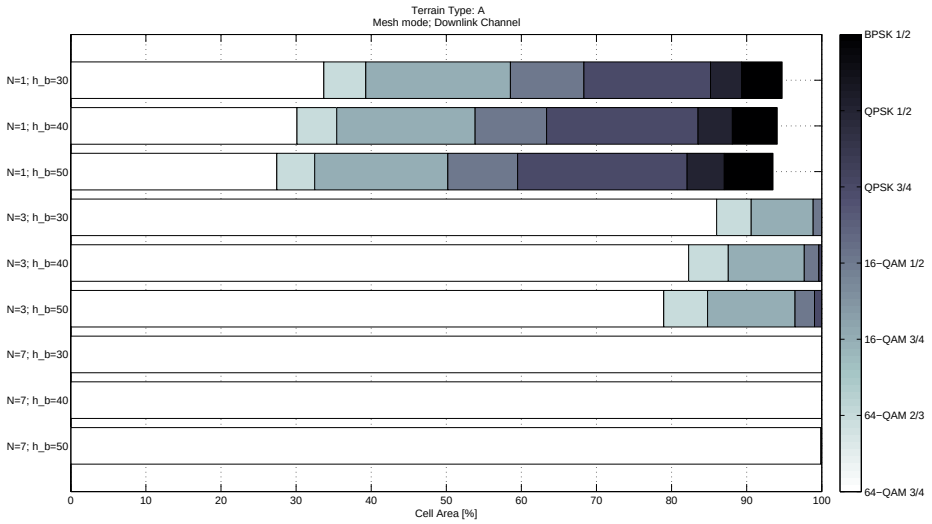

Figure 4.9: Terrain Type: A; Mesh mode; Downlink Channel

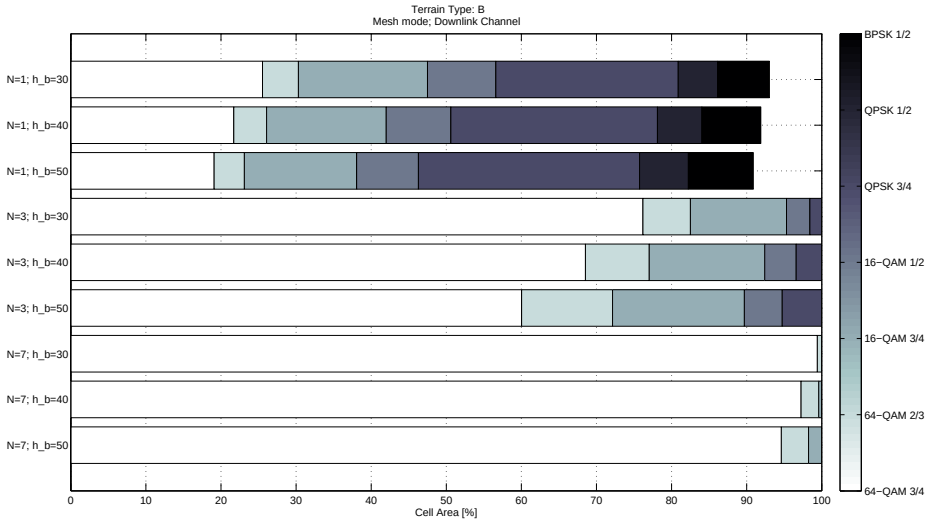

Figure 4.10: Terrain Type: B; Mesh mode; Downlink Channel

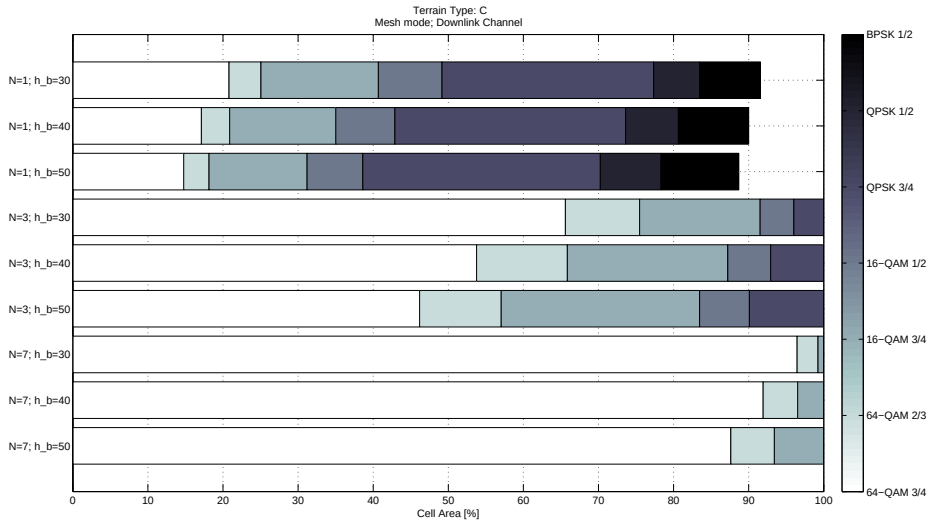

Figure 4.11: Terrain Type: C; Mesh mode; Downlink Channel

Basically, we observe the same behavior as in the PMP mode; bigger BS antenna heights and smaller cluster sizes produce more co-channel interference and more robust modulation schemes are needed throughput the cell.

But the mesh mode show some interesting performances, when the cluster size is equal to seven, practically all the cell can be covered with the 64QAM 3/4 modulation scheme.

4.1.3. Comparative Results

In the results shown in previous section we could notice that bigger antennas result in an unwanted performance due to the interference increment. We could think that smaller antennas result in better performance; however shorter antennas result in a coverage reduction. Because the cases when the BS antenna height (h_b) is equal to 30 meters presented the best performance, we decide to compare the PMP scenario with the Mesh scenario when this value is presented. From Figure 4.12 to Figure 4.14 we are comparing the PMP mode with the Mesh mode for different terrain scenarios.

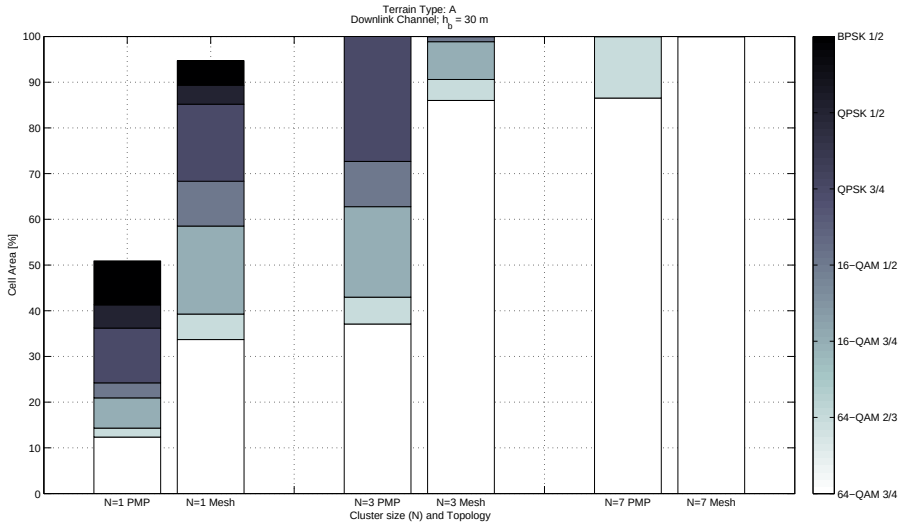

Figure 4.12: PMP mode and Mesh mode comparative for Terrain Type A ($h_b = 30$m); Downlink Channel

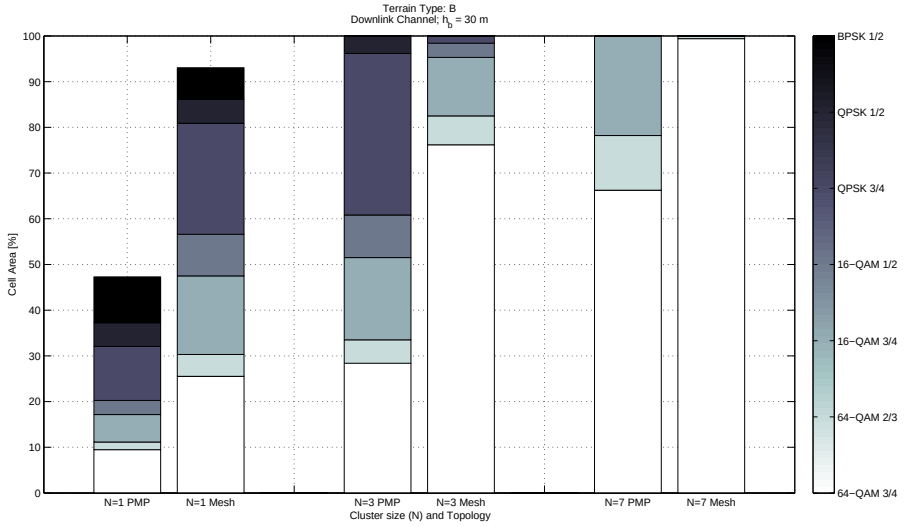

Figure 4.13: PMP mode and Mesh mode comparative for Terrain Type B ($h_b = 30$m); Downlink Channel

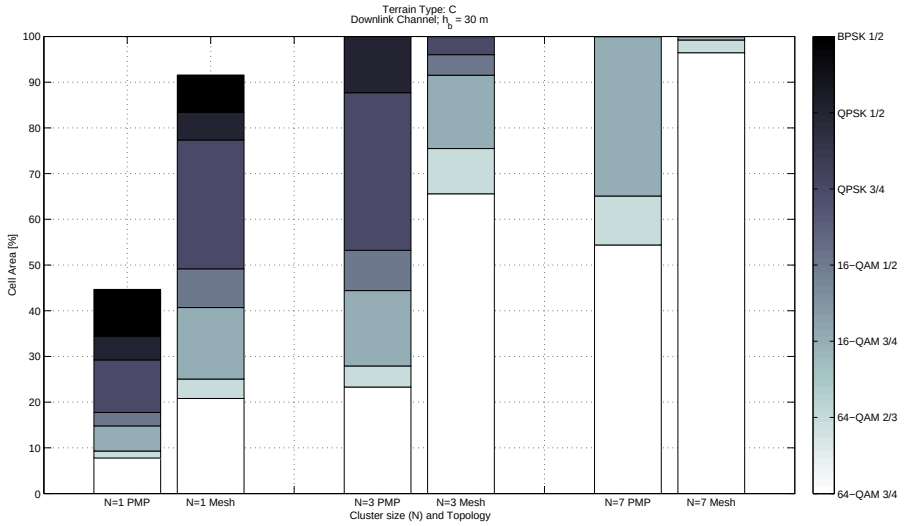

Figure 4.14: PMP mode and Mesh mode comparative for Terrain Type C ($h_b = 30$m); Downlink Channel

In each of these cases the Mesh mode performs better than the PMP mode. In PMP mode more robust modulation schemes are needed throughput the cell while in some Mesh-mode cases just 64QAM 3/4 scheme is needed for covering all the cell. This conclusion can be easily seen in Figures 4.15, 4.16 and 4.17, and in the Table 4.3 where it is summarize the comparative results for the downlink channel in a terrain type B.

Figures 4.15, 4.16 and 4.17 are the graphic representation of the cell for different cluster sizes. The concentric circles are due to the different modulation schemes that can be used; the lightest-blue circles are for the 64QAM 3/4 scheme and the darkest-circles represent the BPSk 1/2 scheme. In these figures is easy to see that with mesh topology we can increase the cell coverage for every cluster size, and also, we can offer a better QoS due to the increase of the high-performance modulation (64QAM 3/4) use.

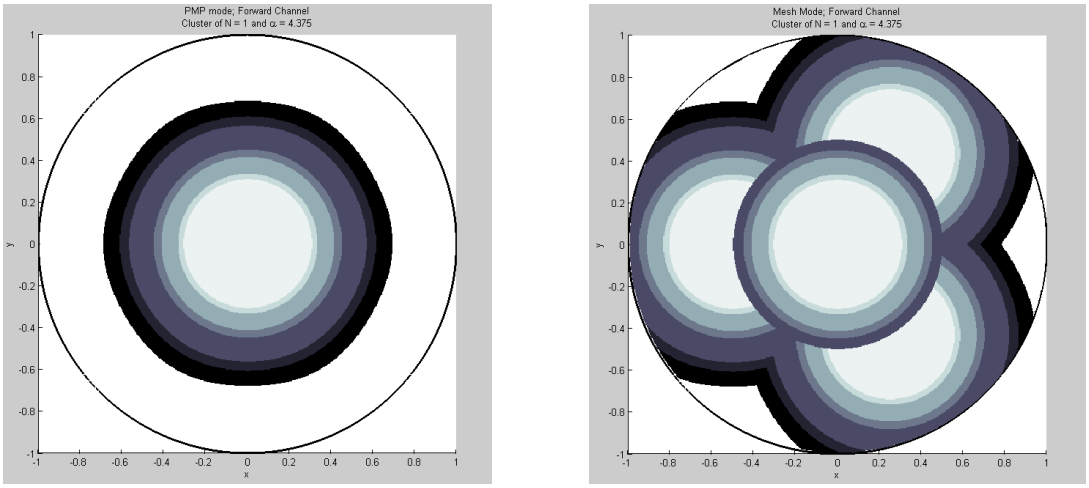

(a) PMP Scenario (b) Mesh Scenario

Figure 4.15: Comparative Results between PMP and Mesh scenarios; Downlink Channel; Cluster Size $N = 1$

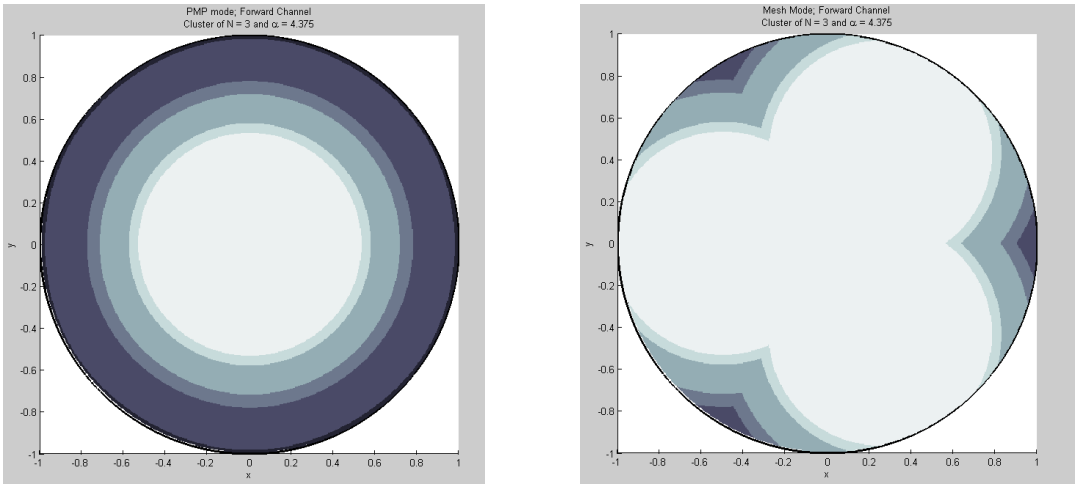

(a) PMP Scenario (b) Mesh Scenario

Figure 4.16: Comparative Results between PMP and Mesh scenarios; Downlink Channel; Cluster Size $N = 3$

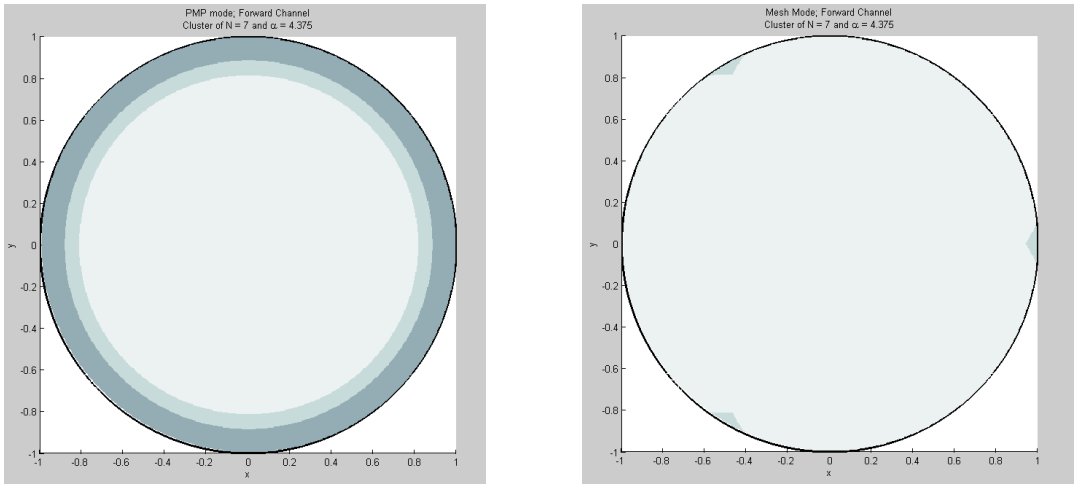

(a) PMP Scenario (b) Mesh Scenario

Figure 4.17: Comparative Results between PMP and Mesh scenarios; Downlink Channel; Cluster Size $N = 7$

Table 4.3: PMP mode and Mesh mode comparative for Terrain Type B ($h_b = 30$m); Downlink Channel

		$N = 1$		$N = 3$		$N = 7$	
		PMP	Mesh	PMP	Mesh	PMP	Mesh
Modulation	Coding Rate	Surface [%]					
BPSK	1/2	10.030	6.919	0	0	0	0
QPSK	1/2	5.170	5.226	3.820	0	0	0
QPSK	3/4	11.814	24.298	35.364	1.575	0	0
16-QAM	1/2	3.104	9.102	9.306	3.113	0	0
16-QAM	3/4	5.999	17.182	17.991	12.805	21.791	0
64-QAM	2/3	1.690	4.788	5.130	6.317	11.957	0.586
64-QAM	3/4	9.471	25.524	28.389	76.189	66.252	99.414
Total Area Covered of the Cell		47.279	93.038	100	100	100	100

In Table 4.3 we can see that when the cluster size equals to seven ($N = 7$), in the mesh mode the 64QAM 3/4 scheme reaches practically all cell size with percentages of 99.414 for the downlink channel. But considering that a cluster size of 7 is unrealistic, we focus in the results for cluster sizes of 1 and 3. In both cases, in the mesh scenario

the use of the 64QAM 3/4 scheme is more than the double compared to the PMP scenario.

4.2. Uplink Channel Interference Calculation

The UL interference is the interference experienced at the base stations from neighboring mobiles transmitting on the same sub-carriers as the desired user (see Figure 4.18). This second type of interference, however, is stochastic in nature because the mobiles can at any given time be at any location within their cell service area. Each of the possible combinations of interference and desired mobile locations could result in different S/Is at the Base stations. Some S/I ratios will occur more frequently than others based on the size, the terrain, as well as the population density of the service areas of both the interfering cells and the cell of interest. The probability distributions of the S/Is at each sector can either be measured or they can be estimated using a prediction tool. In order to simplify this procedure, we decide to estimate the mean value of the MS position with the assumption that the mobiles are uniformly distributed.

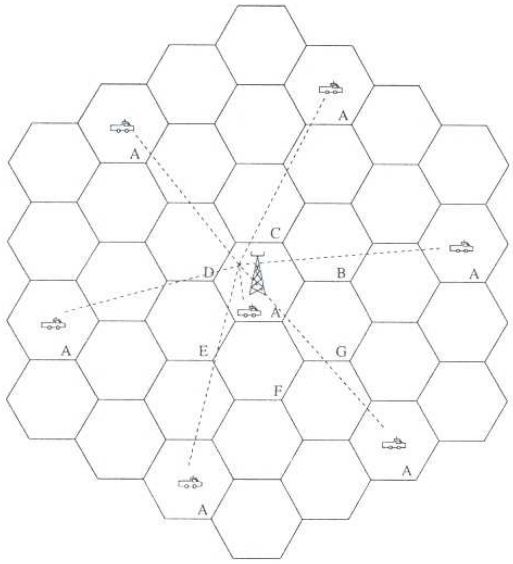

Figure 4.18: Uplink Co-Channel Interference

4.2.1. PMP scenario

Like in the Downlink CCI calculation, we use Figure 4.18, Equation 2.5 and Equation 4.1 and the Uplink Co-Channel Interference was obtained as:

$$\begin{aligned}
\frac{S}{I}_{UL} &= \frac{S}{\sum_{i=1}^{i_0} I_i} \\
\frac{S}{I}_{UL} &= \frac{P_r(R)}{\sum_{i=1}^{i_0} P_r(D_i)} \\
\frac{S}{I}_{UL} &= \frac{\left(\frac{P_{t_{MS}} G_{t_{MS}} G_{r_{BS}}}{L_{t_{MS}} L_{r_{BS}}}\right)\left(\frac{\lambda^2}{(4\pi)^2 d_0^2}\right)\left(\frac{R}{d_0}\right)^{-\gamma}\left(\frac{1}{PL_f PL_h s}\right)}{\sum_{i=1}^{i_0}\left(\frac{P_{t_{MS}} G_{t_{MS}} G_{r_{BS}}}{L_{t_{MS}} L_{r_{BS}}}\right)\left(\frac{\lambda^2}{(4\pi)^2 d_0^2}\right)\left(\frac{D_i}{d_0}\right)^{-\gamma}\left(\frac{1}{PL_f PL_h s}\right)} \\
\frac{S}{I}_{UL} &= \frac{(R)^{-\gamma}}{\sum_{i=1}^{i_0}(D_i)^{-\gamma}}
\end{aligned} \tag{4.6}$$

where R is the distance between the BS and the MS in the cell of interest and D_i is the distance from the BS to the ith interfering co-channel cell mobile station.

We can conclude from Equations 4.2 and 4.6 that when all BSs and MSs within the system work at the same frequency the SIR becomes frequency independent. Also, when the size of each cell is approximately the same and the base stations transmit the same power, the co-channel interference ratio is independent of the transmitted power and becomes a function of the R and D values. For this reason, the results that we are going to show apply for both PMP scenarios.

As in the downlink channel, in order to obtain the interference throughout the cell, Equation 4.6 was applied to each point of a grid drawn over the cell. Then the thresholds from Table 2.6 were applied to the values obtained at each point. Again, the process was repeated several times changing the terrain type and the cluster size. From Figure 4.19 to 4.21 we present the results obtained for the PMP scenarios in the uplink channel.

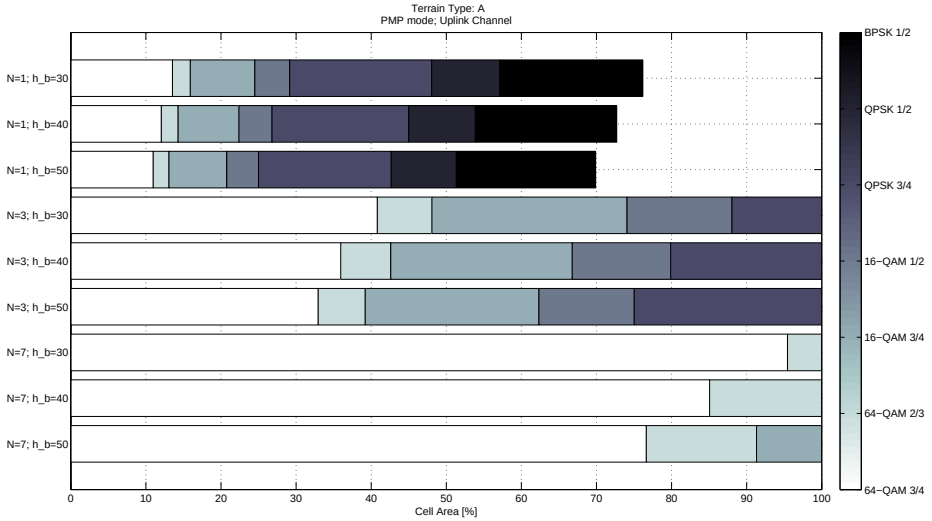

Figure 4.19: Terrain Type: A; PMP mode; Uplink Channel

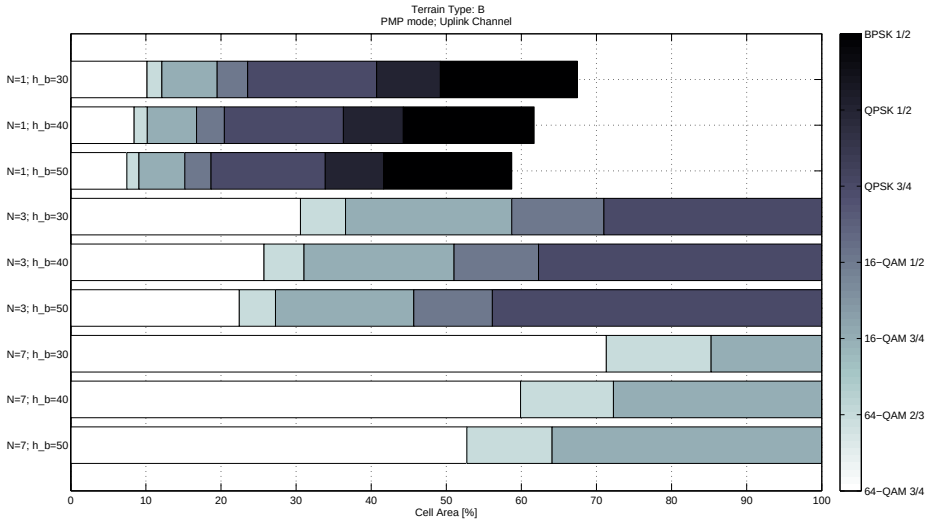

Figure 4.20: Terrain Type: B; PMP mode; Uplink Channel

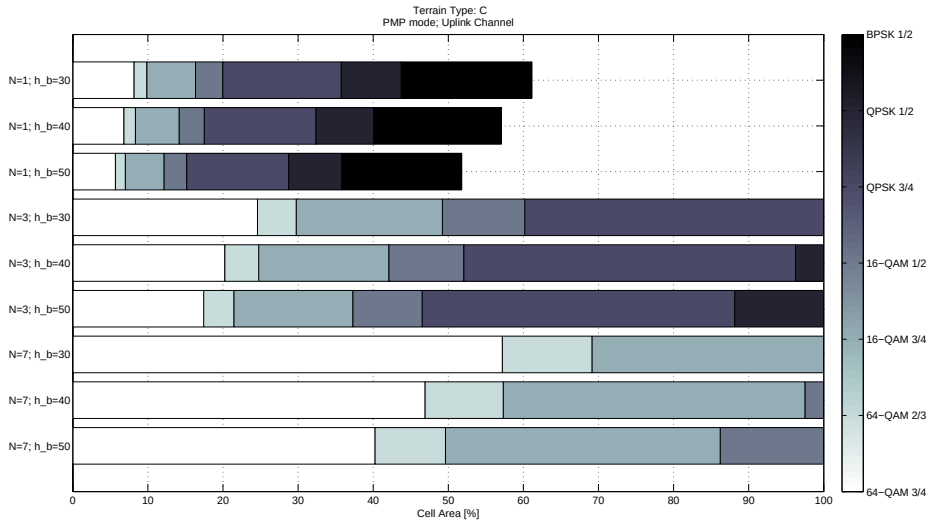

Figure 4.21: Terrain Type: C; PMP mode; Uplink Channel

In the uplink channel we observe similar results to the downlink channel. We observe again that in all cases when the BS antenna height is bigger the co-channel interference increase and more robust modulation schemes are needed throughput the cell. In the same way, smaller cluster size results in a interference increasing due to the signals are more closer and, as a result, the transmitted power is attenuated less.

4.2.2. Mesh scenario

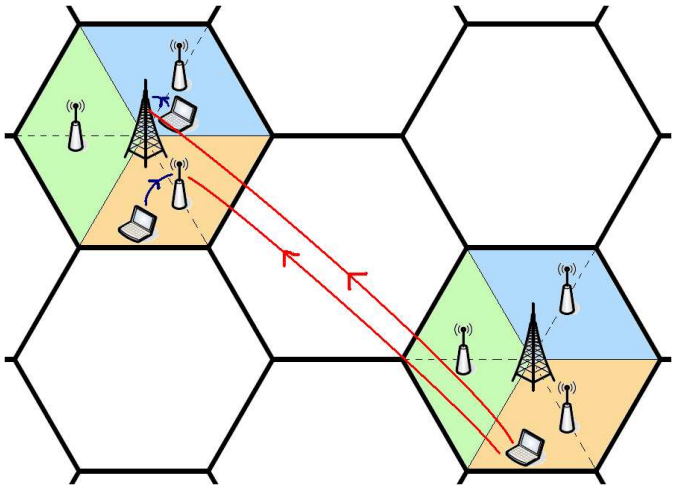

Figure 4.22: Diagram of the interference signals in Uplink Channel for Mesh mode

In the uplink channel (see Figure 4.22) for the mesh scenario we also can see it as two separate parts in order to obtain the desire signal. In the first part the mobile station is located between the BS and the circle formed with the relays so the distance of the desired signal is the one between the BS and MS. The SIR is calculated as follows,

$$\frac{S}{I}_{UL} = \frac{\left(\frac{P_{t_{MS}} G_{t_{MS}} G_{r_{BS}}}{L_{t_{MS}} L_{r_{BS}}}\right)\left(\frac{\lambda^2}{(4\pi)^2 d_0^2}\right)\left(\frac{d^{BS}}{d_0}\right)^{-\gamma}\left(\frac{1}{PL_f PL_h s}\right)}{\sum_{i=1}^{i_0}\left(\frac{P_{t_{MS}} G_{t_{MS}} G_{r_{BS}}}{L_{t_{MS}} L_{r_{BS}}}\right)\left(\frac{\lambda^2}{(4\pi)^2 d_0^2}\right)\left(\frac{D_i^{MS}}{d_0}\right)^{-\gamma}\left(\frac{1}{PL_f PL_h s}\right)}$$

$$\frac{S}{I}_{UL} = \frac{(d^{BS})^{-\gamma}}{\sum_{i=1}^{i_0}(D_i^{MS})^{-\gamma}} \quad \text{for } r \leq \frac{R}{2} \tag{4.7}$$

where $P_{t_{MS}}$ is the MS transmitted power, $G_{t_{MS}}$ is the MS transmitter antenna gain, $G_{r_{BS}}$ is the BS receiver antenna gain, γ is the pathloss exponent factor, L is the system loss factor not related to propagation, and λ is the wavelength in meters. PL_f and PL_h are the correction factor due to the frequency and receive antenna height respectively, while s represent the shadowing effect. d^{BS} is the distance between the BS and the MS in the cell of interest and D_i^{MS} is the distance from the BS to the ith interfering co-channel cell mobile station.

In the second part the mobile station is located beyond the circle formed with the relays and as a result the distance of the desired signal is the one between the relay and the MS. The SIR can be obtained as,

$$\frac{S}{I}_{UL} = \frac{\left(\frac{P_{t_{MS}} G_{t_{MS}} G_{r_{RS}}}{L_{t_{MS}} L_{r_{RS}}}\right)\left(\frac{\lambda^2}{(4\pi)^2 d_0^2}\right)\left(\frac{d^{RS}}{d_0}\right)^{-\gamma}\left(\frac{1}{PL_f PL_h s}\right)}{\sum_{i=1}^{i_0}\left(\frac{P_{t_{MS}} G_{t_{MS}} G_{r_{RS}}}{L_{t_{MS}} L_{r_{RS}}}\right)\left(\frac{\lambda^2}{(4\pi)^2 d_0^2}\right)\left(\frac{D_i^{MS}}{d_0}\right)^{-\gamma}\left(\frac{1}{PL_f PL_h s}\right)}$$

$$\frac{S}{I}_{UL} = \frac{(d^{RS})^{-\gamma}}{\sum_{i=1}^{i_0}(D_i^{MS})^{-\gamma}} \quad \text{for } r \geq \frac{R}{2} \tag{4.8}$$

where d^{RS} is the distance between the RS and the MS in the cell of interest and D_i^{MS} is the distance from the RS to the ith interfering co-channel cell mobile station.

We then follow the same process as in the downlink channel, applying Equations 4.7 and 4.8 to each point of the grid drawn over the cell in order to obtain the interference throughout the cell. The thresholds defined in Table 2.6 are applied to the values obtained at each point and then the area covered by each modulation scheme is quantified. Also, the process was repeated several times changing the terrain type and the cluster size. From Figure 4.23 to 4.25 we present the results obtained for the Mesh mode in the uplink channel.

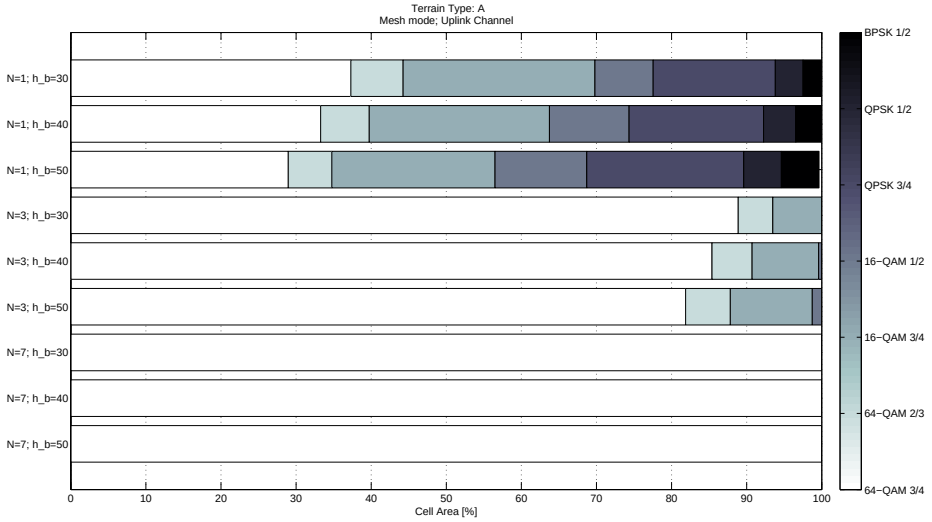

Figure 4.23: Terrain Type: A; Mesh mode; Uplink Channel

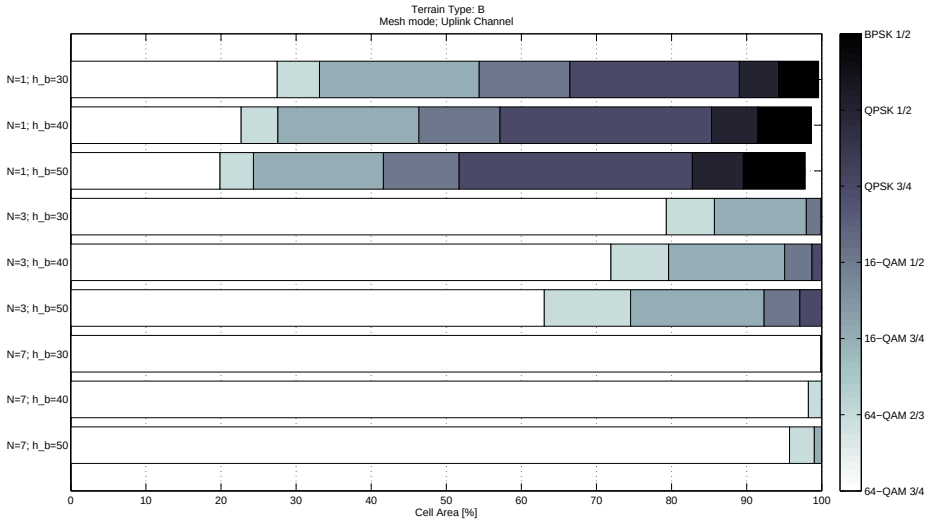

Figure 4.24: Terrain Type: B; Mesh mode; Uplink Channel

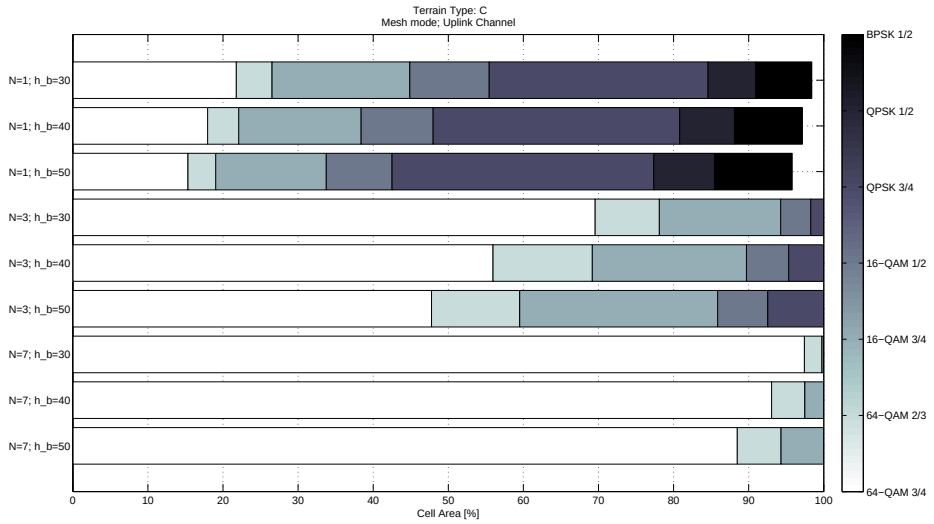

Figure 4.25: Terrain Type: C; Mesh mode; Uplink Channel

Basically, we observe the same behavior as in the downlink channel; bigger BS antenna heights and smaller cluster sizes produce more co-channel interference and more robust modulation schemes are needed throughput the cell. Also the uplink channel of the mesh mode show that when the cluster size is equal to seven, practically all the cell can be covered with the 64QAM 3/4 modulation scheme.

4.2.3. Comparative Results

For the results in the uplink channel we also notice that the cases when the BS antenna height (h_b) is equal to 30 meters presented the best performance. Again, we decide to compare the PMP scenario with the Mesh scenario when this value is presented. From Figure 4.26 to Figure 4.28 we are comparing the PMP mode with the Mesh mode for different terrain scenarios.

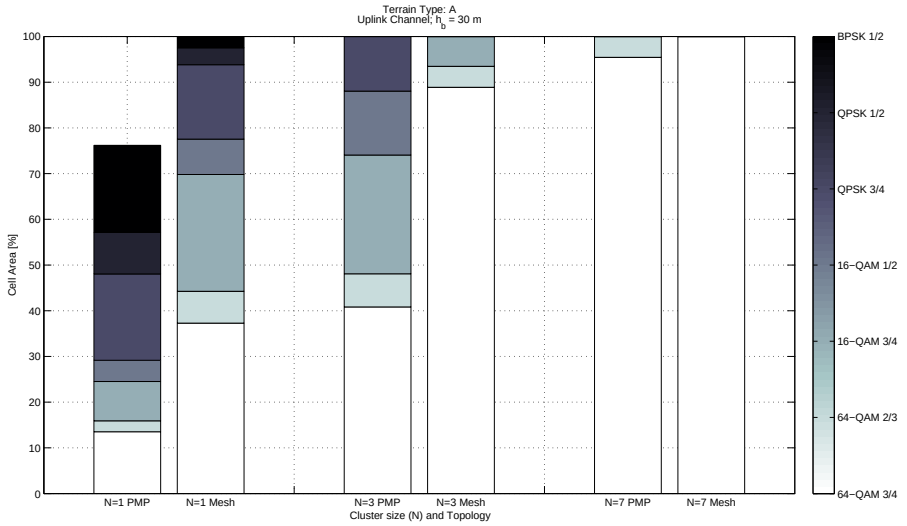

Figure 4.26: PMP mode and Mesh mode comparative for Terrain Type A ($h_b = 30$m); Uplink Channel

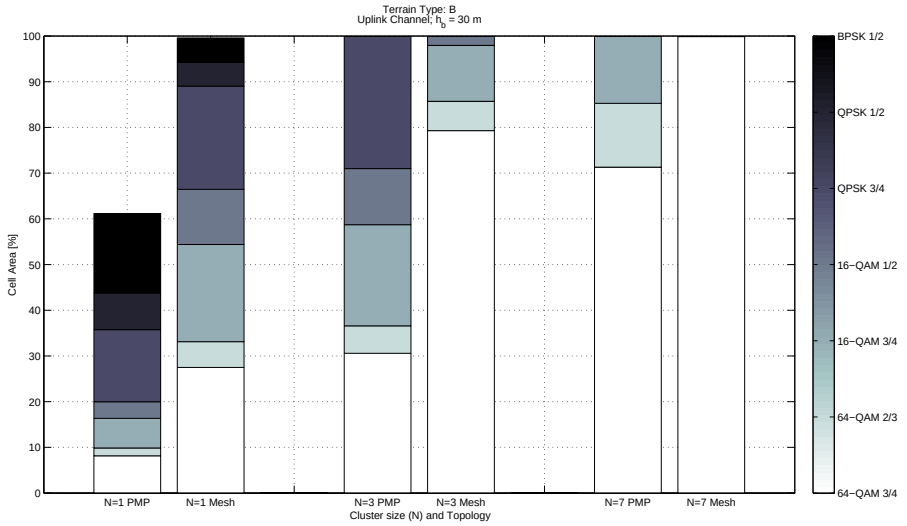

Figure 4.27: PMP mode and Mesh mode comparative for Terrain Type B ($h_b = 30$m); Uplink Channel

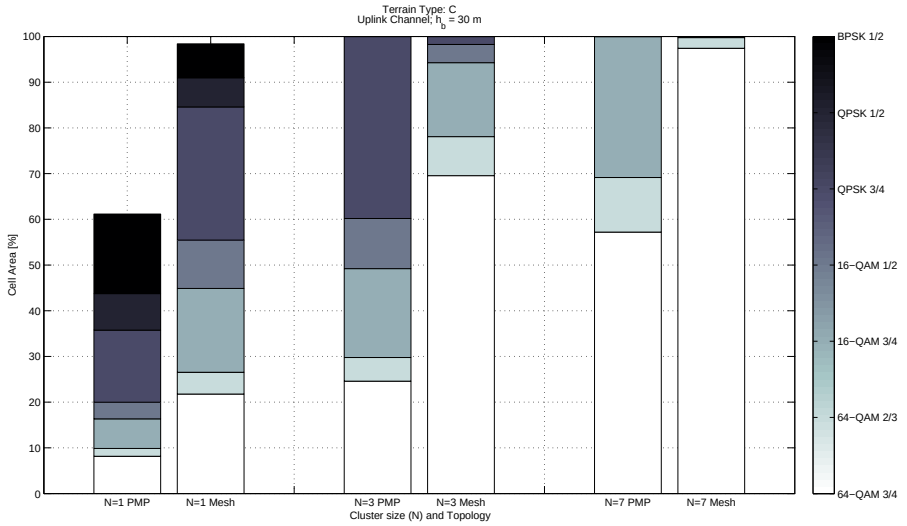

Figure 4.28: PMP mode and Mesh mode comparative for Terrain Type C ($h_b = 30$m); Uplink Channel

As expected, in each of these cases the Mesh mode performs better than the PMP mode. In PMP mode more robust modulation schemes are needed throughput the cell while in some Mesh-mode cases just 64QAM 3/4 scheme is needed for covering all the cell. This conclusion can be easily seen in Figures 4.29, 4.30 and 4.31, and in the Table 4.4 where it is summarize the comparative results for the uplink channel in a terrain type B.

Figures 4.29, 4.30 and 4.31 are the graphic representation of the cell for different cluster sizes in the uplink channel. The concentric circles are due to the different modulation schemes that can be used; the lightest-blue circles are for the 64QAM 3/4 scheme and the darkest-circles represent the BPSk 1/2 scheme. In these figures is easy to see that with mesh topology we can increase the cell coverage for every cluster size, and also, we can offer a better QoS due to the increase of the high-performance modulation (64QAM 3/4) use.

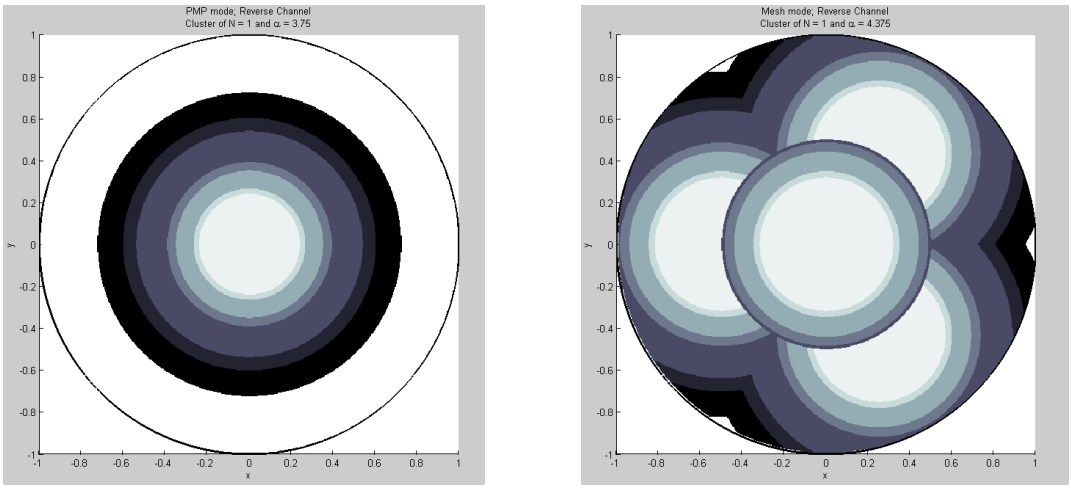

(a) PMP Scenario (b) Mesh Scenario

Figure 4.29: Comparative Results between PMP and Mesh scenarios; Uplink Channel; Cluster Size $N = 1$

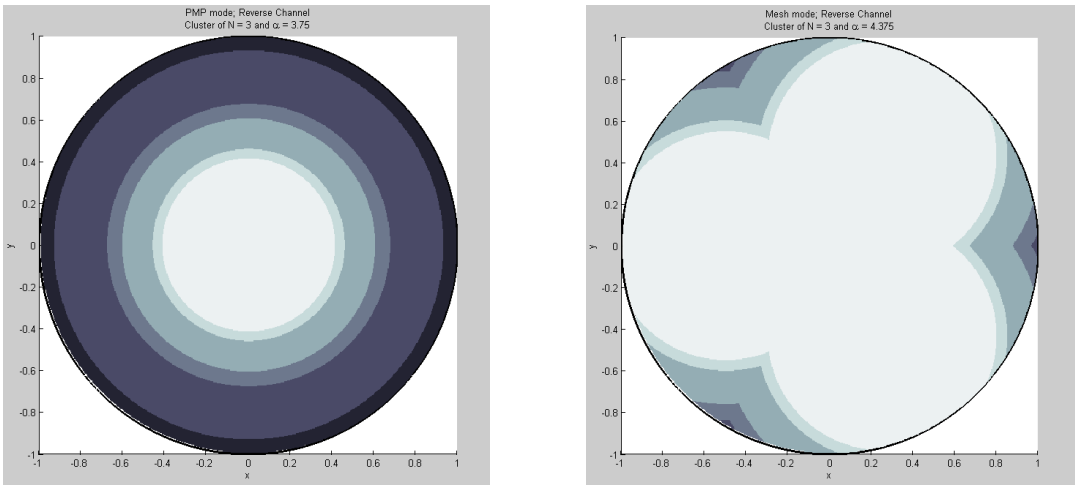

(a) PMP Scenario (b) Mesh Scenario

Figure 4.30: Comparative Results between PMP and Mesh scenarios; Uplink Channel; Cluster Size $N = 3$

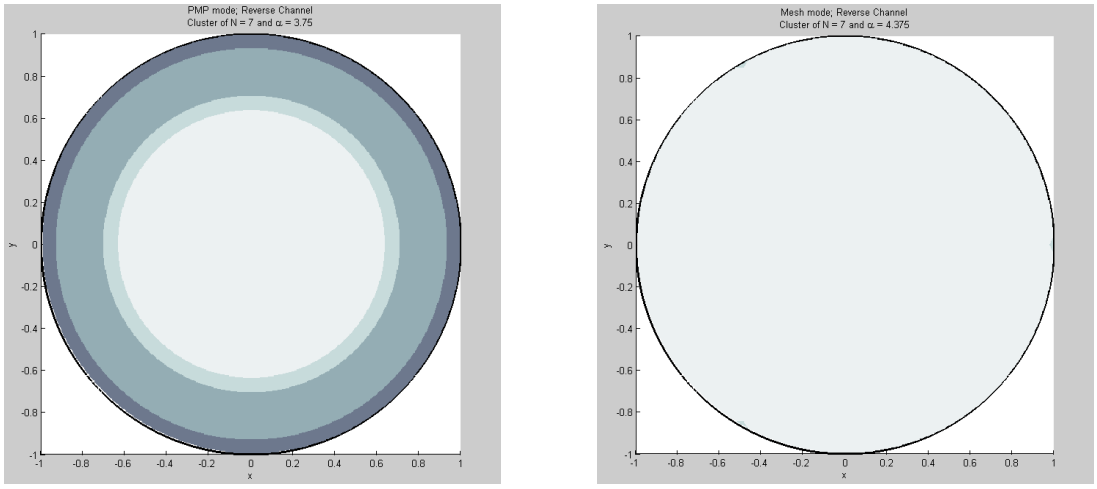

(a) PMP Scenario (b) Mesh Scenario

Figure 4.31: Comparative Results between PMP and Mesh scenarios; Uplink Channel; Cluster Size $N = 7$

Table 4.4: PMP mode and Mesh mode comparative for Terrain Type B ($h_b = 30$m); Uplink Channel

Modulation	Coding Rate	$N = 1$		$N = 3$		$N = 7$	
		PMP	Mesh	PMP	Mesh	PMP	Mesh
		Surface [%]					
BPSK	1/2	18.257	5.307	0	0	0	0
QPSK	1/2	8.485	5.240	0	0	0	0
QPSK	3/4	17.173	22.570	29.011	0.092	0	0
16-QAM	1/2	4.059	12.080	12.268	1.962	0	0
16-QAM	3/4	7.372	21.265	22.139	12.240	14.726	0
64-QAM	2/3	1.979	5.625	6.001	6.400	13.967	0.125
64-QAM	3/4	10.144	27.495	30.581	79.306	71.308	99.875
Total Area Covered of the Cell		67.469	99.582	100	100	100	100

In Table 4.4 we can see that when the cluster size equals to 1 or 3, in the mesh scenario the use of the 64QAM 3/4 scheme is again more than the double compared to the PMP scenario.

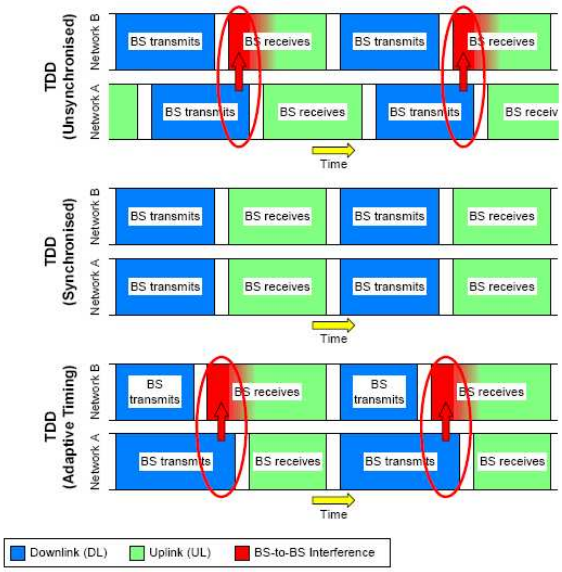

Figure 4.32: DL/UL and UL/DL interferences

4.3. DL/UL and UL/DL interferences

Besides the downlink and uplink interferences, there are, however, other interference possibilities in a TDD system. The 802.16 standard allows for each base station to adaptively set the amount of time that the DL and UL transmissions take up in a frame based on demand in that cell or sector. This means that at some point, a base station could be transmitting in the DL while a neighboring cell is in the UL part of the frame. Under these circumstances there are two additional interference scenarios. The DL/UL interference occurs when a mobile is being interfered by a neighboring mobile transmitting on the UL while receiving information on the DL. Similarly, UL/DL interference could occur at the base station while it is receiving transmissions on the UL and a neighboring cell is interfering on the same sub-carriers while in the DL mode.

These two additional cases, however, usually happen only over a limited time around the transition band between the UL and DL portions of the frame. Figure 4.32, shows a BS-to-BS interference as an example. With unsynchronized BSs (as shown in Figure 4.32 (top)) transmissions from one BS can desensitize the receive path of another. Synchronizing the timing of the transmit and receive windows (as shown in Figure 4.32 (middle)) eliminates this problem. Note that, however, this only works if all systems use a common transmit/receive timing structure; if the timing is adapted to the bandwidth requirements then it becomes virtually impossible to avoid contention

(as shown in Figure 4.32 (bottom))[19].

In order to estimate this interferences we need to consider that the interferers could be in a different state than the cell of interest. So, in the equations defined before we need to add a factor that represents these interferences. Our analysis consider the different possible combinations that would depend on the traffic characteristics of the system.

In Figures 4.33 and 4.34 we can observe the performance results for the different traffic cases when is considered a combination between downlink and uplink channels. In the Downlink/Uplink scenario, when the number of interferers in an opposite state is increased we notice that the area covered increased as well. This result from the fact that the number of BS interferers decreased and the MS interferes affect less the cell of interest.

On the other hand, in the Uplink/Downlink scenario the number of BS interferers increased affecting more the cell of interest, and as a result decreasing the performance of the system. In this scenario the synchronization between cells is very important.

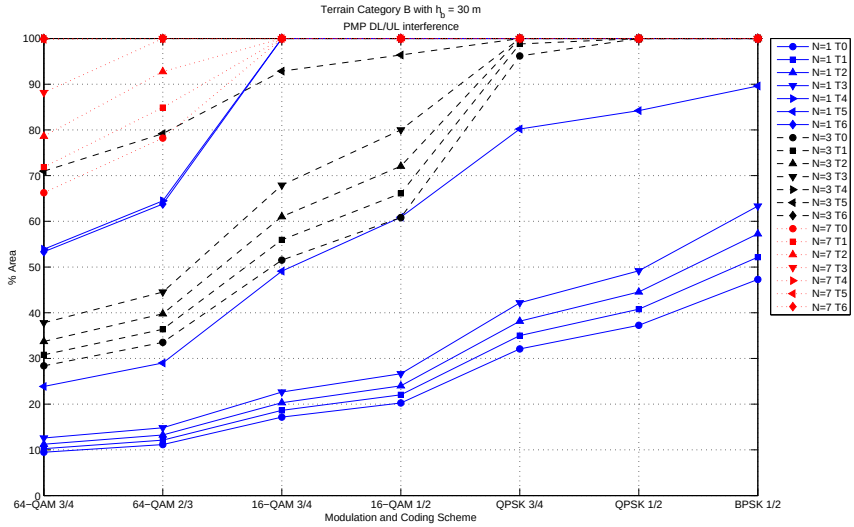

(a) Downlink/Uplink interference

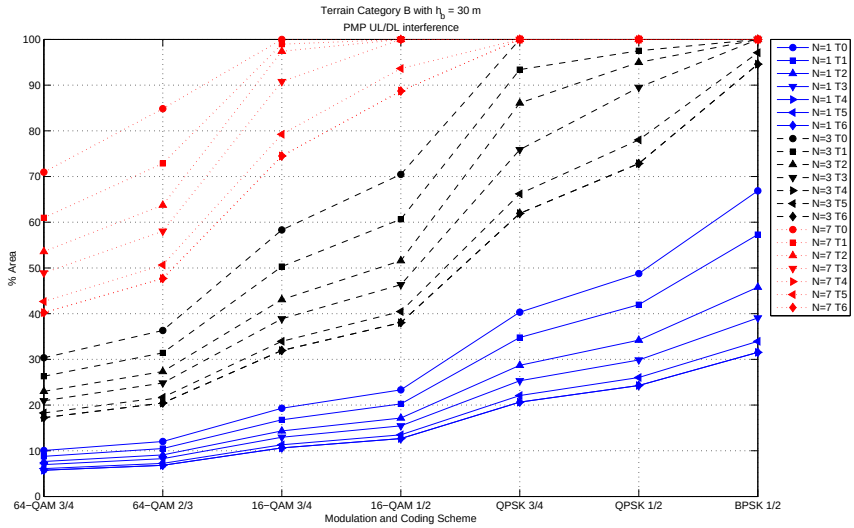

(b) Uplink/Downlink interference

Figure 4.33: Performance results for DL/UL and UL/DL interferences in PMP mode. It was considered different traffic situations; Tn represents each traffic where n is the number of cells in the opposite state

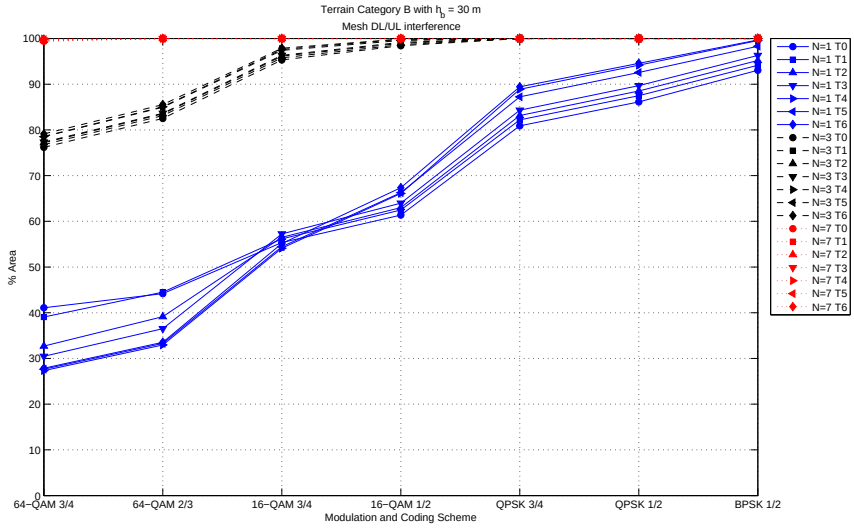

(a) Downlink/Uplink interference

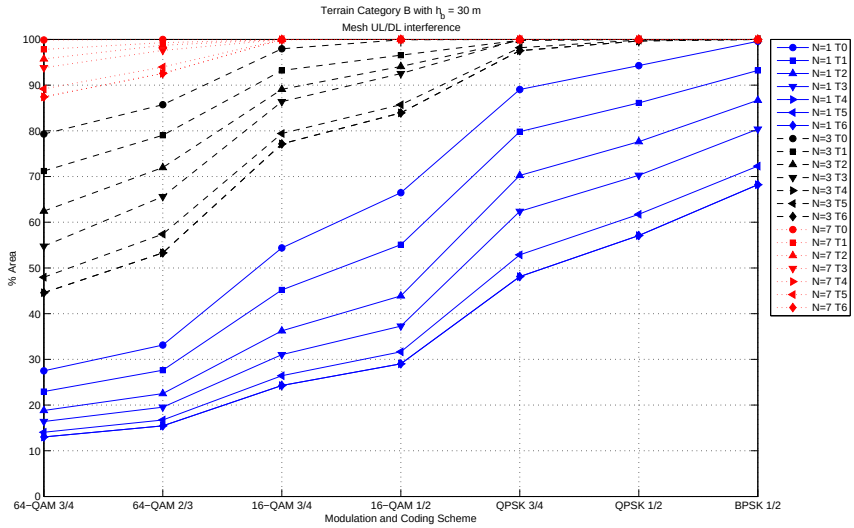

(b) Uplink/Downlink interference

Figure 4.34: Performance results for DL/UL and UL/DL interferences in Mesh mode. It was considered different traffic situations; Tn represents each traffic where n is the number of cells in the opposite state

At the early adoption of WiMAX, the dynamic allocation of the UL and DL time will most likely not be necessary until the systems get more heavily loaded at which point the added spectral efficiency of partitioning the frame becomes useful.

4.4. Interference in Sectoring scenarios

As we said in Section 2.2.3, the co-channel interference in a cellular system may be decreased by replacing a single omnidirectional antenna at the base station by several directional antennas, each radiating within a specified sector. By using directional antennas, a given cell will receive interference and transmit with only a fraction of the available co-channel cells. The technique for decreasing co-channel interference and thus increasing system performance by using directional antennas is called *sectoring*. The factor by which the co-channel interference is reduced depends on the amount of sectoring used. A cell is normally partitioned into three 120° sectors or six 60° sectors as shown in Figure 2.7 on page 21.

When sectoring is employed, the channels used in a particular cell are broken down into sectored groups and are used only within a particular sector. Assuming three-cell reuse, for the case of 120° sectors, the number of interferers in the first tier is reduced from six to three. This is because only three of the six co-channel cells receive interference with a particular sectored channel group. Referring to Figure 4.35, consider the interference experienced by a mobile located in the right-most sector in the center cell labeled "2". There are three co-channel cell sectors labeled "2" to the right of the center cell, and three to the left of the center cell. Out of these six co-channel cells, only three cells have sectors with antenna patterns which radiate into the center cell, and hence a mobile in the center cell will experience interference on the forward link from only these three sector.

In Figure 4.36 is illustrated the 120° sectoring for cluster sizes 1 and 7. In both cases the number of interferers in the first tier is reduced from six to two when the cells have similar dimensions.

In order to increase the SIR in the cells we applied sectoring to the PMP and Mesh scenarios described before. Figures 4.37 and 4.38 shown the results for the PMP mode. Sectoring result in a better performance; this performance was calculated in the same way as in previous sections using AMC. Table 4.5 shows the comparative between the regular PMP scenario and the one which uses 120° sectoring.

In Table 4.5 it could be seen that when we use sectoring the cell coverage is in-

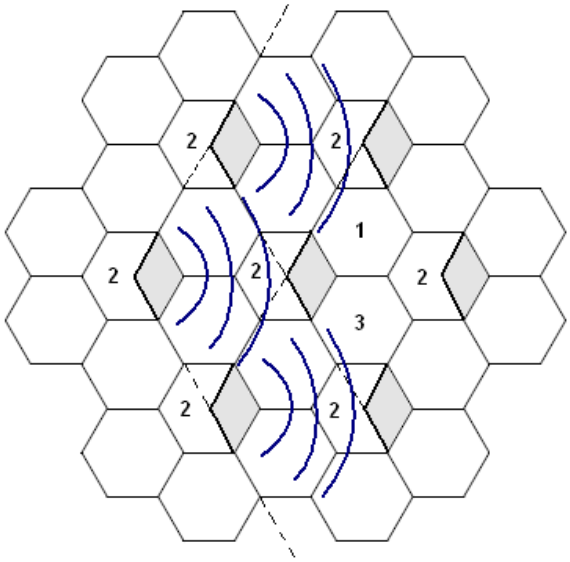

Figure 4.35: Illustration of how 120° sectoring reduces interference from co-channel cells in a three-cell reuse. Out of the six co-channel cells in the first tier, only three of them interfere with the center cell. If omnidirectional antennas were used at each base station, all six co-channel cells would interfere with the center cell.

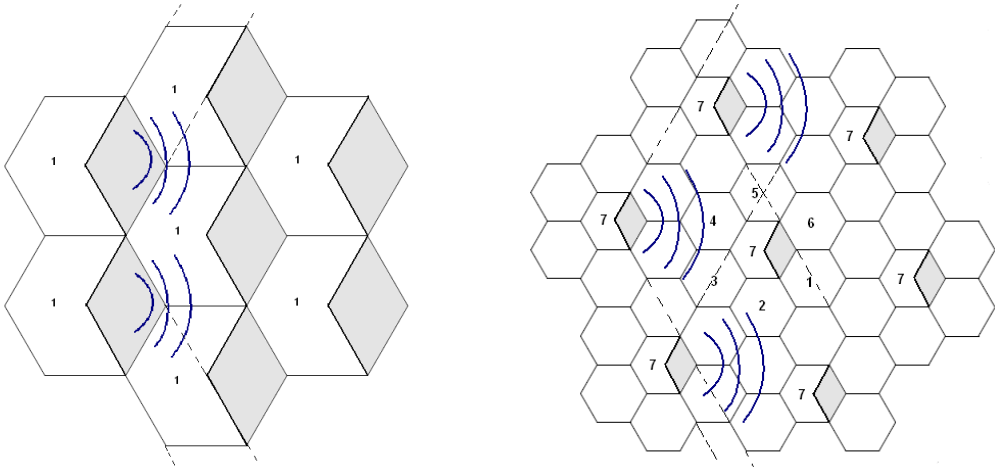

(a) One-cell reuse ($N = 1$) (b) Seven-cell reuse ($N = 7$)

Figure 4.36: Illustration of 120° sectoring with cluster sizes $N = 1$ and $N = 7$

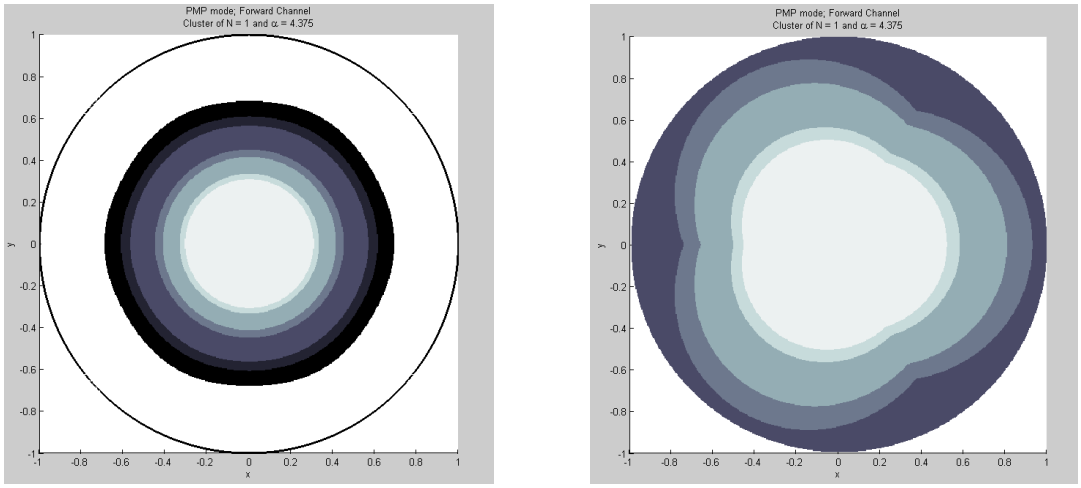

(a) PMP Scenario (b) 3-sector PMP Scenario

Figure 4.37: Comparative Results between PMP and 3-sector PMP scenarios; Downlink Channel; Cluster Size $N = 1$

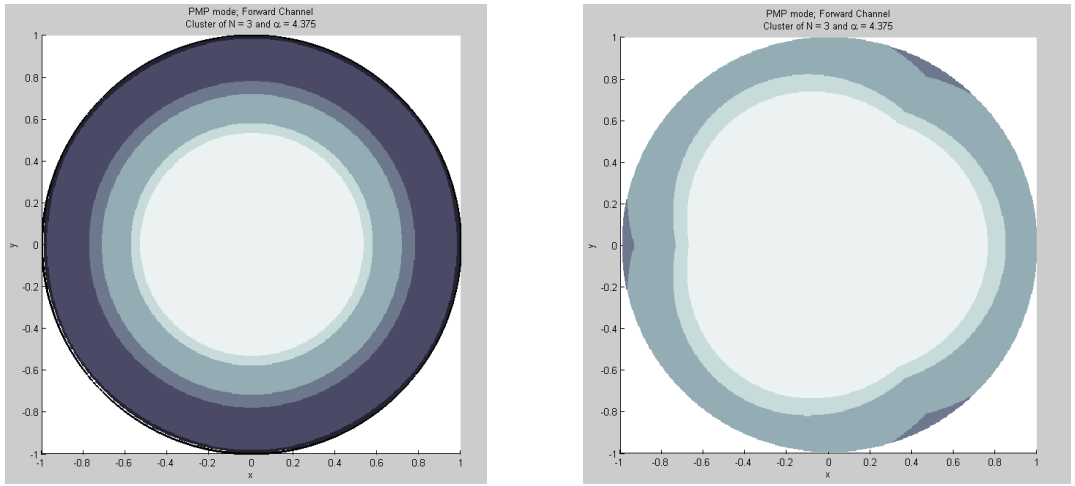

(a) PMP Scenario (b) 3-sector PMP Scenario

Figure 4.38: Comparative Results between PMP and 3-sector PMP scenarios; Downlink Channel; Cluster Size $N = 3$

creased significantly. When we use sectoring with a cluster size $N = 1$ we can cover the entire cell, in contrast to the regular PMP scenario that just cover 47% of the cell. Also the amount of area that use a 64QAM 3/4 modulation scheme is increased in every cluster size.

Table 4.5: PMP mode and 3-sector PMP mode comparative for Terrain Type B ($h_b =$ 30m); Downlink Channel

		$N = 1$		$N = 3$		$N = 7$	
		PMP	3-sect	PMP	3-sect	PMP	3-sect
Modulation	Coding Rate	Surface [%]					
BPSK	1/2	10.030	0	0	0	0	0
QPSK	1/2	5.170	0	3.820	0	0	0
QPSK	3/4	11.814	25.619	35.364	0	0	0
16-QAM	1/2	3.104	17.293	9.306	1.448	0	0
16-QAM	3/4	5.999	26.327	17.991	33.554	21.791	0
64-QAM	2/3	1.690	6.123	5.130	11.958	11.957	0
64-QAM	3/4	9.471	24.638	28.389	53.040	66.252	100
Total Area Covered of the Cell		47.279	100	100	100	100	100

Figures 4.39 and 4.40 shown the results for the Mesh mode. Also in this scenario, sectoring result in a better performance; this performance was calculated in the same way as in previous sections using AMC. Table 4.6 shows the comparative between the regular Mesh scenario and the one which uses 120° sectoring.

In Table 4.6 it could also be seen that when we use sectoring the cell coverage is increased. In the regular Mesh scenario with a cluster size $N = 1$ it could be cover a 93% of the cell. Using sectoring we can cover the entire cell and also increase the amount of area that use a 64QAM 3/4 modulation scheme.

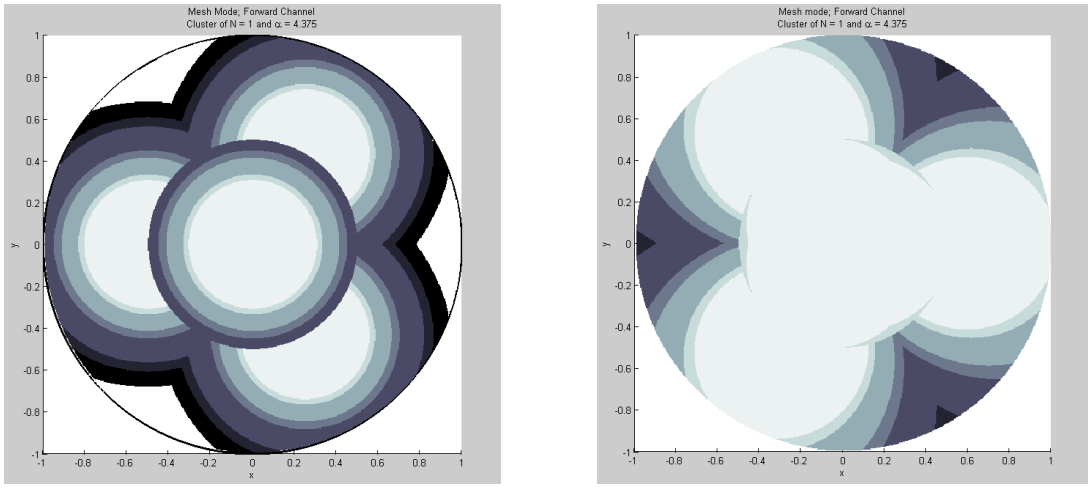

(a) Mesh Scenario (b) 3-sector Mesh Scenario

Figure 4.39: Comparative Results between Mesh and 3-sector Mesh scenarios; Downlink Channel; Cluster Size $N = 1$

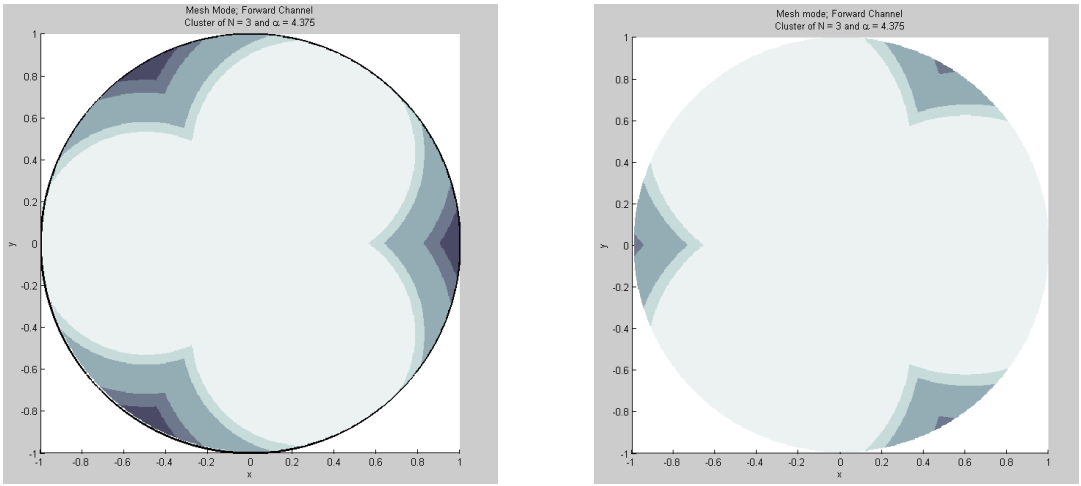

(a) Mesh Scenario (b) 3-sector Mesh Scenario

Figure 4.40: Comparative Results between Mesh and 3-sector Mesh scenarios; Downlink Channel; Cluster Size $N = 3$

Table 4.6: Mesh mode and 3-sector Mesh mode comparative for Terrain Type B (h_b = 30m); Downlink Channel

		$N=1$		$N=3$		$N=7$	
		Mesh	3-sect	Mesh	3-sect	Mesh	3-sect
Modulation	Coding Rate	Surface [%]					
BPSK	1/2	6.919	0	0	0	0	0
QPSK	1/2	5.226	0.657	0	0	0	0
QPSK	3/4	24.298	10.733	1.575	0	0	0
16-QAM	1/2	9.102	5.727	3.113	0.308	0	0
16-QAM	3/4	17.182	14.734	12.805	6.900	0	0
64-QAM	2/3	4.788	6.920	6.317	4.428	0.586	0
64-QAM	3/4	25.524	61.230	76.189	88.364	99.414	100
Total Area Covered of the Cell		93.038	100	100	100	100	100

As in the regular scenarios for PMP and Mesh modes, when we use sectoring the Mesh mode shows a better performance. This can be seen in Figures 4.41 and 4.42 for cluster sizes 1 and 3. In Table 4.7 are the numeric results for the interference estimation when sectoring is used.

Table 4.7 shows that we can offer a better QoS due to the increase of the high-performance modulation (64QAM 3/4) use. When sectorin is used in both modes, in the mesh scenario the use of the 64QAM 3/4 scheme is more than the double in $N = 1$ and double for $N = 3$ compared to the PMP scenario.

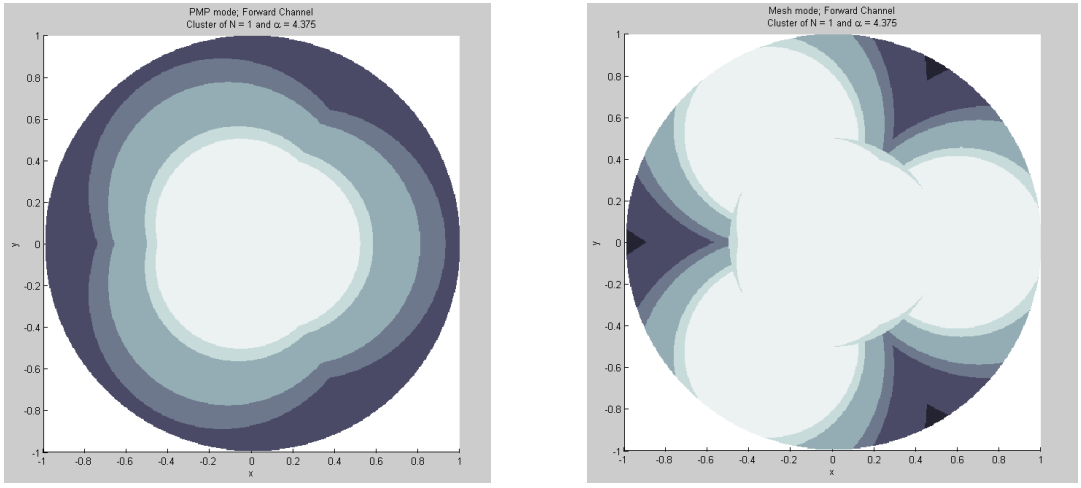

(a) PMP Scenario (b) Mesh Scenario

Figure 4.41: PMP mode and Mesh mode comparative using sectoring (3 sectors); Downlink Channel; Cluster Size $N = 1$

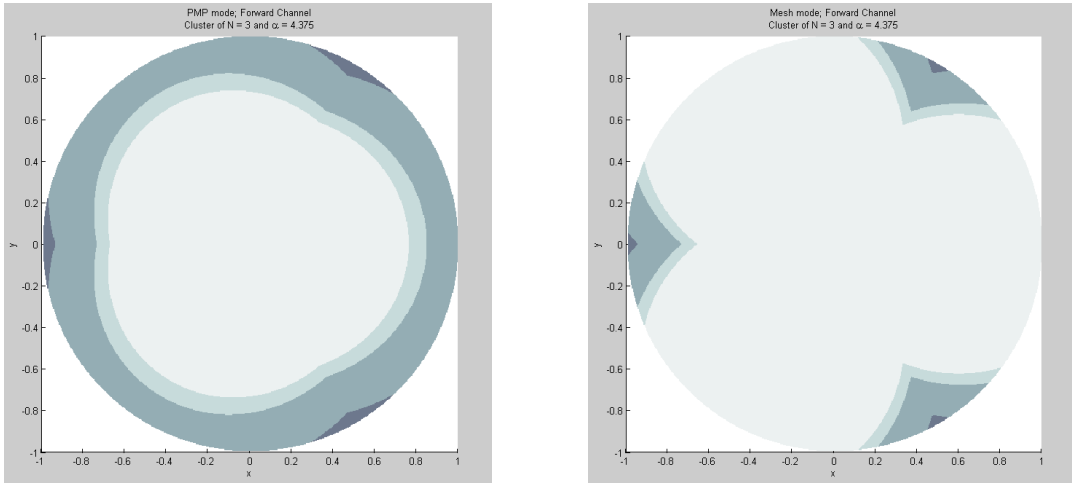

(a) PMP Scenario (b) Mesh Scenario

Figure 4.42: PMP mode and Mesh mode comparative using sectoring (3 sectors); Downlink Channel; Cluster Size $N = 3$

Table 4.7: PMP mode and Mesh mode comparative for Terrain Type B (h_b = 30m) using sectoring (3 sectors); Downlink Channel

		$N = 1$		$N = 3$		$N = 7$	
		PMP	Mesh	PMP	Mesh	PMP	Mesh
Modulation	Coding Rate	Surface [%]					
BPSK	1/2	0	0	0	0	0	0
QPSK	1/2	0	0.657	0	0	0	0
QPSK	3/4	25.619	10.733	0	0	0	0
16-QAM	1/2	17.293	5.727	1.448	0.308	0	0
16-QAM	3/4	26.327	14.734	33.554	6.900	0	0
64-QAM	2/3	6.123	6.920	11.958	4.428	0	0
64-QAM	3/4	24.638	61.230	53.040	88.364	100	100
Total Area Covered of the Cell		100	100	100	100	100	100

In Figure 4.43 were grouped all the interference results for the downlink channel in order to compare the performance when sectoring is used and when it is not. When cluster size equals to one, 120°-sectoring PMP scenario performs better than the regular Mesh scenario, and the 120°-sectoring Mesh scenario has the best performance. But when cluster size equals to three, it could be said that the regular Mesh scenario performs better than the 120°-sectoring PMP scenario due to the significantly increase of 64QAM 3/4 scheme use. Also in $N = 3$ the 120°-sectoring Mesh scenario has the best performance.

4.5. Coverage Simulations for the 700 MHz Band

Much of the globally available bandwidth is at carrier frequencies of several GHz. Lower carrier frequencies are generally considered more desirable, and frequencies below 1GHz are often referred to as "beachfront" spectrum. The reasons for this historically have been twofold.

- First, high-frequency RF electronics have traditionally been more difficult to design and manufacture and hence more expensive. However, this issue is not as prominent presently, owing to advances in RF integrated circuit design.

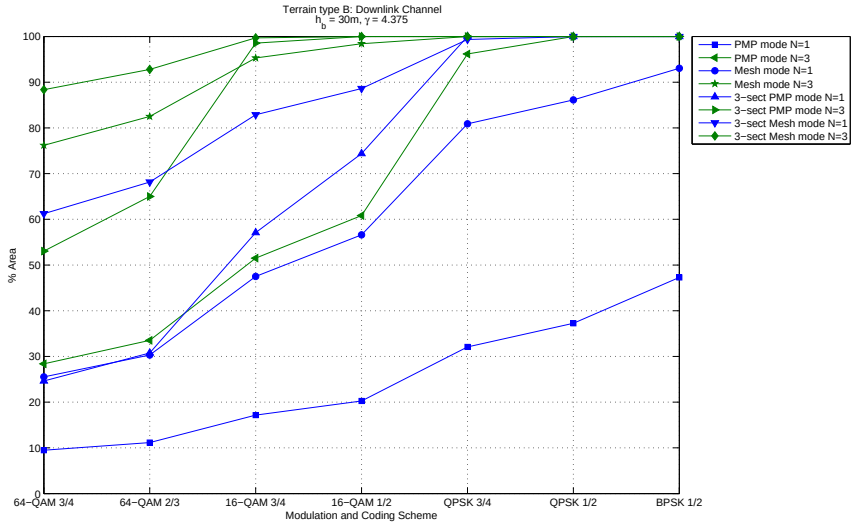

Figure 4.43: Illustration of the performance of non-sectoring scenarios and 120°-sectoring cases in the Downlink Channel

- Second, as easily seen in the free-space pathloss equation, the pathloss increases as f_c^2. A signal at 3.5GHz—one of WiMAX's candidate frequencies—will be received with about 25 times less power than at 700MHz, a popular cellular frequency.

In fact, measurement campaigns have consistently shown that the effective pathloss exponent γ also increases at higher frequencies, owing increased absorption and attenuation of high-frequency signals [20, 21].

As we conclude before, the co-channel interference is independent of the frequency but the coverage range it is not. *Median pathloss models* are useful for getting a rough estimate of the area that can be covered by a given radio transmitter. Since radio signal power tends to decay exponentially with distance, these models are typically linear on a logarithmic decibel scale with a slope and intercept that depend on the overall terrain and clutter environment, carrier frequency, and antenna heights. Median pathloss models are quite useful in doing preliminary system designs to determine the number of base stations (BSs) required to cover a given area.

For correct system work received power P_R must be above sensitivity of receiver S_R: $P_R \geq S_R$. Received power in dB can be calculated by

$$P_R = P_T - L_T + G_T - PL + G_R - L_R \tag{4.9}$$

where P_T is the transmitter power, L_T is the transmitter feeder loss, G_T is the transmitter antenna gain, PL is the pathloss of the transmission medium, G_R is the receiver antenna gain and finally, L_R is the receiver feeder loss. In case when we have receiving power on the threshold (receiver sensitivity which are defined for some BER= 10^{-6} and modulation mode) maximal pathloss can be calculated by

$$PL_{max} = (P_T - L_T + G_T - PL + G_R - L_R) - S_R \tag{4.10}$$

Depending on the pathloss model used we can obtain an equation for the maximum cell radius. For the Erceg model, we use the equations 2.24 and 4.10 and we obtain the following expression,

$$\begin{aligned} 10\gamma \log(d_{max}/d_0) &= PL_{max} - [20\log(4\pi d_0/\lambda) + PL_f + PL_h + s] \\ d_{max} &= d_0 10^{\frac{PL_{max} - \left[20\log(4\pi d_0/\lambda) + PL_f + PL_h + s\right]}{10\gamma}} \\ d_{max} &= d_0 10^{\frac{PL_{max} - \left[20\log(4\pi d_0/\lambda) + PL_f + PL_h + s\right]}{10(a - bh_b + c/h_b)}} \end{aligned} \tag{4.11}$$

where PL_{max} is the maximal pathloss of the transmission medium, PL_f and PL_h are the correction factor due to the frequency and receive antenna height respectively, while s represent the shadowing effect, h_b is the base station antenna height and finally, a, b and c are constants dependent on the terrain category given in Table 2.3.

As we said in Chapter 2 this propagation model cover three terrain categories; A, B, and C. "Category A", being the highest path loss category, is used in this work to predict propagation characteristics in urban environments and "Category C", the lowest path loss terrain category, is used propagation predictions in rural environments. The intermediate path loss condition, "Category B", is assumed for suburban environment range predictions. Treating these terrain categories as urban, suburban, and rural respectively is a suitable assumption for the purposes of this section, but in practice each environment must be assessed on its specific characteristics. It would not be unusual for example, to encounter a rural area with a hilly terrain, extensive trees, and varied building heights making it a candidate for a high-loss propagation condition; "Category A", rather than "Category C". Additionally, some urban areas in smaller cities with low and similar building heights may qualify for an intermediate loss condition, "Category B".

By using equations 2.25 and 2.26 we can obtain expressions which describes cell size for different terrain types. Equation 4.12 defines the maximum cell radius for urban and suburban terrain categories, and Equation 4.13 for rural terrain category.

$$d_{max} = d_0 10^{\frac{PL_{max} - [20\log(4\pi d_0/\lambda) + 6\log(f/2000) - 10.8\log(h_m/2) + s]}{10(a - bh_b + c/h_b)}} \tag{4.12}$$

$$d_{max} = d_0 10^{\frac{PL_{max} - [20\log(4\pi d_0/\lambda) + 6\log(f/2000) - 20\log(h_m/2) + s]}{10(a - bh_b + c/h_b)}} \tag{4.13}$$

In the same way, we can obtain the maximum cell radius expression for the Hata model. The Equation 3.7 is a general expression of the median pathloss for any clutter environment.

$$\begin{aligned}(44.9 - 6.55\log(h_b))\log(d_{max}) = PL_{max} - [69.55 + 26.16\log f - 13.82\log h_b \\ -(3.2(\log(11.75h_m))^2 - 4.97) + \text{Clutter Offset}]\end{aligned}$$

$$d_{max} = 10^{\frac{PL_{max} - \left[9.55 + 26.16\log f - 13.82\log h_b - (3.2(\log(11.75h_m))^2 - 4.97) + \text{Clutter Offset}\right]}{44.9 - 6.55\log(h_b)}} \tag{4.14}$$

where PL_{max} is the maximal pathloss of the transmission medium, h_b is the base station antenna height, h_m is the mobile station antenna height, f is the carrier frequency in MHz and finally, the Clutter Offset is an expression for each terrain category defined in Chapter 3.

Table 4.8 summarizes the parameters for determining the path loss differences among the frequencies bands of interest (700 MHz, 2500 MHz and 3500 MHz).

Table 4.8: Parameters for Path Loss Comparison

Parameter	700 MHz	2500 MHz and 3500 MHz
Propagation Model	Hata	Erceg
Region	Urban, Suburban and Rural	
BS Antenna Height	10–80 meters	
Mobile Terminal Antenna Height	1.5 meters	

Depending on the modulation and coding scheme we can obtain different cell radius. When we use a BPSK 1/2 scheme we can obtain the maximum cell radius; in contrast when we use a 64-QAM 3/4 scheme we obtain the minimum cell radius.

Figure 4.44 and 4.45 show the base station antenna height versus cell radius using BPSK and 64QAM modulation scheme, respectively, for the 700 MHz, 2500 MHz and 3500 MHz frequency bands assuming the Hata model at 700 MHz and the Erceg model in the 2500 and 3500 MHz bands.

As we said these results are useful for getting a rough estimate of the area that can be covered by a given radio transmitter. From the Figures we can observe that the cell radius is inversely proportional to the frequency. This means we can cover a geographical area with less number of base stations when lower frequencies are used. However, it is important to consider other factors in the selection of a frequency.

Antenna Requirements The necessary physical spacing among antennas is determined by the wavelength, with those at 700 MHz being roughly 3.5 times as great as those required at 2500 MHz. The practicality of such spatial techniques at 700 MHz will then depend on the details of the deployments involved and the performance benefits offered. In conclusion antenna spacing considerations may, in general, limit the use of some of the advanced multiple antenna systems supported by WiMAX technology in the 700 MHz band when compared with 2500 MHz deployments. In practice however the specifics of individual deployments and the performance gains offered by the techniques in question will dictate what is acceptable.

Cable Losses Network operators typically prefer base-mounted transmitter power amplifiers rather than tower-mounted amplifiers for ease of maintenance. The amplifier transmit power must therefore be sufficient to overcome cable losses. In the 2500 MHz band cable losses can range from approximately 2 dB for a high performance cable to almost 6 dB for a lower cost cable for a 32 meter tower height. For the same types of cable in the 700 MHz band these losses will range from 1 dB to about 3 dB. To achieve the same transmit power at the base station antenna port, 700 MHz deployments can use lower power base-mounted amplifiers or alternatively lower cost cable. In either case this cost savings would help to mitigate the cost impact of the larger antennas and associated mounting structures.

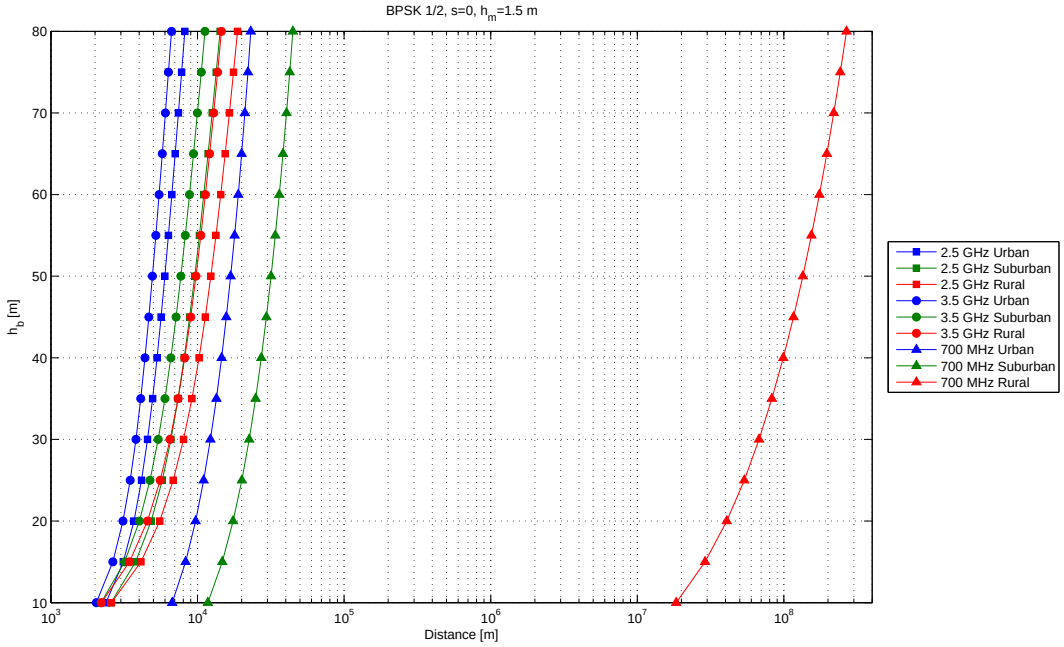

(a) Total Panorama

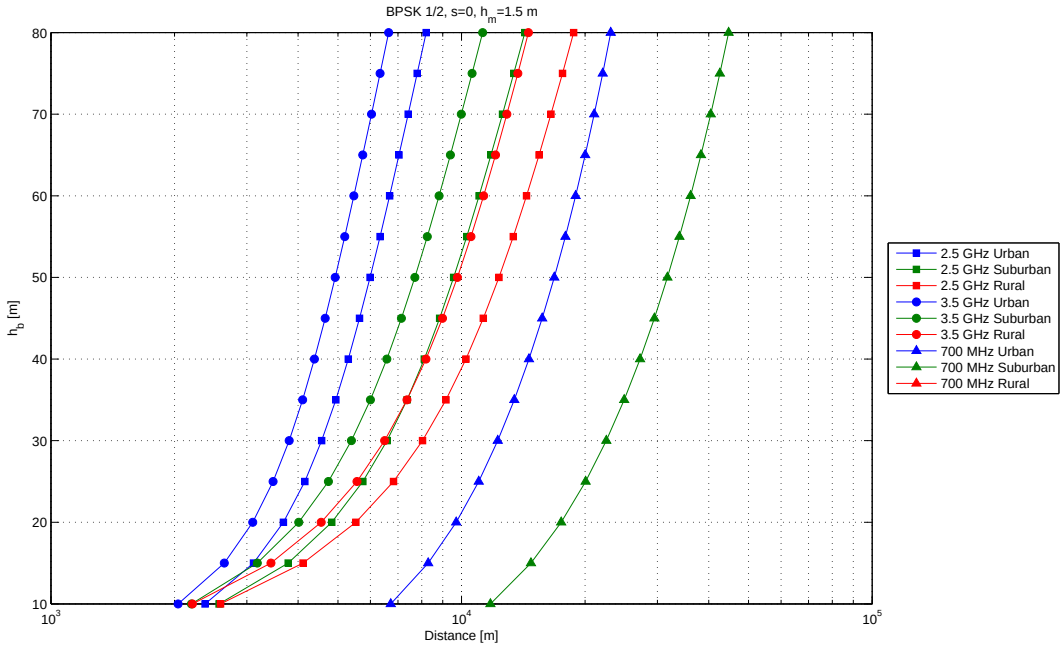

(b) Zoom in Panorama

Figure 4.44: Cell dimensioning with BPSK 1/2 scheme

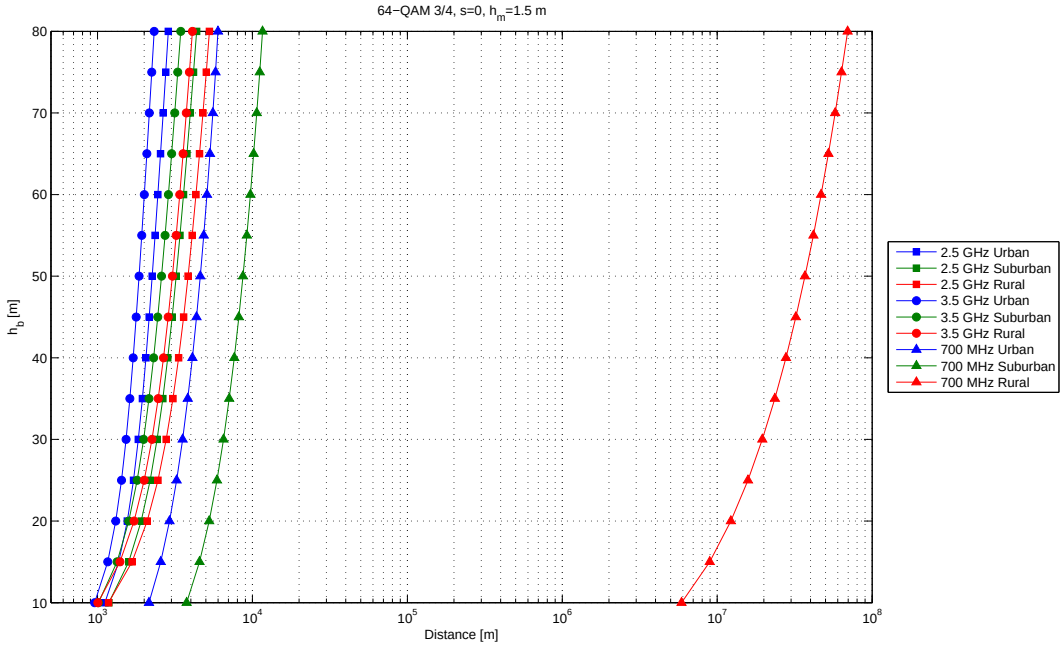

(a) Total Panorama

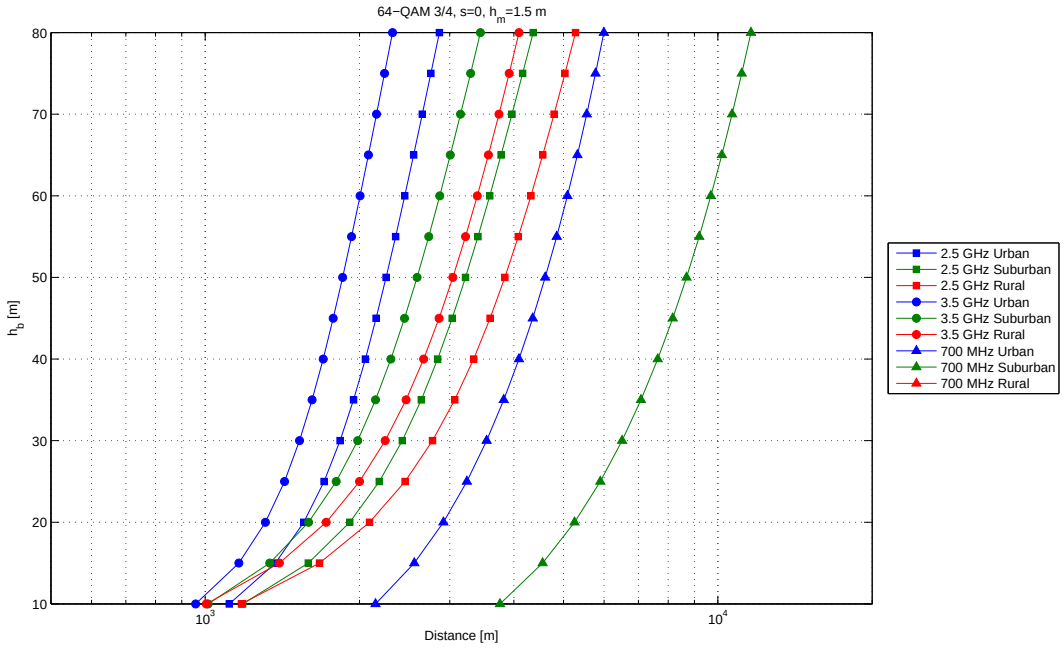

(b) Zoom in Panorama

Figure 4.45: Cell dimensioning with 64QAM 3/4 scheme

Line of Sight True line-of-sight (LOS) is defined as a path free of obstructions within the 1st Fresnel zone[1] to minimize the simultaneous reception of reflected out-of-phase signals and excess losses due to signal diffraction. Although in practice it is common to tolerate obstructions in 30–40% of the 1st Fresnel zone it would be still require higher base stations heights at 700 MHz to achieve the same Fresnel zone clearance that can be achieved at 2500 MHz.

Other Relevant Parameters Other factors that impact range are mobile station antenna gain, transmit power, noise figures, etc.

[1]The radius of the first Fresnel zone is maximum at the midpoint of the LOS path and is directly proportional to the square root of the wavelength times the path length.

Chapter 5

Conclusions and Future Work

5.1. General Conclusions

IEEE 802.16 (WiMAX) is a wireless metropolitan area network standard with high transmission speed and great coverage. There are several ways of quantifying the performance of a broadband system. This thesis considered the factors affecting interference in a WiMAX system. As discussed in this work, uplink and downlink interference analysis have to be approached and analyzed differently. Downlink interference analysis can be computed or measured at each location in the service area and is therefore deterministic in nature. On the uplink, however, the randomness of the distribution of the users in the sectors introduces also a stochastic behavior on the received S/I ratio at the base stations. Channel planning, sub-channel allocations, as well as the use of frequency re-use factor zones all have effects on system wide interference levels.

System capacity is dependent on the distribution of the users in the service area as well as the type of service that is requested. In systems that employ adaptive modulation such as 802.16, capacity is also a function of the S/I ratio since higher modulation orders can achieve higher spectral efficiencies. Channel and, if necessary, sub-channel planning also has an effect on the data rate that can be supported per unit bandwidth. The flexibility in the WiMAX standard allows a system designer to perform tradeoffs between overall system capacity and interference levels to best allocate the resources to supply the customers with their data needs.

In this work we also presented a comparative between the different modes presented in the 802.16e standard: point-to-point and mesh links. We demonstrate that

the mesh mode offers a significantly advantage over the traditional mode. The mesh mode allow to offer best quality of service to more users using a higher rate modulation (64-QAM). It was proven that this results are unsensible to the frequency used.

It was also shown that sectoring improve capacity by increasing S/I using directional antennas instead of omnidirectional antennas. When sectoring is used we can cover the entire cell and also increase the amount of area that use a 64QAM 3/4 modulation scheme even when the cluster size equals to one.

Despite that we show that the interference calculations are unsensible to the frequency we did coverage simulations for the 700 MHz band. We have shown that 700 MHz deployments provide a considerable range benefit compared to scenarios in frequency bands in the order of GHz. This means that in this range of frequency we need less base stations to cover an area. However there are other factors that need to be considered when choosing a frequency.

5.2. Future Work

According to the work done in this thesis, the following ideas can be suggested for further research:

- Consider the effects of dynamic relays instead of the fixed relays that were analyzed here.
- Analyze problems due to the coexistence of TDD and FDD transmissions.
- Estimate interference in hybrid frequency allocation schemes.
- Calculate the intra-cell interference focusing in the impact of Adaptive Modulation and Coding.
- Consider the effects of having different propagation models between hops.
- Evaluate the services that could be offered in terms of the selected WiMAX scheme for a specific scenario.

Appendix A
Abbreviations and Acronyms

AAS adaptive antenna system

AMC adaptive modulation and coding

ARQ automatic repeat request

BCC block convolutional code

BER bit error rate

BPSK binary phase shift keying

BS base station

BTC block turbo code

BW bandwidth

BWA broadband wireless access

C/I carrier-to-interference ratio

C/N carrier-to-noise ratio

CCI co-channel interference

CDMA code division multiple access

CINR carrier-to-interference-and-noise ratio

CP cyclic prefix

CTC convolutional turbo codes

dBi decibels of gain relative to the zero dB gain of a free-space isotropic radiator

dBm decibels relative to one milliwatt

DL downlink

EIRP effective isotropic radiated power

FDD frequency division duplex or duplexing

FEC forward error correction

FFT fast fourier transform

FUSC full usage of subchannels

GPS global positioning system

GS guard symbol

H-FDD half-duplex frequency division duplex

HUMAN high-speed unlicensed metropolitan area network

IFFT inverse fast fourier transform

IP internet protocol

ITU international telecommunications union

LAN local area network

LOS line-of-sight

MAC medium access control layer

MAN metropolitan area network

Mb/s megabit per second

MCS modulation coding scheme

MIMO multiple input multiple output

MS mobile station

MSH mesh

NLOS non-line-of-sight

OFDM orthogonal frequency division multiplexing

OFDMA orthogonal frequency division multiple access

PAPR peak to average power ratio

PHY physical layer

PMP point-to-multipoint

PS physical slot

PUSC partial usage of subchannels

PUSC-ASCA PUSC adjacent subcarrier allocation

QAM quadrature amplitude modulation

QoS quality of service

QPSK quadrature phase-shift keying

REQ request

RNG ranging

RS Reed-Solomon

RSS receive signal strength

RSSI receive signal strength indicator

Rx receiver

SC single carrier

SDMA spatial division multiple access

SIR or S/I signal-to-interference ratio

SNR signal-to-noise ratio

SS subscriber station

TDD time division duplex or duplexing

TDM time division multiplexing

TDMA time division multiple access

Tx transmitter

UL uplink

WirelessMAN Wireless Metropolitan Area Networks

WirelessHUMAN Wireless High-speed Unlicensed Metropolitan Area Networks

Bibliography

[1] J. G. Andrews, A. Ghosh, and R. Muhamed. *Fundamentals of WiMAX: Understanding Broadband Wireless Networking*. Pearson Education, United States, February 2007.

[2] V. Erceg, L. J. Greenstein, S. Y. Tjandra, S. R. Parkoff, A. Gupta, B. Kulic, A. A. Julius, and R. Bianchi. An empirically based path loss model for wireless channels in suburban environments. *Selected Areas in Communications, IEEE Journal on*, 17(7):1205–1211, July 1999.

[3] IEEE Standard for Local and Metropolitan Area Networks Part 16: Air Interface for Fixed and Mobile Broadband Wireless Access Systems Amendment 2: Physical and Medium Access Control Layers for Combined Fixed and Mobile Operation in Licensed Bands and Corrigendum 1, 2006.

[4] IEEE Standard for Local and Metropolitan Area Networks Part 16: Air Interface for Fixed Broadband Wireless Access Systems, 2004.

[5] WiMAX Forum http://www.wimaxforum.org/.

[6] C. Hoymann, M. Dittrich, and S. Goebbels. Dimensioning cellular multihop WiMAX networks. *Mobile WiMAX Symposium, 2007. IEEE*, pages 150–157, March 2007.

[7] Jie Zeng and XiaoFeng Zhong. A novel WiMAX structure with mesh network. *Real-Time Mobile Multimedia Services*, 4787/2007:50–63, 2007.

[8] L. Nuaymi. *WiMAX Technology for Broadband Wireless Access*. Wiley, England, 2007.

[9] J. Oetting. Cellular mobile radio—an emerging technology. *Communications Magazine, IEEE*, 21(8):10–15, November 1983.

[10] Theodore S. Rappaport. *Wireless Communications*. Communications Engineering and Emerging Technologies Series. Prentice Hall, 2002.

[11] V.H. MacDonald. The Cellular Concept. *The Bell Systems Technical Journal*, 58(1):15–43, January 1979.

[12] W. L. Stutzman and G. A. Thiele. *Antenna Theory and Design*. John Wiley & Sons, 1981.

[13] T. Kawano Y. Okumura, E. Ohmori and K. Fukua. Field strength and its variability in UHF and VHF land-mobile radio service. *Rev. Elec. Commun. Lab.*, 16(9), 1968.

[14] M. Hata. Empirical formula for propagation loss in land mobile radio services. *IEEE Trans. Veh. Technol.*, 29:317–325, August 1980.

[15] R. Van Nee and R. Prasad. *OFDM for Wireless Multimedia Communications*. Universal Personal Communications. Artech House, 2000.

[16] Federal Communications Commission http://www.fcc.gov/.

[17] MWG/AWG. A comparative analysis of spectrum alternatives for WiMAX networks with deployment scenarios based on the U.S. 700 MHz band. Technical report, WiMAX Forum, 2008.

[18] WiMAX Forum Mobile System Profile Release 1.0 Approved Specification. Technical report, WiMAX Forum, May 2007.

[19] FDD and TDD coexistence. Technical report, WiMAX Forum, 2007.

[20] P. Stigter G. Janssen and R. Prasad. Wideband Indoor Channel Measurements and BER Analysis of Frequency Selective Multipath Channels at 2.4, 4.75, and 11.5 GHz. *Transactions on Communication, IEEE*, 44(10):1272–1288, October 1996.

[21] Peter Papazian. Basic Transmission Loss and Delay Spread Measurements for Frequencies Between 430 and 5750 MHz. *Transactions on Antennas and Propagation, IEEE*, 53(2):694–701, February 2005.